



# Confocal Ultrasound for the Potentiation of Chemotherapy by Ultrasonic Cavitation without External Nucleation Agents

Maxime Lafond

## ► To cite this version:

Maxime Lafond. Confocal Ultrasound for the Potentiation of Chemotherapy by Ultrasonic Cavitation without External Nucleation Agents. Cancer. Université de Lyon, 2016. English. NNT : 2016LYSE1243 . tel-01593250

**HAL Id: tel-01593250**

**<https://theses.hal.science/tel-01593250>**

Submitted on 26 Sep 2017

**HAL** is a multi-disciplinary open access archive for the deposit and dissemination of scientific research documents, whether they are published or not. The documents may come from teaching and research institutions in France or abroad, or from public or private research centers.

L'archive ouverte pluridisciplinaire **HAL**, est destinée au dépôt et à la diffusion de documents scientifiques de niveau recherche, publiés ou non, émanant des établissements d'enseignement et de recherche français ou étrangers, des laboratoires publics ou privés.



N°d'ordre NNT : 2016 LYSE1243

## **THESE de DOCTORAT DE L'UNIVERSITE DE LYON**

Opérée au sein de  
**L'Université Claude Bernard Lyon 1**

**Ecole Doctorale Interdisciplinaire Sciences-Santé**

**Spécialité de doctorat** : Ingénierie Biomédicale

**Discipline** : Acoustique

Soutenue publiquement le 21/11/2016 par :

**Maxime Lafond**

---

# **Confocal Ultrasound for the Potentiation of Chemotherapy by Ultrasonic Cavitation without External Nucleation Agents**

---

Devant le jury composé de :

BOUAKAZ, Ayache  
LENTACKER, Ine  
UMEMURA, Shin-ichiro  
CANNET-SOULAS, Emmanuelle  
BRIDAL, Lori  
CLEZARDIN, Philippe  
LAFON, Cyril

DR, INSERM U970, Université Rabelais  
DR, Ghent University  
Pr, Tohoku University  
Pr, INSERM U1060, UCBL  
DR, UPMC  
DR, INSERM U1033, UCBL  
DR, INSERM U1032, UCBL

Rapporteur  
Rapporteuse  
Examineur  
Examinatrice  
Présidente du Jury  
Examineur  
Directeur de thèse



## **Utilisation d'ultrasons confocaux pour la potentialisation de chimiothérapie par cavitation ultrasonore sans agents de nucléation extérieurs**

### **Résumé**

Le cancer est reconnu comme l'un des principaux enjeux de santé actuels. Même si de grands progrès ont été réalisés dans ce domaine, les effets systémiques des chimiothérapies et le caractère invasif des procédures actuelles de potentialisation (agents physiques) sont autant d'éléments limitants. Les ultrasons se démarquent néanmoins par leur faible morbidité. Appliqués de façon extracorporelle, ils peuvent pénétrer en profondeur dans les tissus et y induire effets thermiques et mécaniques, incluant entre autres la cavitation. La cavitation peut se définir comme la formation et l'oscillation de bulles dans le milieu de propagation. Il a été montré de potentiels bénéfiques de ce mécanisme dans la potentialisation d'agents thérapeutiques. Bien que la génération de cavitation puisse être aidée par l'ajout d'agents de nucléation extérieurs, le travail présenté ici s'en affranchi afin de rendre la procédure plus versatile. Des simulations numériques ont montré qu'un dispositif ultrasonore basé sur deux faisceaux confocaux permettait des conditions favorables à l'obtention de cavitation dans ces conditions. De plus, études *in vivo* ont montré l'innocuité du phénomène en regard de la stabilité de la doxorubicine, des effets histologiques sur tissus sains ainsi que sur l'éventuelle diffusion métastatique. L'efficacité du traitement combiné n'a en revanche pas pu être démontrée. Pour investiguer la combinaison de chimiothérapie avec de la cavitation stable, une stratégie de régulation est mise en place. Bien que la synergie ait pu être démontrée *in vitro*, l'étude préclinique ne permet pas de conclure sur l'effet *in vivo*. Dans l'hypothèse d'un défaut de localisation du nuage de cavitation, une méthode de localisation spatiale est mise en place et validée.

Mots-clés : ultrasons, cavitation, chimiothérapie

### **Confocal Ultrasound for the Potentiation of Chemotherapy by Ultrasonic Cavitation without External Nucleation Agents**

#### **Abstract**

Cancer is recognized as one of the major health issues of this beginning century. Even if great achievements have been performed, chemotherapies induce systemic toxicity and combinable physical agents are invasive. Ultrasound has shown a great potential as an external physical agent. Applied extracorporeally, it can penetrate in depth in tissue and induce various biological effects, mechanical of thermal. Notably, cavitation, which is the formation and oscillatory motion of bubbles in a media, has effects providing the possibility to enhance the delivery of chemotherapeutic agents. This effect can be induced in biological tissues by using



external nucleation agents such as ultrasound contrast agents. However, to avoid diffusion issues, this work focuses on cavitation without external nucleation agents. For this purpose, a particular setup based on two confocal transducers was designed. Simulations showed its advantages for cavitation applications. A developed preclinical device demonstrated the safety of using unseeded inertial cavitation for the potentiation of doxorubicin (DOX) regarding the drug stability, the effect on healthy tissues and the metastatic spreading. Unfortunately, no effect of combining inertial cavitation with DOX in could have been demonstrated *in vivo*. To investigate stable cavitation phenomenon, a control process was developed. It permitted to evidence *in vitro* the synergistic interaction between DOX and stable cavitation. Again, preclinical studies were not able to prove this synergy *in vivo*. To assess the correct tissue exposures to stable cavitation, a localization method was developed and validated.

Keywords : Ultrasound, cavitation, chemotherapy

## Remerciements

Je tiens tout d'abord à remercier Cyril Lafon pour m'avoir accueilli au sein du LabTAU et encadré au cours de mon stage de Master puis de ces trois années de thèse. Son dynamisme, sa détermination ainsi que ces conseils ont été précieux pour l'aboutissement de ce travail. Je tiens également à remercier Jean-Yves Chapelon, directeur du LabTAU lors de mon arrivée, pour son accueil.

I would like to thank all the members of the committee for their presence and their numerous comments on my work, particularly Ine Lentacker from Ghent University and Ayache Bouakaz from University François Rabelais for having accepted to review the manuscript of this work.

La recherche est un travail d'équipe. J'ai énormément bénéficié et appris de l'aide et du savoir-faire de Jean-Louis, sur la régulation de la cavitation notamment. De Françoise pour les codes de base du simulateur lors de mon arrivée en stage ainsi que pour les diverses conversations sur le sujet. De Fabrice sur le simulateur, notamment pour la partie force de radiation, ainsi que pour les nombreux casse-tête scientifiques. De Jacqueline pour le colossal travail de culture et d'entretien des milliards de cellules tumorales qui auront été sacrifiées sur l'autel de la science durant ces trois ans. Merci à Bernadette et Cécile pour le fantastique travail qui a été fourni sur les études de potentialisation in vitro et les discussions passionnantes amenées ainsi.

This thesis included a three months research stay in Tohoku University, Sendai, under the supervision of Professor Shin-ichiro Umemura. I sincerely thank him for this experience and the amount of things I learned there. I also wish to thank Shin Yoshizawa, Ryo Takagi and all the students that were there for their help and welcoming attitude.

日本で、支援をいっぱいいただきました。この経験をさせてもらった梅村研究所に感謝しています。梅村先生や吉澤先生や高木さんや学生の皆、ありがとうございました。そして、持て成していただきホストファミリーに感謝しています。特別にかやは日本とフランスでいつも支援してくれて感謝しています。

Une des caractéristiques bien connue du LabTAU est la bonne ambiance y régnant. Aux festins, attablés au long des discussions endiablées, les hauts débats se retrouvaient vite sans dessous dessus. On voyait flotter le bon vivre, au coin

d'une porte ou au détour d'un couloir. Les partenaires de sciences, de casse-dalle, de cafés, de galères, de fous rires, partent et arrivent, se succèdent en laissant chaque fois une trace différente, comme un goût de voyage. Je ne citerai pas les noms mais vous savez l'amitié que je vous porte.

J'ai eu quelques compagnons de cordée, et je me dois de les remercier. Tous. Merci à Florence de m'avoir accompagné toutes ces belles longueurs, et merci d'avoir coupé la corde. Merci à Thibault, Corentin et Charlie pour ce long fil tranquille, ces mails à en faire un bouquin qui aurait pu servir à caler les pieds de nos idées bancales. Merci à Joëlle, Elodie et Henri pour ces trois années de création, de plaisir, d'exutoire. Nous aurons fait danser Jupiter et, sans être breton pour un sou, je suis fier de notre belle galette. Merci à Raphaël pour ces falaises, au bout d'une corde coincée dans la Pierra Menta ou en chantant sous la Meije, pour ces moments de vie, pour l'inspiration, pour ton soutien. Merci aux étoiles filantes qui n'ont pas souhaité s'encorder. Merci à mes parents et à Simon de m'avoir assuré dans la dernière longueur. Merci Kaya pour le soutien, la joie, l'espoir. Danse, toujours.

石の上にも三年

« Trois ans sur une pierre »

Merci également à l'ensemble de ma famille, à mes amis, à mes colocataires d'avoir enduré et compris les humeurs variées et la raréfaction des liens sociaux sans pour autant avoir arrêté de m'encourager.

En ces temps d'urgence, en mal de temporalité et de repères, il fait bon admirer l'édifice construit par la science, imaginer le champ des possibles et savoir que l'on a ajouté sa modeste pierre. Il fait bon se jeter, intrépide, dans ce flot de projets animés par la passion de la recherche. Après avoir remercié de façon égoïste ceux qui m'ont aidé, je finirai en remerciant ceux à qui mon travail servira.

Finalement, c'est ce qui compte.

## Summary

Chapter 1: State of the art .....	11
1 Introduction .....	11
2 Physical agent for cancer therapy.....	12
2.1 Radiotherapy .....	13
2.2 Radiofrequency.....	13
2.3 Cryoablation.....	14
2.4 Laser-induced thermotherapy .....	15
2.5 Microwave ablation .....	15
2.6 Ultrasound .....	15
3 Ultrasonic cavitation in cancer therapy .....	17
3.1 Cavitation .....	17
3.1.1 Generation .....	17
3.1.2 Stable vs. inertial.....	19
3.1.3 Controlling cavitation .....	21
3.2 Bioeffects of cavitation .....	23
4 Cavitation-mediated drug delivery .....	25
4.1 Enhanced drug diffusion.....	26
4.2 Encapsulated drugs.....	28
4.2.1 Liposomes.....	29
4.2.2 Micelles .....	30
4.2.3 Nanodroplets.....	31
4.3 Sonoporation .....	32
4.4 Sonodynamic therapy .....	34
4.5 Unseeded cavitation for chemotherapeutic potentiation.....	38
5 Conclusion.....	40
Chapter 2: Numerical study of a confocal ultrasonic setup for cavitation creation.....	43
1 Introduction .....	43
2 The numerical simulator .....	46
2.1 Comparison with single transducers.....	49
2.1.1 Nonlinear distortion.....	51
2.1.2 Influence of the power level on the peak pressure position.....	52
2.2 Improvements of the confocal configuration.....	54
2.2.1 Bulk reduction.....	54
2.2.2 Prefocal crossing.....	56
3 Radiation forces on bubbles.....	58
4 Discussion .....	61

5	Conclusion.....	63
Chapter 3: Unseeded inertial cavitation for doxorubicin potentiation. Safety study .....		
1	Introduction .....	65
2	Material and methods .....	67
2.1	Ultrasound apparatus .....	67
2.2	Doxorubicin integrity.....	70
2.3	Effect on healthy tissues .....	71
2.4	Metastatic spreading.....	71
3	Results .....	72
3.1	Doxorubicin integrity.....	72
3.2	Effect on healthy tissues .....	73
3.3	Metastatic spreading.....	77
4	Discussion .....	79
5	Conclusion.....	84
Chapter 4: Unseeded inertial cavitation for doxorubicin potentiation. Preclinical study on MDA-MB-231 tumors in mice .....		
1	Introduction .....	85
2	Preclinical efficacy study .....	86
2.1	Materials and methods.....	86
2.1.1	Tumor model.....	86
2.1.2	Study design.....	86
2.2	Results .....	87
2.2.1	Macroscopic and histologic observations.....	87
2.2.2	Efficacy study.....	88
3	Evaluation of doxorubicin uptake in tumors .....	89
3.1	Material and methods .....	90
3.2	Results .....	91
4	Discussion .....	92
Chapter 5: <i>In vitro</i> potentiation of doxorubicin by unseeded controlled stable cavitation .....		
1	Introduction .....	95
2	Methods.....	96
2.1	Reproducible stable cavitation generation.....	96
2.2	<i>In vitro</i> enhanced anti-tumor effect .....	99
2.2.1	Cell line and culture conditions .....	99
2.2.2	Chemicals .....	99
2.2.3	DOX delivery by stable cavitation procedure .....	100
2.2.4	Cell viability and DOX internalization.....	100

2.2.5	Cell counting .....	101
2.3	Mechanistic study .....	101
2.3.1	Analysis of DOX internalization.....	101
2.3.2	Influence of the increase in temperature .....	102
2.3.3	Influence of cavitation .....	102
2.3.4	Effect of reactive oxygen species .....	103
2.3.5	Microscope observations .....	103
3	Results .....	104
3.1	<i>In vitro</i> enhanced anti-tumor effect .....	104
3.1.1	Cell viability.....	104
3.1.2	Cell proliferation .....	105
3.2	Mechanistic study .....	106
3.2.1	Effect of temperature .....	106
3.2.2	Effect of the presence of cavitation.....	108
3.2.3	Effect of reactive oxygen species .....	109
3.2.4	Microscope observations .....	111
4	Discussion .....	112
5	Conclusion.....	115
Chapter 6: Unseeded controlled stable cavitation for potentiation of doxorubicin. Preclinical study on 4T1 tumor in mice .....		117
1	Introduction .....	117
2	Methods.....	117
2.1	Cell culture conditions.....	117
2.2	Use of Animals.....	118
2.2.1	Animals .....	118
2.2.2	Induction of 4T1 tumors in animals.....	118
2.2.3	Euthanasia .....	118
2.2.4	Doxorubicin administration.....	119
2.3	Ultrasound conditions .....	119
2.3.1	Ultrasound apparatus.....	119
2.3.2	<i>Ex vivo</i> parametric study for stable cavitation generation .....	119
2.3.3	<i>In vivo</i> ultrasound exposure.....	120
2.4	Experimental design and treatments.....	121
2.4.1	Treatment schedule.....	121
2.4.2	Clinical monitoring.....	122
2.5	Evaluation of metastatic spreading.....	122
3	Results .....	122
3.1	<i>Ex vivo</i> parametric study for stable cavitation .....	122
3.2	Control of stable cavitation.....	124

3.3	Growth inhibition .....	125
3.4	Survival study .....	126
3.5	Metastatic spreading .....	127
4	Discussion .....	128
5	Conclusion .....	130
Chapter 7: Development of a hydrophone-based method for cavitation localization .....		131
1	Introduction .....	131
2	Material and Methods .....	132
2.1	Ultrasonic apparatus .....	132
2.2	High-speed camera observations .....	133
2.3	Acoustical localization of the cavitation cloud .....	133
3	Results .....	134
4	Discussion .....	136
5	Conclusion .....	137
Conclusion .....		139
References .....		143
List of publications .....		157

# Chapter 1: State of the art

## 1 Introduction

Cancer is recognized as one of the major health issues of this beginning century. Particularly, breast cancer represents the quarter of women cancer<sup>1,2</sup>. Since decades, research has been achieved to analyse cancer mechanisms in order to understand its development and explore treatment strategies. Even if great achievements have been performed, there are still limitations in the treatment of some cancers as well as techniques, which do not provide an optimal compliance for the patient. In the case of breast cancer, the standard procedure is surgical resection. However, this method is strongly invasive. Non-invasive methods provide numerous advantages such as a reduced risk of complications from anaesthesia, shortened recovery time and improved cosmetics<sup>3</sup>. Although this point seems superficial, it is a critical parameter for the psychological well-being and the quality of life of the patients<sup>4</sup>. Also, the common use of chemotherapeutic drugs is still linked with a systemic toxicity. This causes troubles such as cardiotoxicity, nausea, hair loss... Thus, even if the chemotherapy happens to show a reduced efficacy along the treatment, the dose cannot be increased. Unfortunately, studies tend to show that tumor can acquire a resistance to

---

<sup>1</sup> Ferlay et al., "Cancer Incidence and Mortality Patterns in Europe"; Bray et al., "Global Estimates of Cancer Prevalence for 27 Sites in the Adult Population in 2008."

<sup>2</sup> Bray et al., "Global Estimates of Cancer Prevalence for 27 Sites in the Adult Population in 2008."

<sup>3</sup> Fleisher et al., "ACC/AHA 2007 Guidelines on Perioperative Cardiovascular Evaluation and Care for Noncardiac SurgeryA Report of the American College of Cardiology/American Heart Association Task Force on Practice Guidelines (Writing Committee to Revise the 2002 Guidelines on Perioperative Cardiovascular Evaluation for Noncardiac Surgery) Developed in Collaboration With the American Society of Echocardiography, American Society of Nuclear Cardiology, Heart Rhythm Society, Society of Cardiovascular Anesthesiologists, Society for Cardiovascular Angiography and Interventions, Society for Vascular Medicine and Biology, and Society for Vascular Surgery."

<sup>4</sup> Al-Ghazal, Fallowfield, and Blamey, "Comparison of Psychological Aspects and Patient Satisfaction Following Breast Conserving Surgery, Simple Mastectomy and Breast Reconstruction."



chemotherapy. This puts the patient and the therapist into a dead-end. Of course, the surgery option is extensively used, showing good results and survival rates. Besides being obviously invasive, this method can be associated with incomplete excision risks as well as potential metastatic spreading.

In order to overcome some efficacy limitations or to increase patient compliance, physical agents came to be used. These can be applied alone with an ablative purpose or in combination to other treatment strategies. Particularly, as an extra-corporeally applicable and non-ionizing agent, ultrasound (US) shows a high compliance. Moreover, it presents a thermal/mechanical effects duality. Thus, it is possible to act on different mechanisms by tuning the US parameters. This therefore provides a wide range of applications. US can be used alone to destroy the tumor cells by thermal or mechanical effect. These applications are respectively known as high intensity focused ultrasound (HIFU) thermal ablation and histotripsy. While the former relies on long US shots to induce a high temperature raise in the tumor area, the latter is based on short pulses with very high pressure. This triggers cavitation, defined as the creation of oscillating gas bubbles inside a media. These created bubbles can oscillate with mild acoustic solicitation (stable cavitation) or be led to collapse if stronger acoustic pressures are applied (inertial cavitation). As these phenomena are strongly nonlinear, their quantifying and monitoring represent a challenge. However, once properly triggered and controlled, these can induce several interesting features. US exposures can act directly on the tumor vasculature to enhance material extravasation. Also, the violent stress induced by cavitation can be used to release drug from capsules that could be brought to the tumor zone by enhanced permeability and retention (EPR) effect of specific targeting. Also, there is evidence that collapsing bubbles can induce pores in the cellular membranes, which enhances the uptake of therapeutic material. This effect is known as sonoporation. These two last strategies (encapsulated drug release and sonoporation) rely on the same purpose: increasing the availability of the therapeutic material to the cell. However, another strategy consists in using US as a stress inducer, which acts synergistically with the chemotherapeutic agent. This strategy is known as sonodynamic therapy.

## 2 Physical agent for cancer therapy

The first tumor cell appears after a cascade of genetic mutations. Succeeding to escape from the immune system, this cell becomes immortal. Then, as it replicates, it gives birth to a small tumor which continues to grow. Eventually, it spreads in secondary locations by the mean of the blood vessels. For a long time,

treatments were composed of surgery or systemic cytotoxic agents. Depending on the drug used, chemotherapy can induce heart failure, blood clots, premature menopause or the emergence of a secondary cancer such as leukaemia. At the beginning of the 2000's, targeted treatments came to be developed. With these agents, signalling pathways responsible for the tumor development can be blocked. It is the case of the Tarveca® for lung and pancreatic cancers or Glivec® for some kinds of leukaemia. However, different pathways can be used by the tumor cells to continue their replication. This phenomenon known as therapeutic escape is responsible for the lack of efficacy of the treatment after a certain time. To overcome this limitation, treatment strategies were explored. These are combining conventional solutions (surgery, chemotherapy) with a physical agent. The role of the physical agent can be local such as destroying tumor cells, increasing their drug uptake or releasing the content of some drug carriers... Also, it can induce a systemic effect by stimulating the immune response. In the following paragraphs, some physical agents are presented. In their light and after explaining the mechanisms of ultrasound, its place amongst the other physical agents is analysed.

## 2.1 Radiotherapy

Radiation therapy – radiotherapy – uses high energy x-rays to kill or prevent the replication of cancer cells. Two types of procedures can be performed. The external procedure is performed from outside the body whereas the internal procedure use a radioactive substance inoculated in the tumor zone by needles, wires, seeds or catheters. As an example, in the specific case of breast cancer, external radiation is performed on the primary tumor. Internal radiation therapy with the strontium-89 radionuclide is used on bones metastasis that was spread by the primary breast tumor<sup>5</sup>. Although not common, radiation therapy is known to induce undesirable effects. Still in the case of breast cancer, radiation therapy can induce lung inflammation (especially in combination with chemotherapy) and arm lymphedema (after surgical lymph node dissection). Also, radiation therapy in a breast increases the risk of developing a cancer in the other breast.

## 2.2 Radiofrequency

Numerous studies are exploring radiofrequency ablation (RFA) as a way to efficiently ablate breast tumors in a minimally invasive fashion. RFA is based on a

---

<sup>5</sup> PDQ Adult Treatment Editorial Board, “Breast Cancer Treatment (PDQ®).”

radiofrequency electrode used to heat and coagulate the targeted tissue<sup>6</sup>. However, minor complications associated to this technique - such as skin burns and mass formation at the electrode site (secondary to fat necrosis) - were reported. Major complications such as tract seeding, cardiac arrest, pulmonary embolism or pneumothorax were reported in 2.2 % of the cases for treatments in the liver<sup>7</sup>. In the specific case of breast cancer, a phase II multicentre clinical study demonstrated the ability for radiofrequency to induce a total ablation of breast tumor in 76% of the cases<sup>8</sup>. In a more recent meta-analysis study, it was shown an 89% total resection achievement<sup>9</sup>. Although no major complication due to RFA was reported, a few complications related with the procedure occurred. Skin burns were reported in 4% of the cases. The proportion of patients who rated their cosmetic result as excellent was 77%.

### 2.3 Cryoablation

Another option to conventional surgery is cryoablation<sup>10</sup>. It consists in freeze-thaw cycles at very low temperatures (in the range of -160°C). These extremes conditions are applied by a cryoprobe of size under 2 mm, inserted in or close to the tumor zone. A noticeable advantage of this technique is the lack of pain<sup>11</sup> and the procedure can be performed with local anaesthesia only. The best indication for breast cancer cryoablation is with solitary invasive tumors smaller than 15 mm in diameter. The posterior wall has to be visible by ultrasound imaging as this will be used to monitor the treatment (the frozen-unfrozen tissue interface is echogenic). The need for small unifocal tumors is one of the major limitations of this technique. However, there are evidences that cryotherapy could be followed by an enhanced immune response<sup>12</sup>. Even if the patient compliance is better with

---

<sup>6</sup> Goldberg, Gazelle, and Mueller, "Thermal Ablation Therapy for Focal Malignancy."

<sup>7</sup> Livraghi et al., "Treatment of Focal Liver Tumors with Percutaneous Radio-Frequency Ablation."

<sup>8</sup> Medina-Franco et al., "Radiofrequency Ablation of Invasive Breast Carcinomas."

<sup>9</sup> Chen et al., "A Meta-Analysis of Clinical Trials Assessing the Effect of Radiofrequency Ablation for Breast Cancer."

<sup>10</sup> Tarkowski and Rzaca, "Cryosurgery in the Treatment of Women with Breast Cancer—a Review."

<sup>11</sup> Niu, Zhou, and Xu, "Cryosurgery of Breast Cancer."

<sup>12</sup> Sabel et al., "Immunologic Response to Cryoablation of Breast Cancer."

cryoablation than it is for surgery or radiofrequency, it is still an invasive method requiring a probe insertion toward the tumoral zone.

## 2.4 Laser-induced thermotherapy

Laser-induced thermotherapy (LITT) is a technique using a neodymium-yttrium aluminium laser (Nd:YAG) or more recently laser diodes to induce thermal coagulation in the tumor zone. The fibre can be inserted through a needle. It can be performed under local anaesthesia with low morbidity. To achieve LITT, a temperature of 60°C has to be reached. The average duration of the procedure for breast tumor is 30 minutes<sup>13</sup>. Under ultrasound monitoring, LITT resulted in only 50% (7) of complete ablation<sup>14</sup>. Also, some complications such as skin burn and a pneumothorax were reported.

## 2.5 Microwave ablation

Microwave ablation (MWA) consists of a probe directly inserted in the tumor area. This probe is used as an antenna to deliver electromagnetic waves in the microwave range, usually 900-2500 MHz. By forcing water molecules to align their dipoles with the oscillating magnetic field, the tissue is heated<sup>15</sup>. This method is supposed to be more reliable than RFA because it does not involve the passage of a current in the tissues. Thus, the treatment is not sensitive on the tissue conductivity heterogeneities. Moreover, it provides the possibility to treat a larger volume. Whereas the centre of the treated zone undergoes necrosis, the sub-lethally treated zones result in the conditioning of dendritic-cells. It is suggested that this would enhance the tumor-free survival by boosting the immune response<sup>16</sup>.

## 2.6 Ultrasound

Ultrasound (US) can be defined as the periodical repetition of compression-rarefaction cycles of a medium at a frequency over 20 kHz. This being said, its fundamental nature is undeniably mechanical. Ultrasounds cannot be propagated in air but because of their strong attenuation in gaseous media. Thus, most of their

---

<sup>13</sup> Fornage and Hwang, "Current Status of Imaging-Guided Percutaneous Ablation of Breast Cancer."

<sup>14</sup> Van Esser et al., "Ultrasound-Guided Laser-Induced Thermal Therapy for Small Palpable Invasive Breast Carcinomas."

<sup>15</sup> Chu and Dupuy, "Thermal Ablation of Tumors."

<sup>16</sup> Ibid.

related applications happen to be in fluids or solids. When an ultrasonic wave encounters an interface with a media having different acoustic impedance, some of the energy is transmitted to this media. However, the over part is reflected. This gave birth to the first application of ultrasound (for military purposes) with the sonar, at the beginning of the 20<sup>th</sup> century. This principle was then transferred for medical imaging in the late 30's. Ultrasound thus became a way to observe non-invasively biological structures (ultrasonography). As it is real-time observations, it can be used to observe the structure but also the movement, like the flow in blood vessels. Sonography has a wide safety record as the technique is non-invasive and non-ionizing. Moreover, the used acoustic intensities are relatively low. Thus, ultrasonography is generally considered safer than other imaging techniques (X-rays notably) by care providers. One of the great advantages of ultrasonic waves is that they can propagate deeper in tissues than electromagnetic waves. This permits the development of non-invasive ultrasound exposures, even for deep targets. However, it is undeniable that as a physical agent, it has the potential to induce dose-dependent bioeffects. To this day, even if almost completely accepted, the Food and Drug Administration (FDA) still consider that long term effects of ultrasound imaging remain unknown<sup>17</sup>. Ultrasound bioeffects are generally divided in mechanical and thermal effects. These will be further detailed later in this chapter. While these effects are considered as side effects for imaging purposes, they can be sought. Indeed, increasing the acoustic intensities, mechanical and/or thermal effects on tissues can be magnified to induce therapeutic effects. A wide range of strategies can be achieved depending on the therapeutic application. High-pressure shock waves can crumble kidney stones. High temperature elevations can induce necrosis of tissues, which can ablate tumors. It is reported that HIFU provides results comparable to RFA for adenocarcinoma ablation, but being non-invasive<sup>18</sup> and providing a potential specific tumor immunity<sup>19</sup>. Cavitation can provide skims to deliver more efficiently therapeutic material in various targets such as brain, eyes or tumors. A large number of tumor sites are currently being targeted. Notably, the efficacy of the existing treatments can be very limited and could benefit from US-mediated potentiation (glioblastoma, sarcomas, pancreatic tumors). Since a

---

<sup>17</sup> FDA, "Guidance for Industry and FDA Staff Information for Manufacturers Seeking Marketing Clearance of Diagnostic Ultrasound Systems and Transducers."

<sup>18</sup> Nishikawa and Osaki, "Comparison of High-Intensity Focused Ultrasound Therapy and Radiofrequency Ablation for Recurrent Hepatocellular Carcinoma."

<sup>19</sup> Huang et al., "M-HIFU Inhibits Tumor Growth, Suppresses STAT3 Activity and Enhances Tumor Specific Immunity in a Transplant Tumor Model of Prostate Cancer."

couple of decades, the thermal effect of US has been brought to clinic by the work on prostate cancer<sup>20</sup>. In addition, the mechanical effects can be used in tumor treatment. Mechanical effects mostly consist in radiation force and cavitation. The present PhD thesis is oriented on this latter particular phenomenon.

### 3 Ultrasonic cavitation in cancer therapy

Acoustic cavitation can be defined as the creation of a bubble in a media and its oscillatory motion. A bubble would be created if the fluid is under a tension stress sufficient to create a rupture in it. This phenomenon can potentiate a chemotherapy-based treatment in several ways. It also presents the challenge to be hard to generate in absence of cavitation nuclei such as ultrasound contrast agents (UCA). Firstly, a large rarefaction pressure, in the range of several MPa has to be generated. Moreover, the created cavitation cloud has to be stable in space and time. Finally, cavitation is a strong mechanical effect, which requires assessments of safety before *in vivo* application.

#### 3.1 Cavitation

##### 3.1.1 Generation

An acoustic wave periodically imposes to the fluid two successive phases: positive and negative pressure (also called rarefaction pressure). Let us consider that a null pressure would be void. Then the negative pressure would be when one creates an emptier void. Actually, as pressure is defined as a force pushing on a surface, the negative pressure can be seen as a force pulling on a surface. It appears now that there is a possibility to create a rupture in the fluid by pulling it with the negative part of an acoustic wave. From that theoretical point of view, in a perfect fluid, creating cavitation with an acoustic wave would be impossible. However, things are not perfect. Indeed, even in cautiously filtered and degassed water, some impurities or gas presence will lower locally the rupture threshold of the fluid. Once created, the now-formed bubble grows by rectified diffusion: there is gas exchange between the bubble and the surrounding media. However, when the bubble is decompressed (high radius), the surface exchange is higher than when the bubble is under pressure (low radius). Thus, the bubble absorbs more gas than it gives back to the surrounding media.

---

<sup>20</sup> Chapelon et al., "Prostate Focused Ultrasound Therapy."

Acoustic parameters having an influence on cavitation initiation have been investigated<sup>21</sup>. Unsurprisingly, beside the ultrasound frequency, the rarefaction pressure plays a preponderant role on the nature of cavitation activity. However, a large number of parameters can interact. Increasing the ultrasound frequency will induce the increase of the rarefaction pressure threshold as well as a decrease of the mean bubble size. It has been shown that cavitation threshold varies linearly with the frequency. While using pulsed US regimen, the pulse repetition frequency (PRF) and the pulse length will also affect the cavitation events. Indeed, in pulsed regimen, cavitation can be favoured by a memory effect: cavitation bubbles remaining from a former pulse acts as cavitation nuclei for the next pulse<sup>22</sup>. Obviously, lowering the PRF will decrease this memory effect and will be deleterious for the cavitation activity. Contrarily, an increase in the pulse length will make easier the cavitation initiation. However, as said before, this will also increase the thermal effects. Once formed, the bubbles then grow and oscillate with the incident acoustic wave (stable cavitation). This regimen is characterized by the emission of a sub-harmonic frequency (half of the excitation frequency). Eventually, at higher pressures, bubbles collapse violently. This regimen of cavitation is called inertial and is associated with the emission of broadband noise. Depending on the sought effect, US parameters can be tuned in different manners. Firstly, the duty cycle (DC) can be reduced in order to limit the time averaged acoustic intensity and thus reduce the temperature elevations. Hyperthermia-based applications could thus benefit of high duty cycles. Contrarily, if cavitation is sought, low DC permits to avoid heating in some extent thus reducing the risk of adverse bio-effects.

For biomedical applications, the nature of the tissue can differ in many points considering the wide range of applications (elasticity, perfusion, geometric distortion of the US beams, etc.). Thus, a general pressure threshold cannot be given. However, for typical therapeutic applications, with US frequency in the range of the MHz, it is considered that the threshold is in the 100 kPa – 1 MPa range in presence of nucleation agents<sup>23</sup>. In unseeded media (absence of

---

<sup>21</sup> Holland and Apfel, "Thresholds for Transient Cavitation Produced by Pulsed Ultrasound in a Controlled Nuclei Environment."

<sup>22</sup> Leighton, *The Acoustic Bubble*.

<sup>23</sup> Holland and Apfel, "Thresholds for Transient Cavitation Produced by Pulsed Ultrasound in a Controlled Nuclei Environment."

intentional cavitation nucleation agents such as UCA), acoustic cavitation requires pressures generally above 10 MPa to occur<sup>24,25</sup>.

### 3.1.2 Stable vs. inertial

Two cavitation regimens can be in existence: stable and inertial. Each one possesses characteristic features. They both induce a wide range of physical effects. The implications of these physical effects on bioeffects and the way that they could be monitored will be detailed later in parts 3.1.3 and 3.2, respectively.

#### ***Stable cavitation***

For moderate acoustic intensities, bubbles oscillate nonlinearly according to the constraint. The liquid-gas exchange surface is larger at the end of the extension phase than at the end of the compression one. Thus, there is a net gas influx over expansion/compression cycles. Known as rectified diffusion, this phenomenon induces the growth of the bubble. Such gentle regimen is termed stable cavitation. Due to its nonlinear oscillation, the stably oscillating bubble is emitting sub- and ultra-harmonics<sup>26</sup>. Figure 1.1 presents the typical frequency content of a cavitation event involving a population of bubble in stable oscillation. This acoustic feature permits to identify the stable cavitation regimen and even to establish a relation with induced bioeffects<sup>27,28</sup>. There are various phenomena associated with stable cavitation. Firstly, oscillations create a liquid flow around the bubble: the microstreaming. If a cell is present in the vicinity of an oscillating bubble, this former will undergo shear stress. Even if very dependent upon the ultrasound parameters and media properties, the induced shear stress was calculated to be approximately in the 10-1100 Pa range<sup>29</sup>.

---

<sup>24</sup> Lafon et al., "Feasibility Study of Cavitation-Induced Liposomal Doxorubicin Release in an AT2 Dunning Rat Tumor Model."

<sup>25</sup> Lafond et al., "Unseeded Inertial Cavitation for Enhancing the Delivery of Chemotherapies," January 1, 2016.

<sup>26</sup> Everbach et al., "Correlation of Ultrasound-Induced Hemolysis with Cavitation Detector Output in Vitro."

<sup>27</sup> Morton et al., "Subharmonic Emission as an Indicator of Ultrasonically-Induced Biological Damage."

<sup>28</sup> Arvanitis et al., "Controlled Ultrasound-Induced Blood-Brain Barrier Disruption Using Passive Acoustic Emissions Monitoring."

<sup>29</sup> Wu, "Theoretical Study on Shear Stress Generated by Microstreaming Surrounding Contrast Agents Attached to Living Cells."



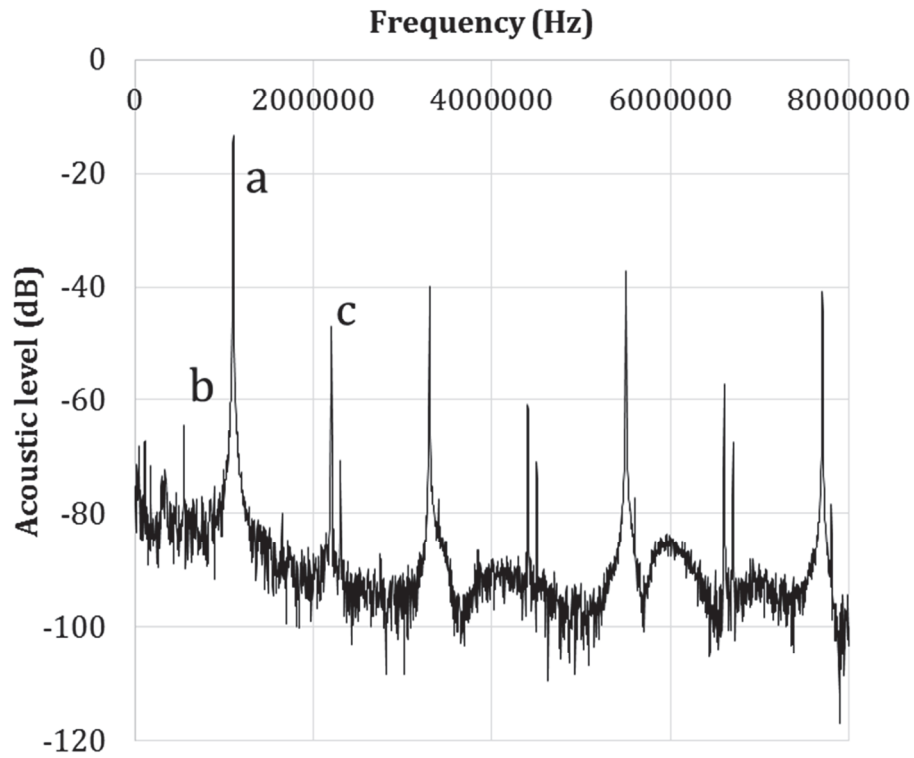


Figure 1.1: For illustration purpose: frequency content of a cavitation event. a) Emission frequency. b) Sub-harmonic at half the emission frequency. c) Ultra-harmonic created both by the stable cavitation and the nonlinear propagation of the excitation ultrasound beam.

### ***Inertial cavitation***

Eventually, at higher pressures, bubbles collapse violently. This regimen of cavitation is called inertial and is associated with the emission of a broadband noise. Inertial cavitation creates an extreme environment. During the collapse, the high velocity of the bubble wall produces a spherically divergent shock wave in the surrounding liquid. Temperatures inside a collapsing bubble can reach thousands of Kelvins<sup>30</sup>. Also, if the bubble happens to collapse with asymmetrical boundary conditions (in the vicinity of a cell for example), it can result in the emission of a microjet. This jet is directed toward the nearby surface with a very high velocity.

---

<sup>30</sup> Leighton, *The Acoustic Bubble*.

Finally, free radicals are created<sup>31</sup>. This can have some implications in quantifying the inertial cavitation activity<sup>32</sup>. Also, the associated bioeffects can result in therapeutic applications such as sonodynamic therapy.

Also, cavitation can result in sonoluminescence (SL): the production of light due to ultrasound-related mechanisms. Precise mechanisms by which light is produced remain uncertain. Several hypotheses were suggested including blackbody radiation, bremsstrahlung radiation, recombination radiation or a combination of these<sup>33</sup>. Although it is generally considered that SL derives from inertial cavitation events, evidences are supporting that stable cavitation can also result in SL<sup>34,35</sup>.

### 3.1.3 Controlling cavitation

There are important differences between the US parameters that can be used to achieve cavitation. Thus, it is difficult to draw conclusions on ideal US parameters. However, this suggests that the important parameter to be adjusted is not the settings itself but the underlying mechanisms such as the amount of stable or inertial cavitation. *In situ*, different factors such as the blood perfusion or tissue heterogeneity can alter the reproducibility of the sought mechanism. Ideally, the monitoring of ultrasound-induced effects such as cavitation or temperature measurement should prevail over direct measurable ultrasound parameters (pressure, intensity...). Thus, the acoustic parameters could be dynamically adjusted using control loops in order to maintain stable and reproducible mechanisms and induced bioeffects. As seen in section 3.1.2, both stable and inertial cavitation can be detected using acoustic features. Such monitoring setup is termed passive cavitation detector (PCD). Stable cavitation is characterized by the emerging sub-harmonic while inertial cavitation induces a rise of the broadband noise. Indexes qualifying stable and inertial cavitation will further be referred as CIs and CI, respectively. Figure 1.2 schematizes the way that

---

<sup>31</sup> Riesz and Kondo, "Free Radical Formation Induced by Ultrasound and Its Biological Implications."

<sup>32</sup> Somaglino et al., "Validation of an Acoustic Cavitation Dose with Hydroxyl Radical Production Generated by Inertial Cavitation in Pulsed Mode."

<sup>33</sup> Byun, Kim, and Kwak, "Sonoluminescence Characteristics from Micron and Submicron Bubbles."

<sup>34</sup> Saksena and Nyborg, "Sonoluminescence from Stable Cavitation."

<sup>35</sup> Gaitan et al., "Sonoluminescence and Bubble Dynamics for a Single, Stable, Cavitation Bubble."

the CI is calculated. It is thus possible to set up control loops in order to adjust the emission intensity with the measured cavitation activity. This was notably achieved for inertial cavitation by Sabraoui et al<sup>36</sup>.

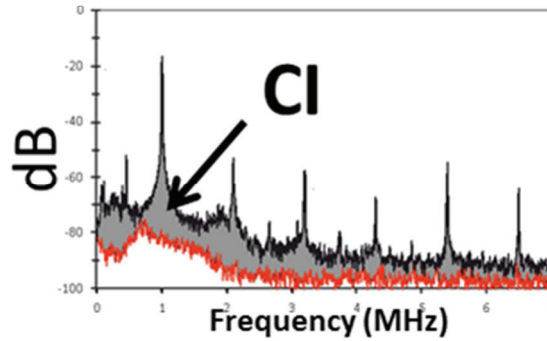


**Figure 1.2: Quantifying the inertial cavitation activity. Frequency content of ambient noise when transducers are not emitting (red) and cavitation noise (black). The difference in intensity between the two curves is the cavitation index (CI), which characterizes the inertial cavitation activity.**

Cavitation has shown to be directly correlated to bioeffects. Morton et al showed that the emission of the sub-harmonic frequency correlated with cellular damage on V79 cells during 1 MHz exposures<sup>37</sup>. With a PCD measuring the broadband noise, Everbach et al showed that adverse bioeffects can be predicted. Indeed, in this study, the CI measured in the sonicated sample correlated with the cell damage induced by hemolysis<sup>38</sup>. More recently, in a different context, Razavi et al demonstrated a cavitation-induced permeabilization of the sclera correlated with his defined CI<sup>39</sup>. Based on these findings, it is relevant to see cavitation as a mean to monitor directly the associated bioeffects in terms of efficacy and/or safety.

For safety concerns, spatial control of cavitation is also an important point. Qualitatively, cavitation cloud can be detected on echo images because of its hyper echo signal. However, using an echo probe, it is also possible to map the cavitation

---

<sup>36</sup> Sabraoui et al., "Feedback Loop Process to Control Acoustic Cavitation."

<sup>37</sup> Morton et al., "Subharmonic Emission as an Indicator of Ultrasonically-Induced Biological Damage."

<sup>38</sup> Everbach et al., "Correlation of Ultrasound-Induced Hemolysis with Cavitation Detector Output in Vitro."

<sup>39</sup> Razavi et al., "Contribution of Inertial Cavitation in the Enhancement of In Vitro Transscleral Drug Delivery."

events by beamforming. This method is known as passive cavitation mapping or passive cavitation imaging. The array-based ultrasound system on receive-only mode is used to measure the cavitation emissions. After beamforming of the signals, a map of cavitation activity can be determined<sup>40</sup>.

### 3.2 Bioeffects of cavitation

Cavitation acts on biological tissues at several levels. On the molecular level, the extreme conditions created by the collapse of bubbles during the inertial regimen induce the formation of reactive oxygen species (ROS)<sup>41</sup>. This creates an oxidative stress for the cells present in the media. Notably, free radicals play an important role in cell membrane permeability<sup>42</sup>. Also, lipid peroxydation caused by the ROS can result in membrane disruption<sup>43</sup>. However, the ROS recombination time is extremely short and mechanical stress induced by cavitation events might prevails over the chemical stress<sup>44</sup>. This suggests a role of ROS specific to low intensities. At the cellular level, there is evidence that the uptake of macromolecular drugs and nanoparticles can be stimulated by stably oscillating bubbles. The two mechanisms involved are the formation of pores<sup>45</sup> and endocytosis<sup>46</sup>. However, mechanical stress impact associated with cavitation varies from slight transient cell deformation to cell lysis. This induced shear stress and the associated surface divergence can result in the stretching and opening of biological structures<sup>47</sup>. The created shear stress can also affect the

---

<sup>40</sup> Gyöngy and Coussios, "Passive Spatial Mapping of Inertial Cavitation during HIFU Exposure."

<sup>41</sup> Riesz and Kondo, "Free Radical Formation Induced by Ultrasound and Its Biological Implications."

<sup>42</sup> Juffermans et al., "Ultrasound and Microbubble-Induced Intra- and Intercellular Bioeffects in Primary Endothelial Cells."

<sup>43</sup> Dhalla, Temsah, and Netticadan, "Role of Oxidative Stress in Cardiovascular Diseases."

<sup>44</sup> Clarke and Hill, "Physical and Chemical Aspects of Ultrasonic Disruption of Cells."

<sup>45</sup> van Wamel et al., "Micromanipulation of Endothelial Cells."

<sup>46</sup> Meijering et al., "Ultrasound and Microbubble-Targeted Delivery of Macromolecules Is Regulated by Induction of Endocytosis and Pore Formation."

<sup>47</sup> Collis et al., "Cavitation Microstreaming and Stress Fields Created by Microbubbles," February 2010.

tissues by disrupting cells<sup>48,49</sup>. Also, radiation force can induce translational movements of microbubbles. Consequently, bubbles are pushed toward cell layers, increasing the cell-bubble interactions<sup>50</sup>. This promotes the delivery of material to the cells<sup>51</sup>. Moreover, compressing bubbles against a cell membrane can result in its disruption. For higher pressures, bubbles can reach their inertial threshold and collapse, inducing a higher stress to cells. Notably, the microjet emitted toward the cells can puncture it, acting as a microsyringe to deliver therapeutic material<sup>52</sup>. However, this threshold depends on the number of acoustic cycles, the PRF and the frequency. The effect on cells of a given parameter set is thus hardly to predict and to generalize for this kind of exposure conditions. It can be found that damage to tissues is very dependent upon the US parameters. When dealing with cavitation, it is more convenient to rely on a cavitation index than on a bench of parameters such as pressure, energy, frequency, which can result in various outputs due to the stochastic nature of cavitation<sup>53</sup>. It has also been shown that US can trigger intracellular biochemical reactions and changes in gene expression<sup>54,55</sup> as well as DNA damage<sup>56,57</sup>. At the tissue level, the structure of the blood vessels can be affected<sup>58</sup>. Histotripsy is a technique that can achieve

---

<sup>48</sup> Wu and Nyborg, "Ultrasound, Cavitation Bubbles and Their Interaction with Cells."

<sup>49</sup> Rooney, "Shear as a Mechanism for Sonically Induced Biological Effects."

<sup>50</sup> Ferrara, "Driving Delivery Vehicles with Ultrasound."

<sup>51</sup> Delalande et al., "Sonoporation at a Low Mechanical Index."

<sup>52</sup> Postema et al., "High-Speed Photography during Ultrasound Illustrates Potential Therapeutic Applications of Microbubbles."

<sup>53</sup> Hallow et al., "Measurement and Correlation of Acoustic Cavitation with Cellular Bioeffects."

<sup>54</sup> Un et al., "Involvement of Activated Transcriptional Process in Efficient Gene Transfection Using Unmodified and Mannose-Modified Bubble Lipoplexes with Ultrasound Exposure."

<sup>55</sup> Yang et al., "Exposure to Low-Intensity Ultrasound Increases Aggrecan Gene Expression in a Rat Femur Fracture Model."

<sup>56</sup> Furusawa et al., "Effects of Therapeutic Ultrasound on the Nucleus and Genomic DNA."

<sup>57</sup> Hassan et al., "Ultrasound-Induced New Cellular Mechanism Involved in Drug Resistance."

<sup>58</sup> Gamarra et al., "High-Energy Shock Waves Induce Blood Flow Reduction in Tumors."

tissue disruption using cavitation<sup>59</sup>. In this last application, US bursts can be very short, but the peak pressures are so high that the cells in the tissue are lysed. Efficient tissue erosion can be efficiently achieved with low time-averaged intensities of 5 W/cm<sup>2</sup> but with peak intensities of 20 kW/cm<sup>2</sup> during short pulses<sup>60</sup>. Distinction has to be made between this mechanical histotripsy based on cavitation and boiling histotripsy, based on thermal effects<sup>61</sup>. This latter happens with lower pressure but longer pulses, for intensities under the range of 1 kW/cm<sup>2</sup>. These techniques are extensively detailed by Maxwell et al<sup>62</sup>.

## 4 Cavitation-mediated drug delivery

Applying ultrasound to enhance delivery of therapeutics can be achieved with four types of strategy. First, cell accessibility can be enhanced by increasing the extravasation of circulating drug in the blood vessels<sup>63</sup> or by overcoming a physiological barrier. The amount of therapeutic agent in a specific area can also be increased by encapsulating the drug in carriers such as liposomes and accumulated in the targeted zone. Second, ultrasound can act as a trigger to damage the carrier, massively releasing their payload in tissues. Third, by the process of sonoporation, US can enhance the penetration of drug into cells. A fourth strategy – termed sonodynamic study – is not a proper enhancement of drug delivery but the synergetic interaction between ultrasound and a chemical agent resulting in a dramatic anti-tumor effect. Although thermal effects and low intensity mechanical effects can be used to achieve some of these delivery strategies, cavitation can be used in each of them<sup>64</sup>.

---

<sup>59</sup> Maxwell et al., “Disintegration of Tissue Using High Intensity Focused Ultrasound.”

<sup>60</sup> Roberts et al., “Pulsed Cavitational Ultrasound.”

<sup>61</sup> Canney et al., “Shock-Induced Heating and Millisecond Boiling in Gels and Tissue Due to High Intensity Focused Ultrasound.”

<sup>62</sup> Maxwell et al., “Disintegration of Tissue Using High Intensity Focused Ultrasound.”

<sup>63</sup> Bohmer et al., “Focused Ultrasound and Microbubbles for Enhanced Extravasation.”

<sup>64</sup> Pitt, Hussein, and Staples, “Ultrasonic Drug Delivery - A General Review.”

#### 4.1 Enhanced drug diffusion

In a tumor environment, the vasculature is very different from that of normal tissues. Tumor vessels show leaky pores and generally lack of lymphatic drainage. This results in a high interstitial fluid pressure (IFP), limiting the transport of material through the interstitium<sup>65</sup>. This high IFP constitutes an important physiological barrier to the delivery of therapeutic material to tumor cells<sup>66</sup>. Also, the high IFP creates an outward force from the tumor core. Thus, even if the retention of therapeutic material can be enhanced in the tumor zone because of the EPR effect, the therapeutic material struggles to diffuse deeply across the vasculature wall. The convectional transport of drugs is reduced. In addition, vessels are forced apart during the tumor growth process, resulting in an increase of the average vessel-cell distance<sup>67</sup>. Thus, to increase the permeability of the vessel walls in the tumor area would constitute an efficient way to enhance the delivery to tumor of blood circulating drugs.

There is evidence that cavitation can be responsible for endothelial disintegration which would allow that increased permeability<sup>68</sup>. Occurring close to vessel walls, cavitation events can result in vascular disruption, vasoconstriction and even shutdown of the vessels<sup>69</sup>. Capillary ruptures can be a consequence of the violent stress inflicted by inertial cavitation<sup>70</sup>. Disruptions can be paracellular (disruption of the tight junctions between the endothelial cells) or transcellular (transcytosis). In the first case<sup>71,72</sup> it results in an increase of

---

<sup>65</sup> Boucher, Baxter, and Jain, "Interstitial Pressure Gradients in Tissue-Isolated and Subcutaneous Tumors."

<sup>66</sup> Jain, "Delivery of Molecular and Cellular Medicine to Solid Tumors."

<sup>67</sup> Minchinton and Tannock, "Drug Penetration in Solid Tumors."

<sup>68</sup> Nixdorff et al., "Dose-Dependent Disintegration of Human Endothelial Monolayers by Contrast Echocardiography."

<sup>69</sup> Goertz, "An Overview of the Influence of Therapeutic Ultrasound Exposures on the Vasculature."

<sup>70</sup> Coussios and Roy, "Applications of Acoustics and Cavitation to Noninvasive Therapy and Drug Delivery."

<sup>71</sup> Bohmer et al., "Focused Ultrasound and Microbubbles for Enhanced Extravasation."

<sup>72</sup> Hu et al., "Insonation of Targeted Microbubbles Produces Regions of Reduced Blood Flow within Tumor Vasculature."

permeability over a duration that depends on the extravasated material size<sup>73</sup>. It has been hypothesized that transcytosis was induced by the vasoconstriction which can occur during the US exposure<sup>74</sup>. In addition, it has been reported that cavitation provides a transient intracellular entrance of calcium and the production of hydrogen peroxide, which facilitate the endocytosis process<sup>75,76</sup>. These effects are modifying the vascular permeability enhancing the extravasation process of the therapeutic material.

As an example, it has been showed that 1 MHz pulsed focused US with 1.2 MPa peak pressure resulted in rupture areas in tumor blood vessels<sup>77</sup>. This increased the vascular permeability and allowed a higher quantity of lipid-coated nanoparticle to deposit in the tumor. This study was performed using ultrasound contrast agents (UCA), which act as cavitation nuclei. Thus, cavitation phenomena can be considered responsible for the benefit on the increased permeability. It should however be noted that mice, which are used in most of the studies presented here, dispose of a very high vasomotor excitability compared to human.

Also, ultrasound has been shown to increase the convectional transport of drug in the interstitium. This is potentially attributable to radiation force. As radiation force consists in a momentum transfer, it induces a transport of the particles in the direction of wave propagation. Eggen et al<sup>78</sup> showed an increased scattering of encapsulated doxorubicin in PC-3 prostate adenocarcinoma in mice. The averaged penetration depth of the material was two-fold the penetration depth without sonication. US parameters consisted in 5% duty cycle pulses at 0.3 or 1 MHz at intensity of 13.35 W/cm<sup>2</sup>. The penetration was higher with the 1MHz frequency, which support the hypothesis of the radiation force being the main mechanism. However, the mechanical index (MI) of 2.2 does not permit to exclude the potential role of cavitation. It should be noted that the improved drug

---

<sup>73</sup> Marty et al., "Dynamic Study of Blood-Brain Barrier Closure after Its Disruption Using Ultrasound."

<sup>74</sup> Sheikov et al., "Cellular Mechanisms of the Blood-Brain Barrier Opening Induced by Ultrasound in Presence of Microbubbles."

<sup>75</sup> De Cock et al., "Ultrasound and Microbubble Mediated Drug Delivery."

<sup>76</sup> Park et al., "Modulation of Intracellular CA<sup>2+</sup> Concentration in Brain Microvascular Endothelial Cells *in vitro* by Acoustic Cavitation."

<sup>77</sup> Lin et al., "Quantitative and Qualitative Investigation into the Impact of Focused Ultrasound with Microbubbles on the Triggered Release of Nanoparticles from Vasculature in Mouse Tumors."

<sup>78</sup> Eggen et al., "Ultrasound Improves the Uptake and Distribution of Liposomal Doxorubicin in Prostate Cancer Xenografts."



diffusion varies within the tumor, notably between superficial and deep zones<sup>79</sup>. This is certainly due to differences in structures and densities. We can therefore hypothesize that this mechanism of drug diffusion enhancement strongly varies with the tumor model.

An original application of the effect of cavitation on vasculature is that it is possible to destroy mechanically the tumor vessels. Combined to the delivery of anti-angiogenic drugs, it is possible to decrease the nutrient supply of the tumor tissue<sup>80</sup>.

## 4.2 Encapsulated drugs

Ultrasound can act as a trigger to damage the carrier, massively diffusing their payload in tissues<sup>81,82,83</sup>. These carriers can be long-circulating liposomes (PEGylated), ligand-targeted liposomes, micelles, nanocups, nanodroplets, etc<sup>84</sup>. They can be loaded with chemotherapeutics drugs, anti-biotics, anaesthetics, genetic material, etc. and thus provide the ability to be transferred to a wide range of applications. Depending on the carrier formulation, the release of the therapeutic agent can be obtained either by mechanical<sup>85</sup> or thermal effect<sup>86,87</sup>. Notably, the shear forces induced by oscillating bubbles can be sufficient to open liposomes and micelles<sup>88</sup>. One of the major advantages of these strategies is that

---

<sup>79</sup> Eggen et al., "Ultrasound-Enhanced Drug Delivery in Prostate Cancer Xenografts by Nanoparticles Stabilizing Microbubbles."

<sup>80</sup> Molema, Meijer, and de Leij, "Tumor Vasculature Targeted Therapies."

<sup>81</sup> Evjen et al., "*In Vivo* Monitoring of Liposomal Release in Tumors Following Ultrasound Stimulation."

<sup>82</sup> Frenkel et al., "Delivery of Liposomal Doxorubicin (Doxil) in a Breast Cancer Tumor Model."

<sup>83</sup> Mestas et al., "Therapeutic Efficacy of the Combination of Doxorubicin-Loaded Liposomes with Inertial Cavitation Generated by Confocal Ultrasound in AT2 Dunning Rat Tumor Model."

<sup>84</sup> Rapoport, "Drug-Loaded Perfluorocarbon Nanodroplets for Ultrasound-Mediated Drug Delivery."

<sup>85</sup> Graham et al., "Ultrasound-Mediated Drug Release from Nanoscale Liposomes Using Nanoscale Cavitation Nuclei."

<sup>86</sup> Lokerse et al., "In Depth Study on Thermosensitive Liposomes."

<sup>87</sup> Novell et al., "Focused Ultrasound Influence on Calcein-Loaded Thermosensitive Stealth Liposomes."

<sup>88</sup> Marmottant and Hilgenfeldt, "Controlled Vesicle Deformation and Lysis by Single Oscillating Bubbles."

using carriers prevents premature and extraneous delivery of the therapeutic material. These promising strategies are extensively being studied<sup>89,90,91</sup>.

#### 4.2.1 Liposomes

Liposomes are spherical bilayered vesicles ranging from 25 nm to 25  $\mu$ m. They consist in an aqueous core and a lipid bilayer membrane<sup>92,93</sup>. Liposomes differ from microbubbles such as ultrasound contrast agents by the nature of their core. Indeed, these formers possess a gaseous core. It is therefore harder to activate liposomes using ultrasound. However, liposomes can be thermosensitive<sup>94,95</sup>. This constitutes an alternative for US, which can induce both mechanical and thermal effects. Notably, Ta et al<sup>96</sup> used Polymer-modified thermosensitive liposomes in rats under MRI guidance. These liposomes are designed to release the carried doxorubicin at 40-42°C temperatures. The induced drug release via ultrasound hyperthermia permitted to decrease significantly the tumor growth of mammary adenocarcinoma. However, non-thermal release may have some advantages. Indeed, non-thermal application makes no longer necessary the control of the local temperature rise, which may represent a safety issue and thus an obstacle toward clinical translation. The drug release using the mechanical effects of ultrasound has been demonstrated<sup>97</sup>. In this study, short pulses (duty cycle DC=1%) were used with high intensity (Spatial Peak, Pulse Average Intensity  $I_{SPPA}$ =10.5 kW/cm<sup>2</sup>) Also, the release can be performed with low-intensity ultrasound. Release was shown with intensities of  $I_{SATA}$ =2.7 W/cm<sup>2</sup> (Spatial Average, Temporal Average, acoustic pressure of p=0.23 MPa at the focus)

---

<sup>89</sup> Mo et al., "Ultrasound-Enhanced Drug Delivery for Cancer."

<sup>90</sup> Hussein, Pitt, and Martins, "Ultrasonically Triggered Drug Delivery."

<sup>91</sup> Ahmed, Martins, and Hussein, "The Use of Ultrasound to Release Chemotherapeutic Drugs from Micelles and Liposomes."

<sup>92</sup> Martins et al., "Lipid-Based Colloidal Carriers for Peptide and Protein Delivery-Liposomes versus Lipid Nanoparticles."

<sup>93</sup> Rawat et al., "Nanocarriers."

<sup>94</sup> Escoffre et al., "Focused Ultrasound Mediated Drug Delivery from Temperature-Sensitive Liposomes."

<sup>95</sup> Ta and Porter, "Thermosensitive Liposomes for Localized Delivery and Triggered Release of Chemotherapy."

<sup>96</sup> Ta et al., "Localized Delivery of Doxorubicin in Vivo from Polymer-Modified Thermosensitive Liposomes with MR-Guided Focused Ultrasound-Mediated Heating."

<sup>97</sup> Evjen et al., "< I> In Vivo</i> Monitoring of Liposomal Release in Tumors Following Ultrasound Stimulation."

in pulsed mode (DC=50%) at 3 MHz<sup>98</sup>. It is possible to monitor the liposome release by encapsulating a paramagnetic agent ( $Mn^{2+}$  or  $Gd^{3+}$  ions based) in the vesicle. Invisible to MRI while still inside the liposomes, they create a contrast when released<sup>99</sup>. This technique was recently used to successfully release doxorubicin and Gadolinium from PEGylated liposomes in a TS/A tumor in mice (murine mammary adenocarcinoma) at low acoustic intensities<sup>100</sup>. The US exposure strategy used was based on a “release” stimulus ( $p=0.28$  MPa,  $I_{SATA}=2.8$  W/cm<sup>2</sup>, 3MHz, DC=50%) and a “sonoporation” stimulus ( $p=0.15$  MPa,  $I_{SATA}=0.78$  W/cm<sup>2</sup>, 1MHz, DC=12%), supposed to increase the vascular permeability. This resulted in very impressive results showing an almost complete regression of the tumor.

#### 4.2.2 Micelles

Micelles are nanosized spherical vesicle (5-30 nm)<sup>101</sup>. They consist in a hydrophobic core surrounded by a hydrophilic corona. Although they provide the ability to extravasate easily due to their small size, polymer micelles present stability issues. Indeed, to be stable in biological fluids, they have to be diluted higher than the critical micellar concentration. However, this concentration of polymers is not tolerated by the body. To solve this issue, copolymers are used in micelles for ultrasound-mediated drug delivery<sup>102,103</sup>. They provide a good structural stability even in blood and other biological fluids and have a long shell life. Moreover, micelles can be targeted by adding antibodies or peptides to their structure<sup>104</sup>. The major limitation of using micelles is that organic molecules and polymers are almost transparent to ultrasound. Thus, the enhanced extravasation of the carrier due to radiation force is hardly beneficial with micelles. Thus,

---

<sup>98</sup> Rizzitelli et al., “In Vivo MRI Visualization of Release from Liposomes Triggered by Local Application of Pulsed Low-Intensity Non-Focused Ultrasound.”

<sup>99</sup> Torres et al., “Improved Paramagnetic Liposomes for MRI Visualization of pH Triggered Release.”

<sup>100</sup> Rizzitelli et al., “The Release of Doxorubicin from Liposomes Monitored by MRI and Triggered by a Combination of US Stimuli Led to a Complete Tumor Regression in a Breast Cancer Mouse Model.”

<sup>101</sup> Pitt, Hussein, and Staples, “Ultrasonic Drug Delivery - A General Review.”

<sup>102</sup> Hussein and Pitt, “Micelles and Nanoparticles for Ultrasonic Drug and Gene Delivery.”

<sup>103</sup> Adams, Lavasanifar, and Kwon, “Amphiphilic Block Copolymers for Drug Delivery.”

<sup>104</sup> Mahmud et al., “Polymeric Micelles for Drug Targeting.”

additional cavitation nuclei such as ultrasound contrast agents are required. As an example, Ugarenko *et al.* showed that low frequency ultrasound (20 kHz, 100 W/cm<sup>2</sup>) resulted in only 7-10% release of doxorubicin carried by Pluronic® micelles<sup>105</sup>. In another study by Staples using encapsulated doxorubicin, DHD/K12/TRb tumor growth was significantly reduced in rats<sup>106</sup>. Two different frequencies were used, 20 kHz and 500 kHz. For both case, the mechanical index MI was 1.22. Surprisingly, the increase of doxorubicin concentration inside the sonicated tumor was very weak. This suggests that the efficacy of ultrasound-micelles combination may not be attributed solely to the drug release from the carrier.

#### 4.2.3 Nanodroplets

During the last decade, breakthrough in nanotechnology and nanomedicine permitted the elaboration of nanosized drug carriers. An application of this technology is the delivery of drug to tumors via nanodroplets, activated by focused ultrasound. Perfluorocarbon (PFC) nanodroplets are made by performing an emulsion of water, surfactant and perfluorocarbon. Other kinds of nanoemulsions have been explored such as perfluoropentane (PFP)<sup>107</sup> and polymer-coated perfluorooctyl bromide (PFOB)<sup>108</sup>. It was shown that these nanodroplets provide the ability to change phase under ultrasound exposure. Moreover, this vaporization process can be induced in diagnostic configuration (7.5 MHz, MI<1). Decafluorobutan (DFB) was also used for its high volatility (boiling point of -2°C). These are very stable in physiological environment and can be activated within the FDA guidelines US parameters<sup>109</sup>. The principal interest of these nanodroplets is that they can convert into microbubbles when exposed to ultrasound (vaporization). They can thus be considered as cavitation nuclei for

---

<sup>105</sup> Ugarenko et al., "Development of Pluronic Micelle-Encapsulated Doxorubicin and Formaldehyde-Releasing Prodrugs for Localized Anticancer Chemotherapy."

<sup>106</sup> Staples, "Pharmacokinetics of Ultrasonically-Released, Micelle-Encapsulated Doxorubicin in the Rat Model and Its Effect on Tumor Growth."

<sup>107</sup> Kripfgans et al., "Acoustic Droplet Vaporization for Therapeutic and Diagnostic Applications."

<sup>108</sup> Reznik, Williams, and Burns, "Investigation of Vaporized Submicron Perfluorocarbon Droplets as an Ultrasound Contrast Agent."

<sup>109</sup> Matsunaga et al., "Phase-Change Nanoparticles Using Highly Volatile Perfluorocarbons."

non-thermal US-based therapy<sup>110</sup>. However, considering the large difference between the droplet size (<6 nm)<sup>111</sup> and the US wavelength, these former are almost transparent to US. Thus the precise mechanism of vaporization is still unclear. It is however suggested that it is the high frequencies induced by the nonlinear beam propagation that interact with the droplet. Satisfying preclinical results have been achieved. Notably, the Rapoport group demonstrated a therapeutic effect of paclitaxel-loaded PFP combined with 1-3 MHz US on breast and pancreatic tumors in mice<sup>112</sup>. An increasing number of promising results is reported<sup>113</sup>. However, much preclinical work and a further comprehension of vaporization mechanisms have to be carried out. Notably, experiments on large animal are lacking. Especially, passive targeting of the nanodroplets in the tumor area is more challenging with large animals because of the lower tumor-body volume ratio.

### 4.3 Sonoporation

Sonoporation is defined as the ability to create transient openings in vessels walls and cellular membranes. As said before, the tumor microenvironment induces several barriers for drug delivery (increased interstitial fluid pressure, limited interstitial transport, increased distance between the tumor cells and the blood vessels). The combination of microbubbles with ultrasound already demonstrated an improvement in the tumor sensitivity to the associated therapeutic material<sup>114</sup>. It is assumed that the mechanistic process is cavitation, both stable and inertial, creating pores on nearby cells, vessels and favouring the drug transport. Moreover, the distance from the vessels reached through the interstitium by the drug is increased<sup>115</sup>. The precise mechanisms responsible for sonoporation are still unclear. Indeed, both microstreaming, jetting, stable and inertial cavitation can play a role. Moreover, two scenarios are susceptible to

---

<sup>110</sup> Rapoport, "Drug-Loaded Perfluorocarbon Nanodroplets for Ultrasound-Mediated Drug Delivery."

<sup>111</sup> Kripfgans et al., "Acoustic Droplet Vaporization for Temporal and Spatial Control of Tissue Occlusion."

<sup>112</sup> Rapoport et al., "Controlled and Targeted Tumor Chemotherapy by Ultrasound-Activated Nanoemulsions/microbubbles."

<sup>113</sup> Rapoport, "Drug-Loaded Perfluorocarbon Nanodroplets for Ultrasound-Mediated Drug Delivery."

<sup>114</sup> Qin, Wang, and Willmann, "Sonoporation."

<sup>115</sup> Eggen et al., "Ultrasound Improves the Uptake and Distribution of Liposomal Doxorubicin in Prostate Cancer Xenografts."

occur: the formation of pores and endocytosis. The formation of crater on cell membranes has been widely reported in the literature<sup>116,117</sup>. Observations at the single cell level evidenced that a direct interaction between the bubble and the cells was required to permit sonoporation<sup>118</sup>. Also, the pore formation correlates with the amplitude of the bubble oscillation. Yet, a large number of parameters can influence the sonoporation process, notably pressure, exposure time and pulse repetition frequency<sup>119</sup>. However, for a given parameter set, sonoporation rate increases as the acoustic pressure increases as well<sup>120</sup>.

Pore sizes can vary in a very large extend. It was reported variations between 1nm and 4.3µm depending on the acoustic pressure (respectively for 190 and 480 kPa, in presence of encapsulated microbubbles)<sup>121</sup>. However, for pressure of 480 kPa, it is suggested that the holes sizes reached a threshold from which the self-sealing mechanism does not operate. It is highly possible that this conducts to the non-reparable sonoporation (sonolysis) of the cell<sup>122</sup>. It is considered that small and large pores are associated to stable and inertial cavitation, respectively<sup>123</sup>. The time of opening of pores has been evaluated. Observation revealed that pores close globally within a short time (from a few seconds to a few minutes) after the US exposure<sup>124,125</sup>. In a recent study<sup>126</sup>, interactions between a single bubble and a single cell of radii of 1.25 and 8.4 µm respectively were studied. Acoustic pressure was 0.12 MPa and the frequency 0.834 MHz. It was shown that the membrane retracted back from signs of rupture in just 38 milliseconds. In this context, it is

---

<sup>116</sup> Zhao et al., "Phospholipids-Based Microbubbles Sonoporation Pore Size and Reseal of Cell Membrane Cultured in Vitro."

<sup>117</sup> Zhou et al., "The Size of Sonoporation Pores on the Cell Membrane."

<sup>118</sup> Van Wamel et al., "Vibrating Microbubbles Poking Individual Cells."

<sup>119</sup> Qiu et al., "The Correlation between Acoustic Cavitation and Sonoporation Involved in Ultrasound-Mediated DNA Transfection with Polyethylenimine (PEI) in Vitro."

<sup>120</sup> Deng et al., "Ultrasound-Induced Cell Membrane Porosity."

<sup>121</sup> Yang et al., "Experimental Study on Cell Self-Sealing during Sonoporation."

<sup>122</sup> Ward, Wu, and Chiu, "Ultrasound-Induced Cell Lysis and Sonoporation Enhanced by Contrast Agents."

<sup>123</sup> Lentacker et al., "Understanding Ultrasound Induced Sonoporation."

<sup>124</sup> Yudina, Lepetit-Coiffé, and Moonen, "Evaluation of the Temporal Window for Drug Delivery Following Ultrasound-Mediated Membrane Permeability Enhancement."

<sup>125</sup> Fan et al., "Spatiotemporally Controlled Single Cell Sonoporation."

<sup>126</sup> Nejad et al., "Reparable Cell Sonoporation in Suspension."

thus particularly important to apply ultrasound when the distribution of the therapeutic material is maximal in the target zone.

#### 4.4 Sonodynamic therapy

Sonodynamic therapy (SDT) consists in the synergetic interaction between ultrasound and a chemical agent. More specifically, SDT refers to sensitizer-dependent sonochemical or sonophotochemical events in an acoustic field leading to cytotoxicity (*Figure 1.3*). This technique, pioneered among others by Umemura and Yumita from 1989<sup>127,128</sup> derives from photodynamic therapy (PDT). PDT is based on photosensitizers and a light source to trigger their cytotoxicity. In both SDT and PDT, the sensitizers alone are considered as relatively non-toxic. This adds a level of control on the treatment. Indeed, the chemical agents will become cytotoxic only after the US stimulus, in the targeted zone. It should be noted that due to its ability to be focused and in depth, SDT provides much more accuracy than PDT.

Originally used in PDT, current sonosensitizers can be of various kinds. Porphyrin-based molecules are proven to produce ROS when exposed to ultrasound. Notably, Photofrin® is a clinically approved hematoporphyrin derivative used in PDT. Xanthene dyes also demonstrated the ability to generate ROS once US-stimulated<sup>129</sup>. However, because of their high and rapid capture by the liver, these agents are contraindicated *in vivo*. Taking advantage of the fact that the uptake of amphiphilic agents by tumors is better, new sonosensitizers were developed. Amphiphilic preparations of rose bengal are realized using alkylation and carboxylation<sup>130</sup>. The resulting drug is known as rose bengal derivative. The variety of sonosensitizers that have been studied is relatively wide as well as the variety of US parameters that can be used. The huge majority of sonosensitizers responds to ultrasound within the 0.4-3 MHz frequency range. This range is particularly convenient for therapeutic applications because of the good ratio propagation depth and accuracy. The reported intensities are generally ranged from 0.5 to 10 W/cm<sup>2</sup>. An up-to-date selection of studies including various

---

<sup>127</sup> Umemura et al., "Mechanism of Cell Damage by Ultrasound in Combination with Hematoporphyrin."

<sup>128</sup> Yumita et al., "Hematoporphyrin as a Sensitizer of Cell-Damaging Effect of Ultrasound."

<sup>129</sup> Umemura et al., "Sonodynamically Induced Effect of Rose Bengal on Isolated Sarcoma 180 Cells."

<sup>130</sup> Sugita et al., "Synthesis of Amphiphilic Derivatives of Rose Bengal and Their Tumor Accumulation."



sonosensitizers, US parameters and the eventual production of ROS can be found in the literature<sup>131</sup>. *Figure 1.3* presents schematically how US is used to interact with sonosensitizers in the context of SDT.

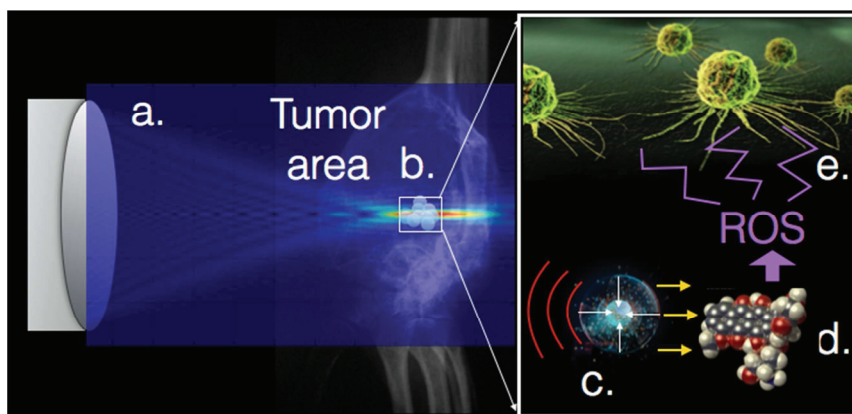


**Figure 1.3: Principle of sonodynamic therapy by ROS creation. a.** The ultrasound transducer emits a focused beam, which can reach high pressure levels inside the tumor area. **b.** The high pressure triggers the phenomenon of cavitation: oscillating bubbles in the medium. **c.** Bubbles undergoing high pressure levels reach the collapse regimen. **d.** Collapsing bubbles interact with sonosensitizers, leading to the creation of radical oxygen species (ROS). **e.** The ROS induce a stress on cancer cells leading to their apoptosis (cell suicide).

A wide range of sonosensitizers as well as numerous US setups was investigated. Also, there are several mechanisms that can be considered as potential activator of the sonodynamic effect. As describe, there is an obvious role of the ROS production. However, the way that US interact with the sensitizers can be multiple.

- Direct generation of ROS: Cavitation regimens induce extreme conditions, permitting sonochemical reactions. The role in cytotoxicity of the formation of oxygen singlet, shown in pioneering work<sup>132</sup>, is debated<sup>133</sup>. It is suggested that bubble collapsing near a sonosensitizer can induce the formation of ROS derived from this sensitizer<sup>134</sup>. It is clear from the

<sup>131</sup> McHale et al., "Sonodynamic Therapy."

<sup>132</sup> Umemura et al., "Mechanism of Cell Damage by Ultrasound in Combination with Hematoporphyrin."

<sup>133</sup> Miyoshi, Igarashi, and Riesz, "Evidence against Singlet Oxygen Formation by Sonolysis of Aqueous Oxygen-Saturated Solutions of Hematoporphyrin and Rose Bengal."

<sup>134</sup> MIŠÍK and Riesz, "Free Radical Intermediates in Sonodynamic Therapy."



literature that the generated ROS because of US exposure depends on the nature of the sensitizer.

- Sonoluminescence: Although the precise mechanism of sonoluminescence remains unclear, its role in SDT has been suggested since early reports<sup>135</sup>. Indeed, as most of the sonosensitizers are also used PDT, it is quite straightforward to hypothesize that the light from SL will activate their photosensitivity. This hypothesis is relevant as SL can be detected *in vivo*<sup>136</sup>.
- Destabilization of cells membranes: It has been observed that hematoporphyrin-sensitized cells were sensitive to US at intensities, which do not induce inertial cavitation<sup>137</sup>. It should however be noted that stable cavitation could have generated SL. In this context, the mechanical disruption of membranes of cells sensitized with rhodamine derivative was investigated<sup>138</sup>. This study suggests the interaction of a hydrophobic entity with a cell membrane, resulting in a hypersensitivity to ultrasound. Moreover, it has been suggested that sonoactivated hematoporphyrin induce the membrane peroxydation, resulting in a reduced membrane fluidity that destabilize the cell<sup>139,140</sup>.

It is clear from the wide variety of phenomena that a given sonosensitizers results in effects that may vary upon the US parameters. Efficacy of SDT has been proven *in vitro*. A wide range of US parameters and sonosensitizers have been combined on various cell lines<sup>141,142</sup>. Further analyses showed that SDT induced cell death by apoptosis. This limits inflammation and immune response, contrarily to necrotic cell death. *In vivo*, ultrasound has to be applied when an optimal

---

<sup>135</sup> Umemura et al., "Mechanism of Cell Damage by Ultrasound in Combination with Hematoporphyrin."

<sup>136</sup> He et al., "In Vivo Sonoluminescence Imaging with the Assistance of FCLA."

<sup>137</sup> Hiraoka et al., "Comparison between Sonodynamic Effect and Photodynamic Effect with Photosensitizers on Free Radical Formation and Cell Killing."

<sup>138</sup> Feril et al., "Apoptosis Induced by the Sonomechanical Effects of Low Intensity Pulsed Ultrasound in a Human Leukemia Cell Line."

<sup>139</sup> Tang et al., "Membrane Fluidity Altering and Enzyme Inactivating in Sarcoma 180 Cells Post the Exposure to Sonoactivated Hematoporphyrin in Vitro."

<sup>140</sup> Yumita and Umemura, "Sonodynamic Antitumor Effect of Chloroaluminum Phthalocyanine Tetrasulfonate on Murine Solid Tumor."

<sup>141</sup> McHale et al., "Sonodynamic Therapy."

<sup>142</sup> Hachimine et al., "Sonodynamic Therapy of Cancer Using a Novel Porphyrin Derivative, DCPH-P-Na(I), Which Is Devoid of Photosensitivity."

quantity of sensitizers in located in the target area. Yumita *et al* applied ultrasound at 2 MHz, 3 W/cm<sup>2</sup> on colon adenocarcinoma in mice, 24 hours after injection of ATX-70 (Gallium-porphyrin sensitizer). At this interval, ATX-70 was present in the tumor during sonication. Results were impressive as tumor size dropped to half the initial size in just 3 days. However, tumor restarted to grow 5-7 days after treatment<sup>143</sup>. The same group performed the same experiment, this time on mammary tumors in rats<sup>144</sup>. In this particular study, the SDT treatment was efficient and no re-growth of the tumors was observed. This illustrates that treatment efficacy depends also on tumor models. Wang *et al* also demonstrated an impressive efficacy of SDT using SF1 sensitizer (porphyrin-based) to treat S-180 sarcoma in mice<sup>145</sup>. US was applied at 1.1 W/cm<sup>2</sup> at 1 MHz frequency. This resulted in a net tumor inhibition as well as inflammation around the target site. Yet, no increased immune response has been demonstrated.

Most of the known sonosensitizers accumulate preferentially in tumor zones. However, residual quantities are still present in other tissues. This was an important challenge for PDT because of the resulting hypersensitivity to light. Of course, as a lot of sensitizers used in PDT and SDT are the same, SDT might result as well in hypersensitivity to light. Thus, SDT may benefit from new targeted drug delivery strategies in order to permit the tumor-specific delivery of sonosensitizers. As an example, issues relatives to rose bengal can be avoided by using microbubbles as sonosensitizers carriers<sup>146</sup>. Also, it has been demonstrated that 20-200 nm particles can accumulate in tumors due to the enhanced retention and permeability (EPR) effect. Thus, conjugation of sonosensitizers with such particles permits to deliver important payloads in the tumor zone<sup>147</sup>.

Sonodynamic therapy accumulated a collection of impressive results on numerous tumor targets and using different sensitizers since 1990's. It is based on relatively non-toxic agents. Moreover it benefits from the records of a similar

---

<sup>143</sup> Yumita et al., "Sonodynamically Induced Antitumor Effect of a Gallium-Porphyrin Complex, ATX-70."

<sup>144</sup> Yumita et al., "Sonodynamic Therapy on Chemically Induced Mammary Tumor."

<sup>145</sup> Wang, Lewis, and Mitchell, "The Tumoricidal Effect of Sonodynamic Therapy (SDT) on S-180 Sarcoma in Mice."

<sup>146</sup> Nomikou et al., "Microbubble-sonosensitizer Conjugates as Therapeutics in Sonodynamic Therapy."

<sup>147</sup> Sazgarnia et al., "A Novel Nanosonosensitizer for Sonodynamic Therapy in Vivo Study on a Colon Tumor Model."

technique: photodynamic therapy. It is therefore at odds that no clinical trial is ongoing to transfer this technology to clinics.

#### 4.5 Unseeded cavitation for chemotherapeutic potentiation

In most of the studies already presented, either cavitation was enhanced by adding cavitation nuclei such as UCA, or carriers bring the drug to the tumor area. Cavitation can also be generated in tissues without adding any nucleation agents. This provides a higher versatility compared to UCA injection as cavitation could be created everywhere and not only in tissues reached by vasculature or closed to the penetration of UCA. In addition, it was demonstrated that controlled unseeded cavitation could be achieved with a coefficient of variation of less than 0.4% while fixed acoustic intensity and UCA led to 22% of variation. Also, unseeded controlled cavitation permits to generate cavitation over a long time while UCA-based cavitation events end up rapidly with the destruction of all the nuclei<sup>148</sup>. It has been proposed a particular setup based on two US transducers matching their respective foci for this purpose (Figure 1.4). Although the mechanisms were not fully understood, it has been shown a great stability of the cavitation cloud using this configuration.

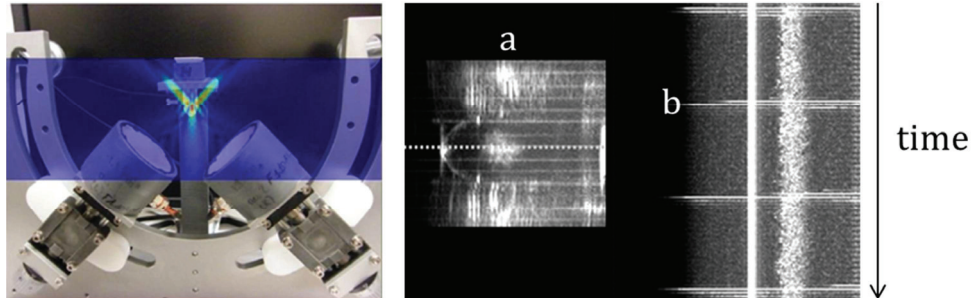


**Figure 1.4: Left: For illustration purpose. Acoustic pressure field produced by a setup composed of two confocal transducers. Right: a) echo imaging of cavitation in an Eppendorf tube. b) Stability of the cavitation cloud over time. The dotted line from a) is displayed along time**

Preliminary experiments as well as other studies evidenced that therapeutic material could be efficiently delivered in tumors. *In vitro*, it was shown that cavitation could enhance the penetration of genetic material inside cells

---

<sup>148</sup> Desjouy et al., "Counterbalancing the Use of Ultrasound Contrast Agents by a Cavitation-Regulated System."

(transfection) even in the absence of cavitation nuclei<sup>149</sup>. Figure 1.5 presents images of cancer cells that were exposed to inertial cavitation. In the absence of ultrasound, the penetration of genes inside these cells was impossible. Fluorescence images witnesses of the penetration of these genes due to the exposure to inertial cavitation. Also, experiments performed on chondrosarcoma in rats permitted to show an increase diffusion of Gadolinium after exposure to an inertial cavitation regimen. Indeed, Figure 1.6 shows that after the US exposure, the intensity of the image (correlated with the uptaken dose of gadolinium) increases in the tumor tissues. The ability to generate controlled activity of cavitation inducing an enhanced material diffusion inside tumors as well as penetration inside cells provide to unseeded cavitation potential for enhancing chemotherapeutic material.

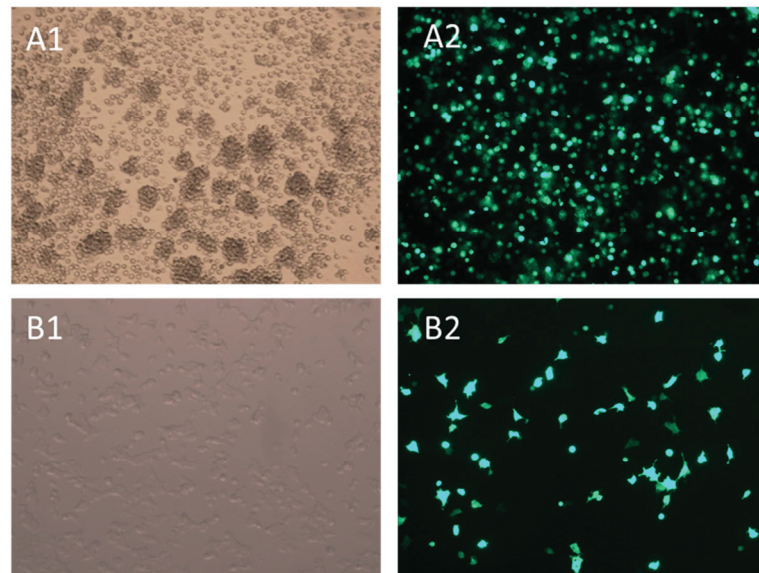


**Figure 1.5: Inertial cavitation permitted to transfect different cancer cell lines which are totally impermeable to the used genetic material without applying ultrasound. A1/2: RL in natural-light/fluorescence microscopy. B1/2: 293-T in natural-light/fluorescence microscopy.**

---

<sup>149</sup> Chettab et al., "Spatial and Temporal Control of Cavitation Allows High In Vitro Transfection Efficiency in the Absence of Transfection Reagents or Contrast Agents."

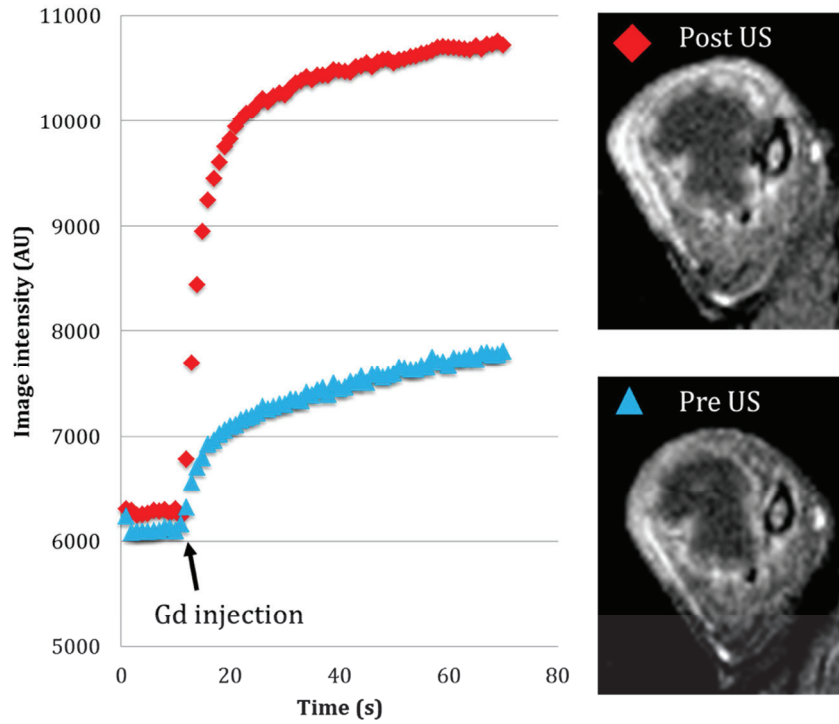


**Figure 1.6: The amount of gadolinium penetrating inside the tumor increases after exposure to inertial cavitation.**

## 5 Conclusion

As seen in this chapter, the classic anticancer treatments find benefits in their conjugation with some physical agents. Amongst these physical agents, ultrasounds provide interesting features. Indeed, they can be applied non-invasively in an extra-corporeal way. Their ability to be focused enables to reach high intensity levels in deep tissue without harming intervening layers. Moreover, different physical mechanisms can be solicited depending on the US parameters. Continuous waves and high duty cycle pulsed modes will favour thermal effects whereas high pressure short pulses will favour the occurrence of cavitation. This last effect was shown to induce various bioeffects, which can promote the efficacy of anticancer treatments (enhanced extravasation, sonoporation, synergetic interactions...). Considering the phenomena of cavitation and temperature elevation, we can consider ultrasound as a non-invasive surgical tool. Moreover, with proper monitoring, ultrasonic techniques provide the possibility to control directly the bioeffects, beneficial and adverse. Compared to other strategies currently applied for cancer treatment, this feature is a considerable advantage.

Most of the studies presented here combine ultrasound to microbubbles to facilitate the occurrence of cavitation. However, nucleation agents of drug carriers mainly remain in the tumor vasculature, preventing cavitation to occur inside the tumor, close to the tumor cells. Thus, the choice was made to orient the present work on unseeded cavitation for enhancement of chemotherapeutic treatments. To do so, work has to be done on multiple aspects: efficient cavitation generation, safety assessments, and mechanistic study on potential efficacy on chemotherapy potentiation. A particular ultrasonic configuration based on confocal transducers is used. Through simulations and experiments, we investigate the features that permit to enhance the cavitation activity. Moreover, the developed simulator provides the possibility to optimize parameters for cavitation generation. The effect on inertial cavitation activity of the interference pattern created by the crossing of the two beams was then studied experimentally. Preliminary results showed an increase of material diffusion in tumors after inertial cavitation exposure. However, strong damages induced on tissues highlight the need to develop safe exposure conditions. In a first place, the assessed safety points are potential damages on healthy surrounding tissues, chemical stability of the therapeutic material and the absence of metastatic spreading due to ultrasound exposures. With considered safe US exposure parameters, a preclinical study was designed in order to attempt to potentiate chemotherapeutic agents with cavitation. These studies aimed at potentiating doxorubicin on MDA-MB-231 breast tumor in mice. *In vitro* experiments showed that stable cavitation could create a strong synergetic effect with doxorubicin, contrarily to inertial cavitation that only resulted only in cells death. After developing a control loop strategy to generate stable cavitation in a reproducible way, a mechanistic study was performed to investigate the synergetic effect between stable cavitation and doxorubicin on 4T1 tumor cells. A preclinical study was designed to evaluate the synergy between stable cavitation and doxorubicin on 4T1 tumors in mice. This study aimed also at evaluating the reproducibility of stable cavitation generation *in vivo* as well as the metastatic spreading with this different cavitation regimen. The *in vivo* study permitted to evidence the need for cavitation to be precisely located, notably to discriminate cavitation events from the actual target from cavitation at the surface of the skin. The possibility to employ a three hydrophones-based source localization technique was explored. Cavitation clouds located with this technique were compared to high-speed camera observations.





## Chapter 2: Numerical study of a confocal ultrasonic setup for cavitation creation

### 1 Introduction

In the field of ultrasound and particularly in medical applications, high intensity focused ultrasound (HIFU) is of both research and clinical interest<sup>150,151</sup>. HIFU presents many advantages for therapeutic applications, such as the capability to create high acoustic pressures deep within tissue, thus allowing focused treatment at a site of interest. These pressures result in effects such as tissue heating due to absorption, radiation force and cavitation. Ultrasound tissue heating has been used in a variety of clinical applications such as tissue ablation, and physical therapy for a variety of sports injuries<sup>152,153</sup>. With sufficient pressure, HIFU can result in cavitation: the creation, oscillation, and implosion of bubbles in the fluid due to the acoustic field. Cavitation has been used for targeted drug delivery<sup>154,155,156,157</sup>, as well as a non-thermal destruction techniques such as histotripsy for tissues<sup>158,159,160,161</sup> and lithotripsy for kidney stones<sup>162,163,164</sup>.

---

<sup>150</sup> Bailey et al., "Physical Mechanisms of the Therapeutic Effect of Ultrasound (a Review)."

<sup>151</sup> Pichardo et al., "New Integrated Imaging High Intensity Focused Ultrasound Probe for Transrectal Prostate Cancer Treatment."

<sup>152</sup> Diederich, "Thermal Ablation and High-Temperature Thermal Therapy."

<sup>153</sup> Gelet et al., "Transrectal High-Intensity Focused Ultrasound."

<sup>154</sup> Koch et al., "Ultrasound Enhancement of Liposome-Mediated Cell Transfection Is Caused by Cavitation Effects."

<sup>155</sup> Lafon et al., "Feasibility Study of Cavitation-Induced Liposomal Doxorubicin Release in an AT2 Dunning Rat Tumor Model."

<sup>156</sup> Mestas et al., "In-vitro and in-vivo siRNA transfection by an ultrasonic confocal device."

<sup>157</sup> Schroeder, Kost, and Barenholz, "Ultrasound, Liposomes, and Drug Delivery."

<sup>158</sup> Maxwell et al., "Noninvasive Thrombolysis Using Pulsed Ultrasound Cavitation Therapy-histotripsy."

<sup>159</sup> Roberts et al., "Pulsed Cavitational Ultrasound."

<sup>160</sup> Wang et al., "An Efficient Treatment Strategy for Histotripsy by Removing Cavitation Memory."

<sup>161</sup> Xu et al., "High Speed Imaging of Bubble Clouds Generated in Pulsed Ultrasound Cavitational Therapy-Histotripsy."



Confocal acoustic apparatus have been used for cavitation purpose notably by Ciuti *et al.* whom added a secondary low frequency field to enhance cavitation activity<sup>165,166</sup>. Chen *et al.*<sup>167</sup> also used confocal ultrasound to trap bubbles and determine focal sizes of HIFU transducers. Also, confocal ultrasound has been used by Mestas *et al.* in a drug delivery context<sup>168</sup>. In this particular study, two confocal spherical transducers are arranged so that their respective focal points are superimposed, with a 90° angle between the acoustic axes. It is shown that inertial cavitation is obtained in an efficient and reproducible manner. Crossing the two beams creates an interference pattern in the focal area with nodes and antinodes. Early studies have already shown that the confocal configuration provides a better spatial control of the cavitation cloud and an increase of cavitation activity<sup>169</sup>. Thus, this configuration seems well adapted for cavitation applications.

In the present work we study the acoustic features provided by a confocal configuration. Particularly, we focus on the features that are relevant for cavitation applications. As peak negative pressure is a crucial parameter in its generation<sup>170</sup>, the following work focuses on the resultant pressure fields and peak negative pressures from a confocal device. Also, depending of the application, spatial accuracy could be a prominent feature. In addition to investigating the properties of a confocal system, a numerical approach also allows comparison with a single transducer with parameter variation which

---

<sup>162</sup> Chaussy, Chaussy, and others, *Extracorporeal Shock Wave Lithotripsy*.

<sup>163</sup> Nguyen et al., "Optimization of Extracorporeal Shock Wave Lithotripsy Delivery Rates Achieves Excellent Outcomes for Ureteral Stones."

<sup>164</sup> Ponchon et al., "Gallstone Disappearance after Extracorporeal Lithotripsy and Oral Bile Acid Dissolution."

<sup>165</sup> Ciuti et al., "Cavitation Activity Stimulation by Low Frequency Field Pulses."

<sup>166</sup> Iernetti et al., "Enhancement of High-Frequency Acoustic Cavitation Effects by a Low-Frequency Stimulation."

<sup>167</sup> Chen et al., "A Novel Method for Estimating the Focal Size of Two Confocal High-Intensity Focused Ultrasound Transducers."

<sup>168</sup> Mestas et al., "Therapeutic Efficacy of the Combination of Doxorubicin-Loaded Liposomes with Inertial Cavitation Generated by Confocal Ultrasound in AT2 Dunning Rat Tumor Model."

<sup>169</sup> Moussatov et al., "Stabilisation of Cavitation Zone for Therapeutic Applications."

<sup>170</sup> Holland and Apfel, "Thresholds for Transient Cavitation Produced by Pulsed Ultrasound in a Controlled Nuclei Environment."

would be impractical in an empirical study. Also, it has been shown that the maximum pressure is not localized at the very geometrical focal point but rather closer toward the transducer. The distance between the geometrical focus and the actual acoustic focus is inversely proportional to the focusing gain of the transducer. Moreover, the acoustic focus is slightly changed with the considered nonlinear regimen<sup>171</sup>. Indeed, strong nonlinear effect will also shift the peak negative toward the transducer<sup>172</sup>. Thus, the developed simulator will be used to compare both the geometrically confocal alignment and the acoustically confocal alignment. The Khokhlov-Zabolotskaya-Kuznetsov (KZK) equation<sup>173,174</sup> is often used to model the acoustic fields of ultrasonic device at high intensities. This equation describes the acoustic propagation while accounting for nonlinearity, thermo-viscous absorption, and diffraction. The KZK equation is appropriate for modelling single transducers but, as the opening angle values for confocal device are significant, this equation is no longer valid. To model wider propagation angles, the Westervelt equation has to be used<sup>175</sup>.

After describing the numerical scheme used in this study, the simulator, termed CFcode, is tested by a comparison with measurements. Features of the confocal configuration are therefore investigated both numerically and experimentally. The nonlinear distortion induced by the single transducer configuration and the confocal configuration is investigated numerically to show the potential benefits of using the confocal configuration for cavitation generation. Finally, the calculation of the radiation forces exerted of scatterers such as bubbles is implemented. The radiation force fields are compared in both the confocal and single transducer cases.

---

<sup>171</sup> Camarena et al., "Nonlinear Focal Shift beyond the Geometrical Focus in Moderately Focused Acoustic Beams."

<sup>172</sup> Bessonova et al., "FOCUSING OF HIGH POWER ULTRASOUND BEAMS AND LIMITING VALUES OF SHOCK WAVE PARAMETERS."

<sup>173</sup> Kuznetsov, "Equations of Nonlinear Acoustics."

<sup>174</sup> Zabolotskaya and Khokhlov, "Quasi-Plane Waves in the Nonlinear Acoustics of Confined Beams."

<sup>175</sup> Westervelt, "Parametric Acoustic Array."

## 2 The numerical simulator

### 2.1 Basic equations

The Khokhlov-Zabolotskaya-Kuznetsov (KZK) equation (Kuznetsov, 1971; Zabolotskaya and Khokhlov, 1969) is often used to model the acoustic fields of ultrasonic device at high intensities. This equation describes the acoustic propagation while accounting for nonlinearity, thermo-viscous absorption, and diffraction. The KZK equation is appropriate for modelling single transducers but, as the opening angle values for confocal device are significant, this equation is no longer valid. To model wider propagation angles, the Westervelt equation (1) has to be used (Westervelt, 1963).

$$\frac{\partial^2 p}{\partial z \partial \tau} = \frac{c_0}{2} \Delta p + \alpha \frac{\partial^3 p}{\partial \tau^3} + \frac{\beta}{2\rho_0 c_0^3} \frac{\partial^2 p^2}{\partial \tau^2} \quad (1)$$

Here,  $\Delta$  is the Laplacian,  $p$  the acoustic pressure,  $z$  the distance along the acoustic axis,  $\tau = t - z/c_0$  the retarded time. Water was chosen as the simulated acoustic medium, with the sound velocity in the medium defined as  $c_0 = 1500 \text{ m/s}$ , density defined as  $\rho_0 = 1000 \text{ kg/m}^3$ . The nonlinearity parameter is defined as  $\beta = 3.5$ . The parameter  $\alpha = 2.2 \cdot 10^{-3} \text{ Np/m/MHz}^2$  is the absorption coefficient of sound in water at a standard ambient temperature (Culjat et al., 2010). The most commonly used method for the numerical resolution of this equation is the operator splitting method (Tavakkoli et al., 1998). This method consists in splitting the Westervelt equation into three elementary equations: one for each physical effect. Then, each operator is applied sequentially in the frequency domain and stepwise along the main propagation direction ( $z$  in our case).

The coupled system Eq. (2) (Yuldashev and Khokhlova, 2011) is used to solve for nonlinear effects.

$$\frac{\partial p_n}{\partial z} = \frac{in\beta\omega}{\rho_0 c_0^3} \left( \sum_{k=1}^{N_{\max}-n} p_k p_{n+k}^* + \frac{1}{2} \sum_{k=1}^{n-1} p_k p_{n-k} \right) \quad (2)$$

In Eq. (2),  $N_{\max}$  is the maximum number of frequency components (harmonics) taken into account,  $\omega$  is the angular frequency of the source and  $n$  is the index of the frequency component being calculated.  $p^*$  denotes the complex conjugate of the pressure. The initial value of  $N_{\max}$  is 3 and is increased by steps of 10 if the  $N_{\max}-1$  amplitude reaches 50 Pa. This value was chosen so that the result

converges without adding unnecessary harmonics. For the absorption, Eq. (3) is applied for each frequency component  $n$ .

$$p_n(z + \Delta z) = p_n(z) \exp(-\Delta z \alpha \omega_n^b) \quad (3)$$

The exponent ( $b$ ) on the angular frequency  $\omega$  depends on the nature of the medium: proportional law for biological tissues ( $b=1$ ), quadratic law for thermo-viscous losses ( $b=2$ ). Arbitrary law could also be used ( $1 < b < 2$ ).

Diffraction is solved using the angular spectrum method (Christopher and Parker, 1991; Varslot and Taraldsen, 2005; Williams, 1999). This method consists in calculating the spatial Fourier transform of the pressure field (termed 2DFT) in a plane perpendicular to the propagation direction, then multiplying it by a phase factor which represents the propagation. An inverse spatial Fourier transform (I2DFT) is then calculated from this data, generating a new, adjusted pressure field. Thus, the following relation is applied for calculating the pressure in the plane  $z+\Delta z$  from that in the plane  $z$ :

$$p_n(x, y, z + \Delta z) = I2DFT[H_W \times 2DFT[p_n(x, y, z)]] \quad (4)$$

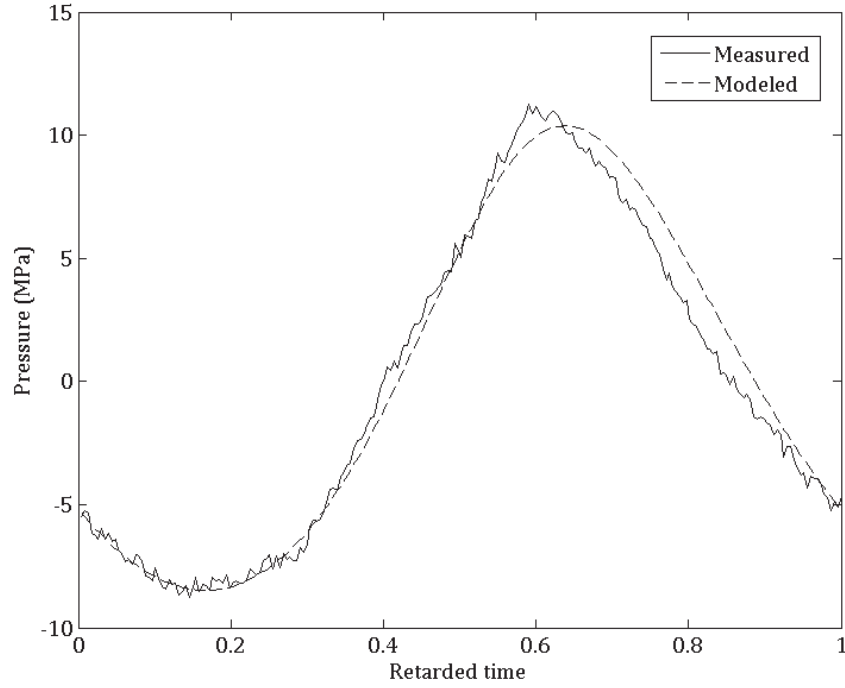
Here,  $H_W(k_x, k_y) = e^{i\Delta z(\sqrt{k_n^2 - k_x^2 - k_y^2} - k_n)}$  is the phase factor corresponding to the elementary equation for diffraction). The variables  $k_x$  and  $k_y$  denote the wavenumbers over the plane in the wavenumber domain and  $k_n$  is the wavenumber of the  $n$ -th harmonic:  $k_n = n\omega/c_0$  with  $\omega$  the angular frequency of the fundamental component. The relation (4) is applied for each frequency component. As a validation, in addition to comparison to KZKTexas code for the single transducer with and without angle (data not shown), the waveform simulated for the confocal case is compared to experiment. There is a strong drawback for simulations of confocal configuration which is the considerably reduced symmetry against a single transducer. In the single transducer case, the axial symmetry reduces considerably the calculation time. With the confocal configuration, the only symmetry that can be applied is the division in four quarters. Although the difference in a case of a single transducer varies from the order of the minute with KZKTexas2 code to one hour with the CFcode, all the simulations for single transducers were performed with the four quarters symmetry only.

## 2.2 Experimental setup

The experimental setup consists of two 1.1 MHz transducers with a diameter of 50 mm and a focal distance of 50 mm, placed with  $90^\circ$  separation angle. The acoustic axes of the transducers are crossing at 50 mm. For clarity purpose, this device configuration is hereafter referred to as CF90. The acoustic axis of the confocal head is defined as the bisector between the acoustic axes of the two transducers crossing at the geometric focus. The CF90 device was placed in a tank filled with degassed water to avoid cavitation. 110-cycle pulses were generated by a Tektronix AFG3022B (Tektronix, Beaverton, OR) pulse generator with a pulse repetition frequency of 100 Hz and amplified with a 400W RF power amplifier 1040LA (E&I, Rochester, NY). An instantaneous acoustic power of 109 W (based on known transducer efficacies and wattmeter measurement) was applied to the transducers. This corresponded to a calculated pressure of 0.279 MPa on the transducer surface. Acoustic pressure measurements were performed with a calibrated fiber optic hydrophone FOPH-2000 (RP Acoustics, Leutenbach, Germany). The measured waveforms were de-convolved using the manufacturer's software.

## 2.3 Validation of the simulator

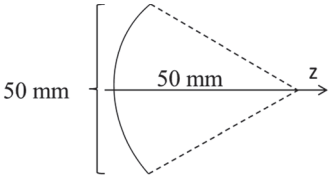
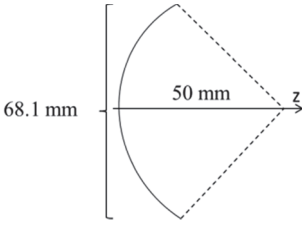
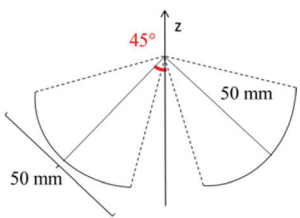
For all simulations with the CFcode, the spatial resolution is 0.1 mm in both lateral directions  $x$  and  $y$ . The distance between two planes (in the  $z$  direction) is also set at 0.1 mm. This resolution provides a good accuracy while maintaining an acceptable computation time (a dozen of minutes for linear simulations to a couple of hours for strong nonlinearities implying approximately 70 harmonics). Figure 2.7 shows a good agreement between the measured and the simulated waveforms for a total acoustic power of 109W (simulation included realistic nonlinear and attenuation parameters for the water). Simulation and measurement differ by 3% and 6% for peak negative and positive pressures, respectively. These differences can be considered slight and are attributed to measurement uncertainties which might come from potential imperfect confocal alignment of the two confocal beams, hydrophone noise and positioning. Overall, we can consider the simulator relatively reliable to model for the CF90 configuration.



**Figure 2.7: Simulated waveform and measurement at the focal point of the CF90 confocal setup. Total acoustic power is 109 W.**

#### 2.4 Comparison with single transducers

To evaluate the benefit of using confocal configuration, the developed simulator was used to compare three configurations: 1) a single spherical transducer with a diameter of 50 mm, focused at 50 mm (termed T1); 2) a single spherical transducer with a doubled surface i.e. with a diameter of 68.1 mm, and focused at 50 mm (termed T2); 3) a confocal configuration composed of two spherical transducers T1 with an angle of  $90^\circ$  between them (termed the CF90). The emission frequency is 1.1 MHz in all cases. For clarity, the Figure 2.2 summarizes the various setups used in this study.

T1	T2	CF90
Diameter $d=50$ mm focal distance $df=50$ mm emission frequency $F=1.1$ MHz	$d=68.1$ mm $df=50$ mm $F=1.1$ MHz	$d=50$ mm $df=50$ mm $F=1.1$ MHz Separation Angle = $90^\circ$
		

**Figure 2.8: Summary of the transducers configurations used in the comparison between confocal and single transducers configurations**

Comparing these configurations in linear mode, it appears that configurations T2 and CF90 induce the same pressure at the acoustic focal point for the same acoustic power while a quadruple power is needed for T1 configuration. Moreover, the shapes of the focal regions of the single and confocal configurations are inherently different. Firstly, the focal volume (defined as the volume in which the pressure is equal or greater than half the peak linear pressure) is 22 mm<sup>3</sup> for T1 and only 8 mm<sup>3</sup> with both the T2 and CF90 configuration. However, the shapes are very different as T2 induces a focal region that is 6 mm in length whereas CF90 induces only a 2 mm long focal region. This provides a better spatial accuracy in the lateral direction to the confocal setup. Secondly, although the single transducers T1 and T2 create a lobe-shaped focal region (see Figure 2.14), the crossing of two beams creates an interference pattern. It is possible that the interferences contribute to trap material (bubbles, cells, liposomes...) in the focal zone. This is investigated in a latter part (Radiation forces on bubbles) of the study.

## 2.5 Nonlinear distortion

All along the propagation axis and for a set of increasing acoustic powers, the pressure waveforms are calculated in linear and nonlinear mode ( $\beta=0$  and  $\beta=3.5$  respectively). For the three configurations (T1, T2 and CF90), figure 2.2 presents the extreme positive and negative pressure peaks reached on this axis in nonlinear mode as a function of the pressure amplitude calculated in linear mode. Nonlinear effects are known to distort the waveform toward a saw-tooth-shaped shape. In association with focusing, the phase shifts, resulting in an asymmetry of the waveform: the negative pressure at the focal point is reduced and the positive pressure is increased. Figure 2.9 presents the peak positive and negative pressures that are reached depending on the pressure obtained at the focus without taking into account the nonlinear effects. This pressure is termed peak linear pressure and its absolute value is equal for positive and negative pressure as the waveform is symmetrical in this case. These results are presented for each type of transducer configuration (T1, T2 and CF90). They differ because of the combined effect of nonlinear distortion and diffraction. Comparing T1 and T2, it appears that doubling the emitting surface reduces the decrease of the peak negative pressure while limiting the increase of the peak positive pressure. Moreover, the comparison between T2 and CF90 shows that splitting the emitting surface in two distinct beams limits further the pulse asymmetry.



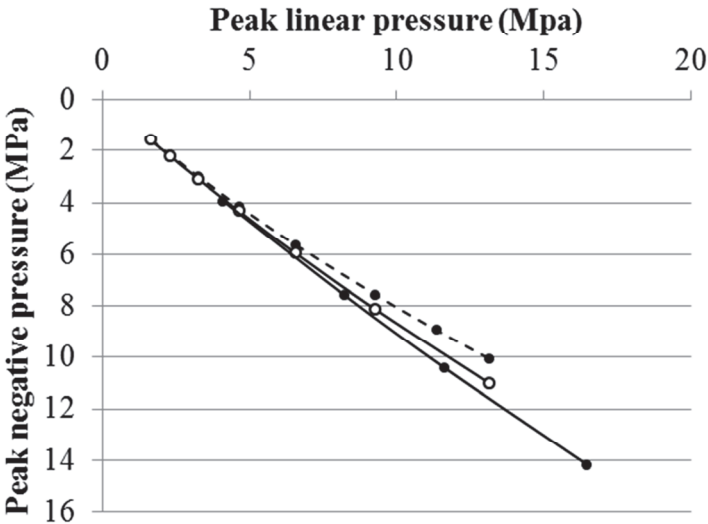


**Figure 2.9: Peak negative pressure (bottom) and peak positive pressure (top) against the peak linear pressure. The decrease of negative pressure and increase of positive pressure are consequences of the asymmetric distortion of the beam. T1 corresponds to the single transducer, T2 is a single transducer with a doubled emission surface and CF90 is the confocal configuration based on two transducers T1 with their acoustic axes tilted of  $45^\circ$  each relatively to the former acoustic axis.**

## 2.6 Peak pressure position

Theoretically, as the power increases, the location of the peak negative pressure tends to move toward the transducer. This phenomenon is well

reproduced by the developed simulator. Indeed, Figure 2.10 shows that with low pressure amplitude (linear regime), the peak negative pressure is located at 49.1 mm from T1 and 49.5 mm from T2. Increasing the power, the position of this peak continues to move toward the transducer. Contrarily, in the confocal case, the position on the peak negative pressure remains almost steady even if the same phenomenon of peak negative pressure shifting occurs for each transducer constituting the confocal configuration. Nevertheless, the spatial sum of the two beams has a preponderant influence. Consequently, the spatial position of the peak pressure is much less influenced by the nonlinear effects in the confocal case.

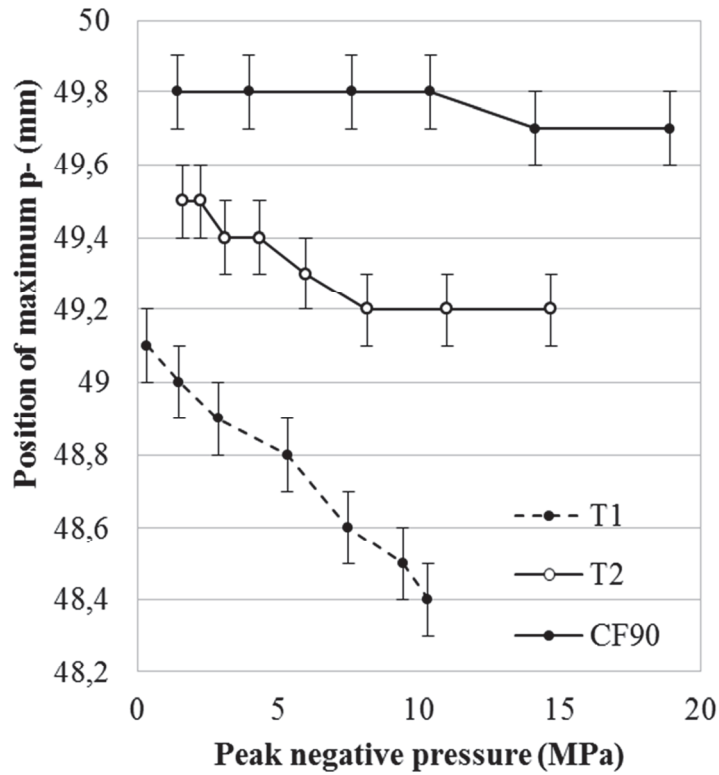


**Figure 2.10: Position of the peak negative pressure depending on its value. As the reached peak negative pressure increases, its location moves toward the transducer in the case of the single transducer. Errors bars represent the 0.1 mm step in the diffraction scheme. This induces a limit in the precision of the estimation of the focal point. With the confocal configuration, the location of the peak negative pressure stands still.**

### 3 Improvements of the confocal configuration

#### 3.1 Size reduction

The confocal configuration used for comparisons with the single transducer setups is based on two transducers angled of  $90^\circ$ . In a practical situation (e.g. in clinical context), one would need to reduce the size of the device for convenience. Thus, decreasing the separation angle provides an efficient manner to reduce this size. However, this may also impact the advantages of the confocal configuration previously demonstrated. To assess the effect of the angle modification, another configuration is modelled based on the same previous configuration but reducing the separation angle to  $70^\circ$ . This configuration is termed CF70-G. The CF90 and CF70-G configurations are compared on the basis of the negative and positive pressure peaks relatively to the linear case, as performed in a previous part. Figure 2.11 shows both the decrease of peak negative pressure and increase of peak positive pressure obtained with both the CF70-G and CF90 setups. The data corresponding to T2 configuration is also displayed as a reference.

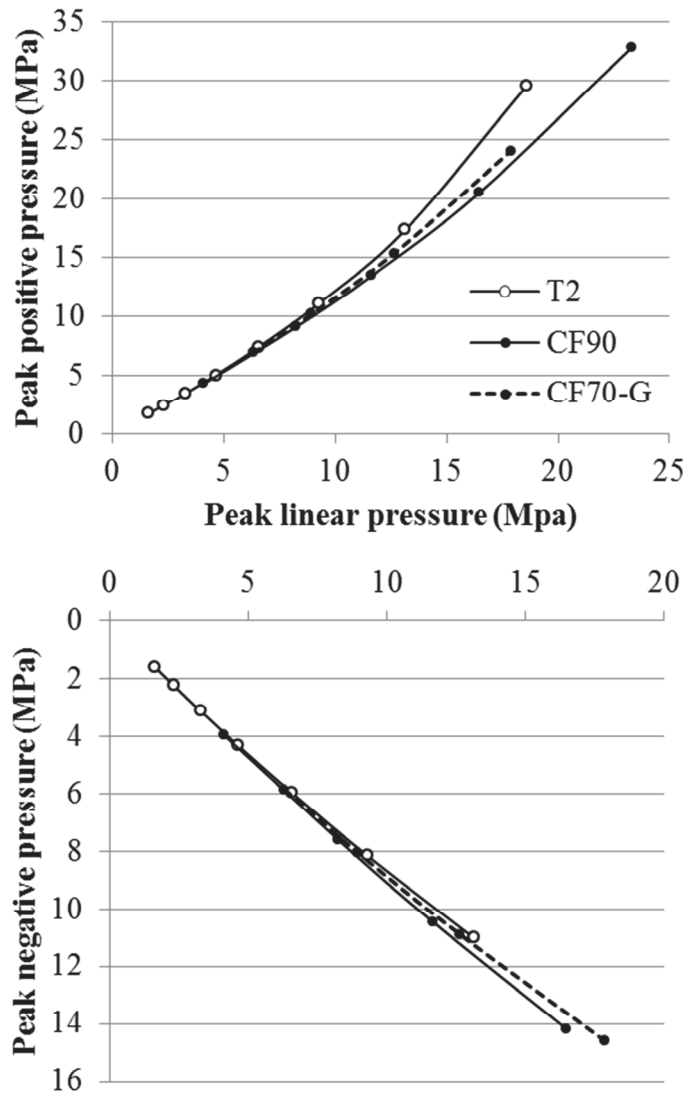


**Figure 2.11: Peak negative pressure (bottom) and peak positive pressure (top) against the peak linear pressure. When reducing the size of the setup by decreasing the separation angle from 90° (CF90) to 70° (CF70), the nonlinear effects are increased. Still, these are reduced compared to a single transducer with the same emission surface (T2), displayed here as a reference curve.**

The CF90 provides the lowest distortion due to nonlinearity. However, there is not a strong difference with the CF70 configuration that still provides better results than the T2 configuration. As an example, around the relevant value of 15 MPa in peak linear pressure, while the peak rarefaction pressure is reduced to 12.94 MPa in the CF90 case, it is reduced to 12.6 MPa using the CF70-G (2.6%

difference). Compared to T2, this reduction is of 4.6%. When reaching 15 MPa on peak linear pressure with CF90, CF70-G, T2 configurations the peak positive pressures are 18.07 MPa (20.5% increase compared to the linear case), 19.0 MPa (26.7% increase) and 19.86 MPa (32.4% increase) respectively. Thus, reducing the angle from  $90^\circ$  to  $70^\circ$  permits to reduce strongly the size of the ultrasonic setup while maintaining almost all the advantages of the confocal configuration in term of reduced nonlinear distortion compared to single transducer setups. As it enhances the practical aspect and relevancy for future experimental purposes, the further investigations focuses on the CF70 configuration.

### 3.2 Crossing at the acoustic focus

As the initial pressure increases, the location of the peak negative pressure tends to move toward the transducer with single transducer setups, as shown in Figure 2.10. According to the simulations previously performed, for a focal peak negative pressure of 9.42 MPa obtained with T1, the location of the peak negative pressure is at 48.5 mm. We try to take advantage of this in the confocal setup by crossing the axes of each transducer at 48.5 mm distance instead of 50 mm. To investigate the consequences of this shift toward the transducers in a confocal context, two configurations are compared. The first one is the previously modelled CF70 such as the two beams cross at 50 mm, the geometrical focus (termed CF70-G as for “Geometric crossing distance” for clarity). The second configuration is based on the same configuration but the two beams cross at 48.5 mm, the location of the peak negative pressure for each single transducer when the peak negative pressure in the confocal case is around the 10 MPa range. This second configuration is termed CF70-A as for “Acoustic crossing distance”. These two configurations are synthesized in Figure 2.12.

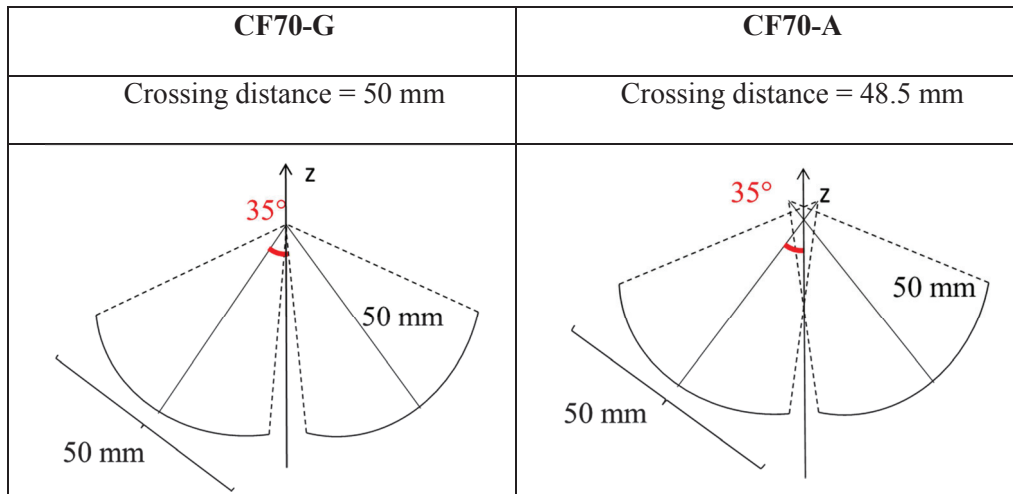


**Figure 2.12: Schematics of the confocal configurations used for the comparison between geometrical (CF70-G) and acoustical (CF70-A) crossing distance.**

Figure 2.13 presents the negative and positive pressure peaks, while crossing the two acoustic beams at the geometric or the acoustic focal distance. The geometrically confocal setup CF70-G is not as advantageous as the CF90 configuration regarding the nonlinear effects. However, by crossing the beam around the acoustic focus, the nonlinear propagation is reduced in some extent that it almost compensates for the lower performance of the 70° angle compared to the 90°. In the linear case, peak negative pressure of 25.28 MPa and 25.12 MPa for CF70-G and CF70-A respectively (0.6% difference) result in peak negative pressure of 19.29 MPa and 19.65 MPa for CF70-G and CF70-A respectively while accounting for the nonlinear effects (1.9% increase with the acoustic crossing). For these same configurations, the peak positive pressure is 40.54 MPa and 38.12 MPa for CF70-G and CF70-A respectively (6% decrease with the acoustic crossing). It should be noted that unlike for the single transducer cases, the position of the peak negative pressure in the CF70-A configuration indeed correspond to the position of the geometric crossing of the beams (48.5 mm).

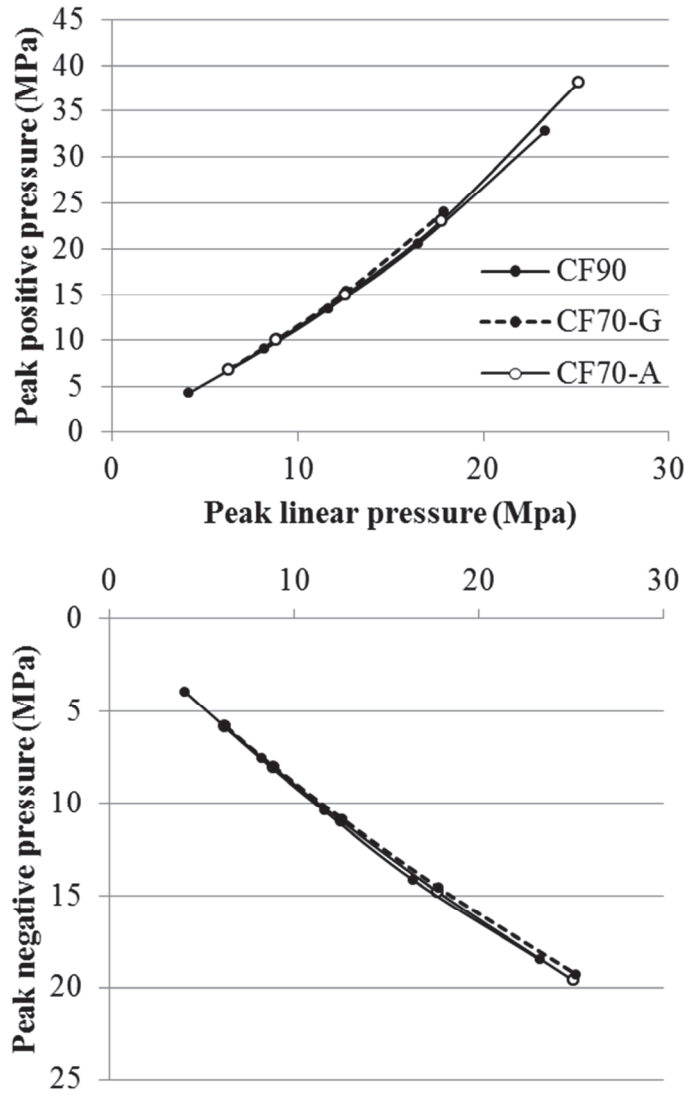


Figure 2.13: Peak negative pressure (bottom) peak positive pressure (top) attributable to the nonlinear effects. When crossing the two acoustic beams according to the acoustic focal distance (CF70-A), the nonlinear effects are increased compared to the geometric crossing (CF70-G).

#### 4 Radiation forces on bubbles

Beside the difference in the nonlinear propagation, the crossing of the two beams results in constructive and destructive interactions leading to an interference pattern (see Figure 2.14). Those are susceptible to change the forces that are exerted on the bubbles. Thus, the radiation force calculation has been integrated into the simulator as described by Sapozhnikov *et al.* (2013). This

study fully describes the calculation of the scattered field and the resulting radiation force for an arbitrary beam incident on an elastic sphere in a lossless medium. In our particular study, we consider the case for which the scatters are small ( $ka \ll 1$ ). In the present study, we modelled scatters that are 150  $\mu\text{m}$  in radius, located in the focal area during the ultrasonic pulse. Also, it should be noted that these radiation force simulations are done for a lossless medium which is a reasonable simplification when considering fresh water with a negligible attenuation.

Figure 2.14 presents the direction of the radiation forces calculated for the T2 and CF70-A configurations in relation to the acoustic pressure field. A major difference can be observed. In the first case (T1), the radiation force and the beam propagation direction are oriented in the same way (away from the transducer). Thus, the scatters will be pushed and flushed from the focal area. Contrarily, in the CF70-A case, the radiation force around the main propagation axis is directed away from the transducer before the focal point ( $z < 48 \text{ mm}$ ) but towards the transducer beyond focus ( $z > 49 \text{ mm}$ ) effectively keeping the scatters around focus. It also appears that lateral forces on each side of the nodes ( $x = \pm 0.7 \text{ mm}$ ) push the scatters toward the pressure nodes of the interference pattern. We can thus hypothesize that the presence of bubbles in the focal area during the pulse will be favored. The interference pattern would therefore act as an acoustic trap for the bubbles. These properties are known and used, notably to perform acoustic levitation. .



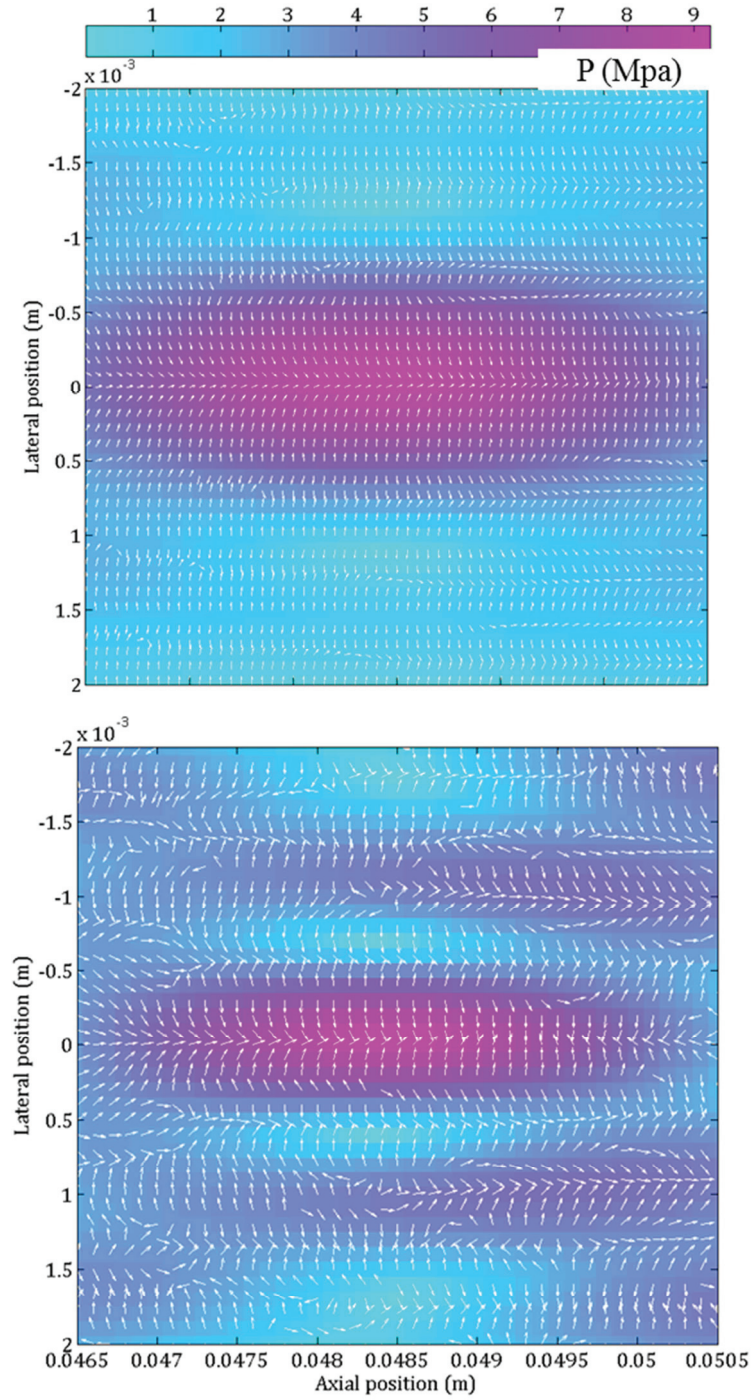


Figure 2.14: Direction of the radiation force (arrows) exerted by the T2 (top) and the CF70-G (bottom) configurations on a  $150\text{ }\mu\text{m}$ -radius elastic sphere. The length of the arrows is normalized by the radiation force. The colour background shows the pressure field (in linear regimen). The interference

**pattern generated from the confocal setup is clearly visible with nodes around  $\pm 0.7$  mm and  $\pm 1.7$  mm and antinodes around 0 mm and  $\pm 1$  mm.**

## 5 Discussion

A simulator that models the pressure fields in nonlinear regimen of confocal transducers was developed. It is based on Westervelt equation and uses an operator splitting method in the frequency domain to model the ultrasonic beams along the volume. This simulator was used to compare a confocal configuration (CF90) versus single transducer setups: T1 and T2, this latter having twice the T1 emission surface. Although the comparison with T1 is not completely relevant as the emission surface is varying, the comparison with T2 permits to observe the effect of splitting the beam in two separated beams. The observed differences between T2 and CF90 are a reduction of nonlinear distortion as well as a change in the shape of the focal volume. These differences would lead to a different configuration choice considering therapeutic applications. Indeed, for cavitation applications, the higher level of negative pressure induced by the confocal device makes it a better choice. The focal volume also has to be considered in the light of the needed spatial accuracy and the volume to be exposed to ultrasound. Thus, the confocal device is well adapted when spatial accuracy is needed. Contrarily, if one is interested in larger exposed zones, a single transducer configuration might be a better choice. Also, the higher nonlinear distortion is linked to a transfer of energy toward the higher frequencies. Therefore, as the acoustic absorption of tissues increases with frequency, the nonlinear effects are favoring the heating. Thus, not only the confocal configuration is reducing the needed energy to reach a certain rarefaction pressure but also reduces the local heating resulting from this energy. The modification of the focal point position depending on the nonlinear regimen has been investigated for both the confocal and the single transducer configurations. While the position of the peak negative pressure is shifted toward the single transducer when increasing the intensity, its position with the confocal setup remains unchanged. For this reason the confocal configuration is favoured for applications requiring a great accuracy.

In a second part of the study, possible improvements were investigated. Obviously, the confocal configurations are less practical than a single transducer at first sight. However, as our target is the breast cancer, the accessibility to the targeted zone is not such an issue as it would be in the case of the liver for example. Nevertheless, reducing the separation angle between the two

transducers can be seen as beneficial considering that the two propagation paths are most likely to have similar acoustic properties. This study permitted to show that reducing the separation angle from  $90^\circ$  to  $70^\circ$  reduces the size of the device while still providing the demonstrated advantages of the confocal configuration, although less pronounced than with the CF90 setup. As shown in the first part, the actual acoustic focus for a single transducer is not localized at the geometric focus but slightly toward the transducer. Moreover, the position of the focus shifts even more as the intensity increases. Thus crossing the two acoustic beams in the confocal setup slightly before the geometric focus is a second lead for improvement. The CF70-G and CF70-A are setups with beams crossing at 50 mm and 48.5 mm respectively. The reduced nonlinear distortion provided by the CF70-A configuration permits to reach higher rarefaction pressure while maintaining a lower peak positive pressure. To that extend, it is quite obvious that the acoustic-based crossing distance in the CF90 case (which would have been termed CF90-A) would result in an improvement of the results compared to the CF70-A case. However by reducing the separation angle from  $90^\circ$  to  $70^\circ$  and changing the crossing distance, we designed a configuration that is less cumbersome than the initial device (CF90) while providing the same advantages thanks to the change in the crossing distance. Depending on the application, the improvement on the size reduction with the CF70-A could appear much more consistent than reaching a few percent more rarefaction pressure with a hypothetical CF90-A. This is for example the case for the biomedical that are intended to be developed in which the accessibility of the target and the versatility of the apparatus is of utmost relevance.

In this study, the criteria that were used to determine if a configuration was advantageous were the steadiness of the focal point, the focal volume, and the nonlinear propagation. Although the steadiness of the focal point is an undeniable advantage, the two others have to be considered carefully. As previously discussed, the reduced focal volume can be either an advantage or a limitation depending on the application. In the same way, the reduced nonlinear propagation can be considered as such. Firstly, a reduced nonlinear propagation reduces the heating. More interestingly, the change in the positive/negative pressure ratio will have implications in the cavitation activity. Indeed, while it is now well established that a high rarefaction pressure is favoring the initiation of cavitation, the positive pressure also plays a role on the resulting cavitation activity. At the fluid/bubble interface the acoustic beam encounters an interface between water (high acoustic impedance) and gas (low acoustic impedance). This

induces a polarity change in the pulse in the reflected wave (positive and negative pressures are inverted). As a result, the reflection-induced higher negative pressure will also trigger the induction of cavitation (Maxwell et al., 2011). Thus, strongly distorted waveforms are not antagonist with strong activity. However, if no low-impedance reflector is present in the focal zone, this effect does not occur. In a clinical context, strong cavitation activity can result in damages in tissues (healthy and tumoral). Although it can be the objective, as for histotripsy, some studies intend to limit the damages and use cavitation only as a trigger for the enhanced drug efficacy and/or diffusion in the tumor zone. Thus, the interest is in initiating cavitation easily while limiting deleterious effects. For this reason, a configuration that provides the ability to maximize the rarefaction pressure while keeping the positive pressure as low as possible can be a safer alternative. Finally, simulations of the radiation force exerted on scatters in the focal zone show that the confocal configuration provides the possibility to create a bubble trap. This result is of great interest for cavitation application. Indeed, a longer flushing time of the bubbles from the focal zone provides the opportunity that bubbles are remaining from one pulse to another. As these remaining bubbles act as cavitation nuclei, the cavitation would thus be easier to initiate. This last point would explain the great temporal stability of the cavitation clouds that was observed during previous experiments (Prieur et al., 2015). One could notice that the 150  $\mu\text{m}$  used in the simulations corresponds to the size range of cells. It is therefore possible that the cells are flushed out from the focal area with the single transducer and contrarily remaining in the focal zone in the confocal case for *in vitro* experiments. This would explain the impressive results of the configuration to perform transfection (Chettab et al., 2015).

## 6 Conclusion

A simulation tool for confocal ultrasonic devices has been developed. Comparisons with numerical and experimental references show good agreement. The simulator can be used to design efficient confocal devices, and permits a way to predict physical effects even at high pressure (beyond 15 MPa in water, which is adapted to cavitation concerns). Numerical comparisons showed that the confocal configuration provides a pressure field inherently different from the single transducer, with a smaller focal region, reduced nonlinear behaviour, inducing the increase of the negative pressure in the focal area. By its enhanced accuracy, the reduction of nonlinear distortion and the potential effects of the interference pattern, the confocal configuration is well adapted for cavitation applications.



## Chapter 3: Unseeded inertial cavitation for doxorubicin potentiation. Safety study

### 1 Introduction

It was previously described how ultrasound and its related effects such as cavitation can induce consequences at different levels. Even if no effect on drug molecular structures has been demonstrated in the literature, inertial cavitation can act at the molecular level. For example, hydroxyl radicals can be induced by cavitation-induced sonolysis of water molecules. The molecular structure of drug exposed to intense inertial cavitation activity and its cytotoxicity have to be assessed to avoid eventual altered bioeffects. Over one hundred anti-cancer drugs are approved by the US FDA, doxorubicin (DOX) is one of the most potent antineoplastic drugs. However, its cytotoxic effects are multidirectional. Studies combining DOX with unseeded inertial cavitation are rare in the literature. However, many studies were described with this combination with UCA which – although the acoustic intensities are much lower – allows the surrounding media to be subject to equivalent variety of stress as in unseeded cavitation<sup>176,177</sup>.

There are several known effects of cavitation on biological tissues, at different levels<sup>178</sup>. At the cellular level, cavitation can cause transient or permanent pores in cells. Hwang *et al* also showed a correlation between cavitation activity and the presence of damages on endothelial cells using UCA<sup>179</sup>. At the tissue level, strong mechanical effects can affect the structure of blood vessels. For example, shock waves were shown to decrease tumor perfusion in certain cases<sup>180</sup>. In this last study, a lithotripter was used to generate pressures of 80 MPa. Also, significant tissue disruption can be achieved with inertial cavitation as a function of the

---

<sup>176</sup> Escoffre et al., "Doxorubicin Delivery into Tumor Cells with Ultrasound and Microbubbles."

<sup>177</sup> Ghoshal, Swat, and Oelze, "Synergistic Effects of Ultrasound-Activated Microbubbles and Doxorubicin on Short-Term Survival of Mouse Mammary Tumor Cells."

<sup>178</sup> Pitt, Hussein, and Staples, "Ultrasonic Drug Delivery - A General Review."

<sup>179</sup> Hwang et al., "Correlation between Inertial Cavitation Dose and Endothelial Cell Damage in Vivo."

<sup>180</sup> Gamarra et al., "High-Energy Shock Waves Induce Blood Flow Reduction in Tumors."

ultrasonic parameters<sup>181</sup>. Inertial cavitation for drug delivery can therefore be problematic if local damage occurs on healthy tissues surrounding the target zone.

Finally, there are concerns about applying such intense mechanical stress on tumors. Indeed, a possible dissemination of tumor cells and/or change in the tumor kinetics has to be assessed. Hoshi *et al*<sup>182,183</sup> showed that 1 MPa peak pressure shock waves do not promote lung metastasis in urinary bladder cancer model implanted on rabbits. In contrast, Oosterhof *et al*<sup>184</sup> showed that high-energy shock waves (10 MPa p- / 64 MPa p+) increase the metastatic spreading of rat AT-6 prostate tumor cells in lung. Additionally, Miller *et al*<sup>185</sup> showed that cavitation could induce metastatic spreading combining shock waves (10 MPa on p-, 64 MPa on p+) with ultrasound contrast agents. In another study, 1 ms-long pulses at 5 MPa pressures (p-) with 1 Hz rate increased also metastatic spreading of mouse B16 melanoma cells in the lungs of animals<sup>186</sup>. These results suggest that inertial cavitation could promote dissemination of metastases depending on the exposure conditions and on the tumor model.

We intend to develop drug delivery application with unseeded inertial cavitation. The second chapter of this thesis reports how the confocal configuration is adapted to cavitation applications. Typically, our exposure conditions consisted in short pulses (40  $\mu$ s) at high negative pressure levels (13 MPa) but with the particular feature of inhibiting considerably the formation of shock wave. These parameters were chosen in preliminaries studies for their ability to induce inertial cavitation in a consistent manner *in vivo* minimizing the total energy to reduce the thermal elevation. The aim of the present study is to assess some safety features of such exposure conditions in breast tumors. The actual efficacy of combining DOX with unseeded inertial cavitation is not studied here. To begin with, experiments were performed to verify that doxorubicin was

---

<sup>181</sup> Maxwell et al., "Noninvasive Thrombolysis Using Pulsed Ultrasound Cavitation Therapy-histotripsy."

<sup>182</sup> Hoshi et al., "High Energy Underwater Shock Wave Treatment on Implanted Urinary Bladder Cancer in Rabbits."

<sup>183</sup> Hoshi et al., "Shock Wave and THP-Adriamycin for Treatment of Rabbit's Bladder Cancer."

<sup>184</sup> Oosterhof et al., "The Influence of High-Energy Shock Waves on the Development of Metastases."

<sup>185</sup> Miller, Dou, and Song, "Lithotripter Shockwave-Induced Enhancement of Mouse Melanoma Lung Metastasis."

<sup>186</sup> Miller and Dou, "The Potential for Enhancement of Mouse Melanoma Metastasis by Diagnostic and High-Amplitude Ultrasound."



not altered by our ultrasonic conditions, both on its molecular structure and on its biological effects. Then, local damages were evaluated on healthy tissues in rats. Finally, mouse 4T1 tumors implanted in syngeneic animals were sonicated to evaluate the impact of the selected exposure conditions on local tumor growth and metastatic spreading.

## 2 Material and methods

### 2.1 Ultrasound apparatus

The ultrasonic setup is composed of two piezoceramic focused transducers positioned in a confocal manner with a focal distance of 50 mm. Each transducer is a spherical cap, with a diameter of 50 mm truncated in the lateral direction at 40 mm. Thus, the f-number – defined as the focal length over diameter ratio – of these two transducers is 1 (based on the non-truncated geometry). The acoustic beams of the transducers are separated by an angle of  $66,6^\circ$ . Each transducer was independently driven with a 2-channel amplifier (ADECE, Veigné, France). This device is well adapted for cavitation initiation as showed in the second chapter of this thesis. It permits to lower the nonlinear effects leading to the formation of shock wave and increased heating due to the higher absorption of high frequencies by tissues. It is thus supposed to induce safer exposures. Also, it creates a standing wave pattern that was hypothesized to “trap” the bubble cloud and reduce the acoustic radiation forces that push the bubbles away from focus. Focal pressures were measured with an optic fiber hydrophone FOPH 2000 (RP Acoustics, Leutenbach, Germany). The waveform measured at the focal point is presented in Figure 3.1. The peak positive and negative pressures were respectively 20.5 MPa and 13 MPa. One could note that because of the distortions induced by nonlinear effects, the peak positive and negative pressures are not exactly co-located. The ultrasonic setup emitted a 40  $\mu$ s pulse of 1-MHz center frequency. The pulse repetition frequency was 250 Hz (1% duty cycle).



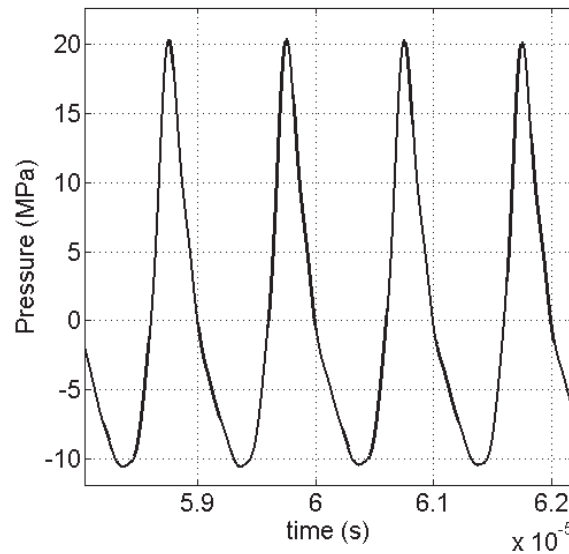


**Figure 3.1: Measured waveform at the focal point for the confocal device for a maximum negative peak pressure of 13 MPa. Here, the peak negative and peak positive pressure were not exactly co-located. The waveform presented here was recorded at the location of the peak positive pressure, where the distortion of the waveform is greatest. Although the pulse is distorted, the shock front is less pronounced than those obtained with lithotripsy or histotripsy.**

For *in vivo* applications, the device was immersed in a tank filled with degassed water (Figure 3.2). The tank is divided in two by a silicone membrane on top of which the anaesthetized animal can be installed. This silicone membrane induces a loss of acoustic pressure of approximately 12% at the focal point (measured pressures given above were done with this membrane in place). To improve image quality (dust in suspension creating speckle) and avoid excessive gas dissolution in the water surrounding the animal, the tank where the animal is placed was regularly emptied and refilled with newly degassed water. A separation of the tank in two distinct parts by a thin membrane reduces the amount of water that has to be changed, thus speeding up the procedure. A 3D motion stage allows displacing the transducers for sonicating a pre-defined volume. An imaging probe Telemed Echo Blaster 128 (Telemed, Vilnius, Lithuania) positioned between the confocal transducers allows defining the volume to sonicate and visualizing the bubble cloud during treatment.

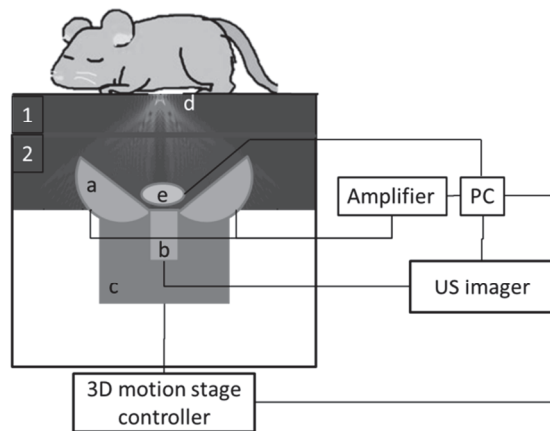


**Figure 3.2: Schematic view of the ultrasonic apparatus used for sonications.** The tank 2 is filled with degassed water. The tank 1 is filled with a smaller amount of degassed water which is replaced between each exposure in order to keep it clean and degassed. The two water tanks 1 and 2 are separated by a silicone membrane. Device composed of two independently driven piezoceramic transducers (a), an imaging probe (b) and a 3D motion stage controller (c). The animal is placed on a plastic plate and the zone of interest is sonicated through a hole in that plate (d). A computer controls the whole procedure with an in-house software. A PVDF hydrophone fitted to the ultrasonic head and oriented towards the focal zone allows a monitoring of the inertial cavitation activity (e).

To assess the inertial cavitation activity, an in-house PVDF hydrophone is fitted on the ultrasonic head and points towards the focal point. This hydrophone records the signal backscattered by the medium. This signal's frequency spectrum is used to compute a cavitation index (CI) representative of the inertial cavitation activity. The CI is defined as the mean of the spectrum amplitude expressed in dB between 100 kHz and 20 MHz minus the mean of the electronic noise frequency spectrum over the same frequency band. An increase in CI translates an increase of the broadband noise. Calculating the mean CI in every location, the overall events of mean cavitation activity can be displayed for every rat to assess reproducibility.

Treatment sessions consisted of 2s-long exposures per discrete locations each distant of approximately 2 mm in each direction. This 2 mm spacing is chosen relative to the size of the cavitation cloud<sup>187</sup>. As the volume of this cloud is smaller

<sup>187</sup> Prieur et al., "Observation of a Cavitation Cloud in Tissue Using Correlation between Ultrafast Ultrasound Images."

than volume delimited by the -6dB beam profile (in linear regimen), the high pressure areas inevitably overlap. The treated volume was defined manually as a cuboid. For *in vivo* exposures of healthy tissues, each sonicated volume was approximately 2 cm<sup>3</sup>. For tumors, the defined volume included the whole tumor. The whole ultrasonic apparatus, termed CaviStation, was used along the thesis for all *in vivo* applications.

For *in vitro* exposures, 1 mL of 1 mM doxorubicin (diluted in PBS before ultrasound exposure) solution was placed at room temperature (approximately 21°C) in a 2 mL Eppendorf tube (Eppendorf, Hamburg, Germany) at the focal point. The duration of the exposure was 0.25 s/mm<sup>3</sup> in order to keep the ratio time/volume identical to the *in vivo* setup (2 s sonications for 8 mm<sup>3</sup> treated volume). No scanning was necessary because of the strong streaming taking place in the exposed samples.

## 2.2 Doxorubicin integrity

The molecular integrity of doxorubicin was evaluated by liquid chromatography and mass spectrometry (LC-MS) analysis. An ultra-high performance liquid chromatograph IClass chain (Acquity Waters, Milford, MA) was used with an ultraviolet detector (diodes arrays) (Acquity Waters, Milford, MA) and an aerosol detector loaded with Corona Ultra RS (Thermo Scientific, Sunnyvale, CA). The first step consisted in the LC-MS analysis of a sample of doxorubicin to evaluate the retention time of the molecule. Then a mass spectrum was performed on the found retention time for a sonicated sample and a control sample. The integrity of the molecule is validated if the molecular mass remains identical between the two samples and if no additional product is detected in the sonicated sample.

Cytotoxicity of doxorubicin exposed or not to ultrasound was evaluated with 3-(4,5-dimethylthiazol-2-yl)-2,5-diphenyl (MTT) assay. MDA-MB231 carcinoma cells were seeded on 96 well plates with a density of  $8 \cdot 10^3$  cells per well in 100 mL of opti-MEM and incubated for 24 hours to allow cells to attach. Then, different concentrations of doxorubicin diluted in PBS ranging from 0.01  $\mu$ M to 3  $\mu$ M were added and cells were incubated for another 72 hours before living cells were quantified with the MTT assay. Twenty micro liters of MTT solution (5 mg/mL) was added into each well. Cells were incubated for 2 hours at 37°C. Finally MTT solution was removed and replaced with 100 $\mu$ L of isopropanol – HCl 1N. The plate was further incubated for 15 minutes at room temperature and the absorbance of the wells was estimated using Multiskan EX microplate spectrophotometer (Thermo Scientific, Waltham, MA).

### 2.3 Effect on healthy tissues

The purpose of this study was to evaluate the local effect of unseeded inertial cavitation on healthy tissues in the rat 72 hours and 2 weeks post-treatment. Different types of tissues were exposed: skin, liver, bone (femur), muscle, vein and nerve. Thirteen rats were used in the study. The rats received intraperitoneal ketamine/diazepam anesthesia and were shaved before each exposure to ultrasound in order to avoid cavitation at the skin due to the air and various dust particles trapped in the hair and acting as cavitation nuclei. Each of them received sonication on one thigh and six received an additional treatment in the liver. Six rats (including 3 that had the liver exposed) were euthanized 72h post-treatment. The seven remaining rats were euthanized 2 weeks post-treatment.

The rats exposed to ultrasound were kept under observation until sacrifice. After complete fixation in 10% Neutral-Buffed Formalin (NBF) (at least 24 hours), the bones (femurs) were decalcified at 37°C in ethylene diamine tetra acetic acid (EDTA) solution before initiation of the histological preparation. After complete decalcification in EDTA (demonstrated by null radio opacity), the femurs and all the others specimens were dehydrated in alcohol solutions of increasing concentration, cleared in xylene and embedded in paraffin. Three sections (approximately 5 µm thick) were prepared for each treated and non-treated sites using a microtome (Microm Microtech, Francheville, France). Two sections were stained with Safranin-Hematoxylin-Eosin (SHE) and one section was stained with a modified Masson Trichrome (MT). For the femur only one section was stained with SHE and one section was stained with MT. Semi-quantitative histopathological evaluation of the local tissue effects at each implanted site were conducted. Each injury was scored between 0 (no damage) and 4 (severe) by an independent histopathologist in a blinded manner. A score of 2 was globally considered as a tolerated damage. A total of 217 sections were analyzed. The mean score of each injury for each tissue was computed.

### 2.4 Metastatic spreading

4T1 cells (syngeneic mammary carcinoma) were injected in the fourth mammary gland of 20 female Balb/c mice. Twelve days after tumor cell injection (D12), mice were randomly divided into two groups of 10 animals each. At D15, all of the mice received gaseous anesthesia and 10 of them received an ultrasound exposure at the primary tumor site. The whole tumor volume was sonicated. The tumor size was measured using a Vernier caliper at D12, D15, D19, D22 and before sacrifice at D25. Lungs and bone marrow were collected in order to evaluate the presence of metastatic 4T1 cells in these organs, as previously

reported<sup>188</sup>. Cell suspensions from lungs and bone marrow from each animal were cultured and exposed to the cytotoxic agent 6-thioguanine allowing the specific growth of 6-thioguanine-resistant 4T1 cells. Tumor cell colonies were then counted in a blinded manner.

Primary tumors were harvested right after euthanasia (D25) for fixation in paraformaldehyde and inclusion in paraffin. Immunohistochemical analyses were performed on 3 serial slices per tumor at 10 random locations per slice with a Ventana Discovery XTautomated system (Roche Meylan, France) using antibodies targeting blood vessels (rabbit anti-CD31 polyclonal antibody, Anaspec, Fremont, CA), cell proliferation (rabbit anti-Ki67 monoclonal antibody, SP6 clone, Spring Bioscience, Pleasanton, CA) and cell apoptosis (rabbit anti-caspase-3 monoclonal antibody, clone 5A1E, Cell Signaling, Danvers, MA). Tumor sections were stained with 3,3'-diaminobenzidine (DAB). Magnifications for Ki67, CD31 and Caspase-3 observations were x20, x10 and x10, respectively. The mitotic and apoptotic indexes and the tumor microvasculature density were quantified, as described Croset *et al.*<sup>197</sup>.

**All animal experiments were approved by an independent ethics committee and in agreement with the national ethical laws for animal experimentation.**

## 3 Results

### 3.1 Doxorubicin integrity

The retention times and the corresponding molecular mass were measured for the two doxorubicin solutions (sonicated or not). The measured retention time was 2.99 min in both cases. The corresponding molecular mass was 543 g/mol for both solutions. Moreover, no additional product was detected between the control and the sonicated samples. Thus, the inertial cavitation at the selected conditions did not alter the doxorubicin molecules.

---

<sup>188</sup> Croset *et al.*, "TWIST1 Expression in Breast Cancer Cells Facilitates Bone Metastasis Formation."

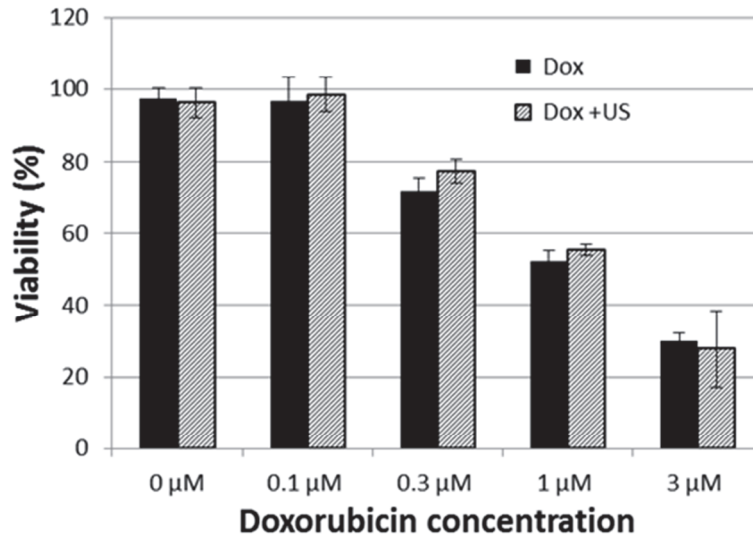


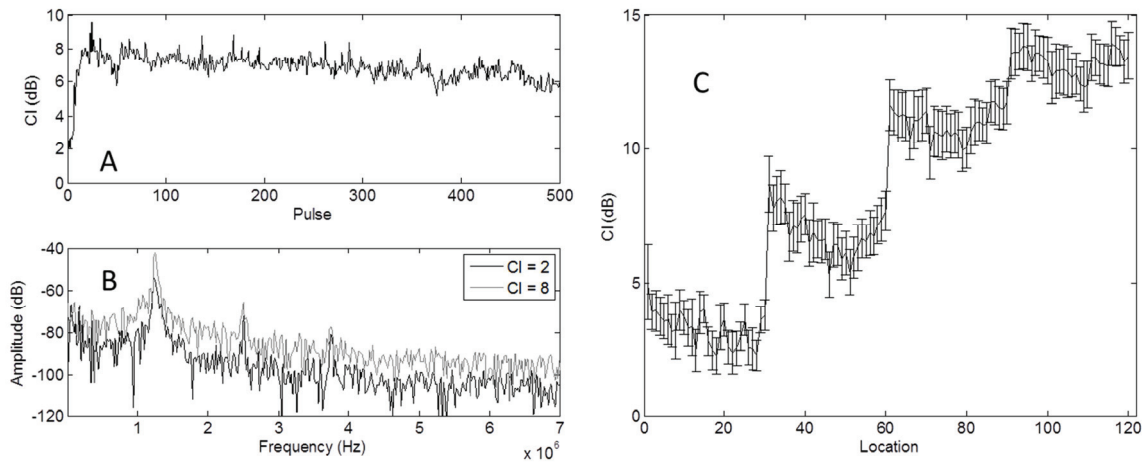
**Figure 3.3: Percentage of viable cells when incubated with various concentrations of normal (plain bars) or sonicated (white black-striped bars) doxorubicin. Error bars indicate the standard deviation between the samples (n=3). There is no significant difference between control and sonicated samples.**

For doxorubicin concentration from 0 to 3  $\mu\text{M}$ , no significant difference was observed on viability of tumor cells exposed to standard and preliminarily sonicated doxorubicin (Figure 3.3). Thus, it can be assumed that exposure to inertial cavitation at the selected conditions did not induce changes that could alter the cytotoxicity of doxorubicin.

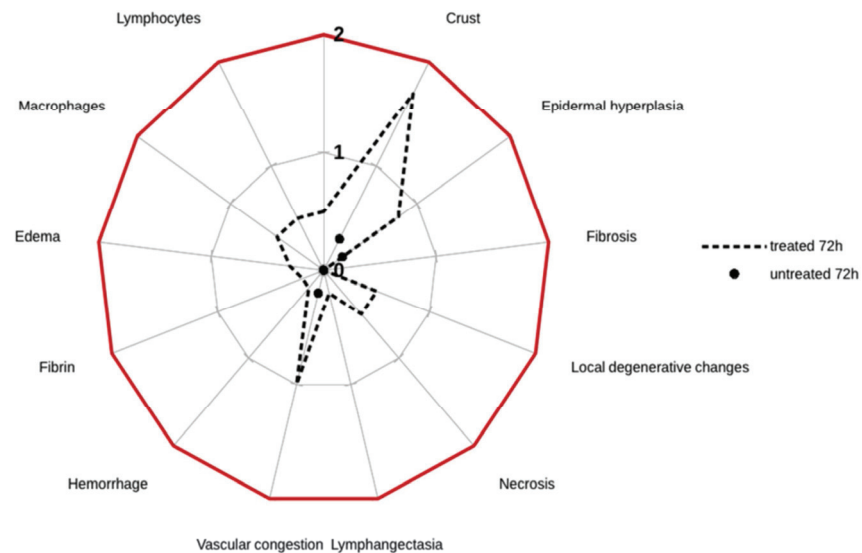
### 3.2 Effect on healthy tissues

Figure 3.4 shows a representative evolution of the CI during a 2-s exposure. The CI varies by approximately 10 dB over the 500 pulses (Figure 3.4.A). Comparing the frequency content of a pulse with a high CI and one with a low CI we observe an elevation of the broadband noise (Figure 3.4.B), characteristic of collapsing bubbles. Figure 3.4.C presents the mean CI over 2-s exposures for all point exposures of a treated volume. The step shape is due to the different depths – thus different attenuation of the broadband noise – at which cavitation was produced. For every depth, cavitation activity is obtained with a satisfactory reproducibility. The semi-quantitative histopathological analysis of the impact of inertial cavitation on the skin 72 hours post-treatment is presented on Figure 3.5. 1/6 untreated sites and 5/6 treated sites showed cellular crusts associated with

slight focal epidermal hyperplasia (Figure 3.6). Additional anecdotal histopathological findings were observed in the treated sites only, suggesting an effect of the selected exposure conditions.



**Figure 3.4: Representative example of the variations of the CI during exposure of a rat thigh. A: variations of the CI during a 2-s exposure at one location. B: Comparison of the frequency spectra for a signal with a low CI and one with a high CI. The increase in the broadband noise level is characteristic of collapsing bubbles. C: Variations of the mean CI over 2-s exposures for all exposed locations of a treated volume. The error bars denotes the standard deviation of the CIs at each location.**



**Figure 3.5: Semi-quantitative histopathological analysis of the effect of inertial cavitation in the skin after 72 hours. Mean score for six rats in each**



group. The solid line is the fixed limit of score 2 that corresponds to moderate acceptable injuries, 0 is for intact tissues.

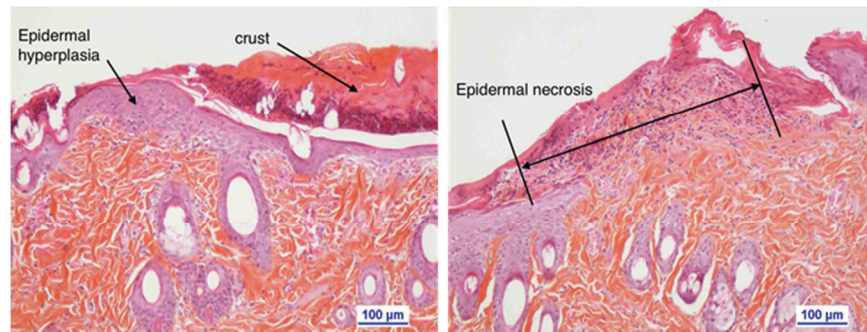


**Figure 3.6: Representative images of treatment-related histopathologic findings in the skin of rats 72 hours post-treatment. Left: epidermal hyperplasia and crust. Right: epidermal necrosis.**

After 2 weeks (Figure 3.7), all treated sites had focal/multifocal areas with changes of slight severity distributed in the superficial dermis and epidermis. These changes consisted in fibrosis in the superficial dermis, inflammatory cell infiltration, vascular congestion in the superficial dermis, epidermal hyperplasia, local degenerative changes in the epidermis and dermal adnexa.

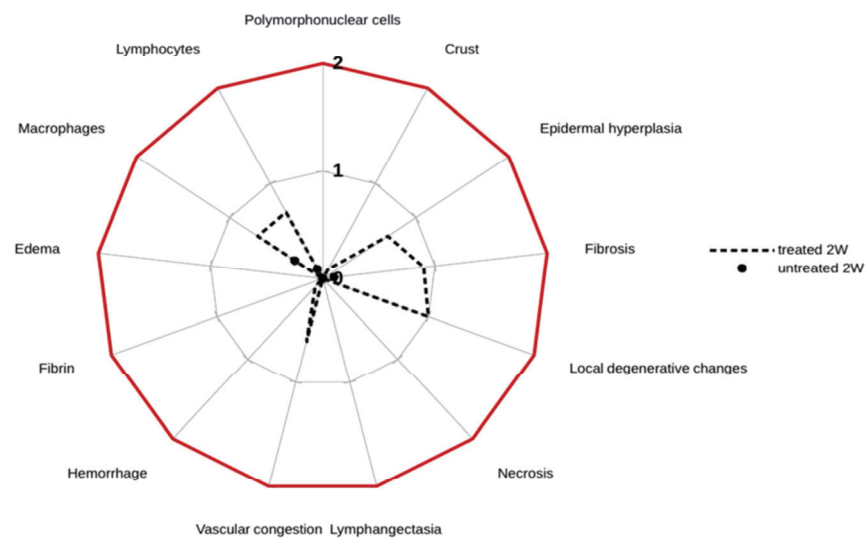


**Figure 3.7: Semi-quantitative histopathological analysis of the effect of inertial cavitation in the skin after 2 weeks. Mean score for seven rats in each**



group. The solid line is the fixed limit of score 2 that corresponds to moderate acceptable injuries, 0 is for intact tissues.

The semi-quantitative histopathological analysis of the impact of inertial cavitation on the skeletal muscle is presented on Figure 3.8. No histopathological findings were observed after 72 hours. After 2 weeks, histopathological findings of minimal severity were observed in 3/7 treated sites (none in untreated). In 2/7 treated sites, these findings consisted in focal decrease in the diameter of myofibers, cellular rounding, cytoplasmic basophilia, nuclear enlargement, nuclear centralization, as well as typical rows of central nuclei. These findings are considered typical of skeletal muscle regeneration and are associated with fibrosis.

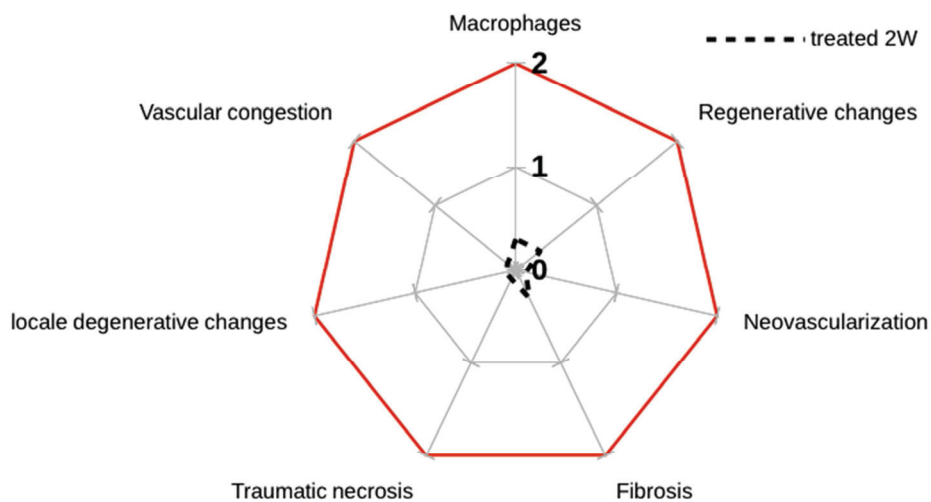


**Figure 3.8: Semi-quantitative histopathological analysis of the effect of inertial cavitation in the skeletal muscle. The solid line is the fixed limit of score 2 that corresponds to moderate acceptable injuries.**

No severe histopathological findings were observed in the bone after 72 hours. Slight local degenerative changes were present within the adjacent skeletal muscle. These changes consisted in degenerative and necrotic changes affecting the myofibers adjacent to the femoral bone, associated with subacute inflammatory cell infiltration and early signs of muscle regeneration. Although these findings were not specific and may be encountered as a background finding in the skeletal muscle, an effect of the treatment was considered possible. After 2 weeks, no histopathological findings were observed.

At both time points, some microscopic changes were observed in some treated and untreated livers (dissociation of the hepatocytes and loss of the

cellular detail with preservation of the cell outlines). Also, these changes were considered artefactual and no treatment-related because the microscopic appearance was similar at both time points and in both treated and untreated groups and because there were no associated inflammatory cells. At both time points, no histopathological findings were observed in both veins and nerves.

### 3.3 Metastatic spreading

*Ex vivo* analyses of the bone marrow and lungs from 4T1-tumor bearing mice which did not receive the ultrasound treatment showed that 7 out of 9 animals (78%) had lung metastasis and 3 of them (33%) had medullary metastasis (Figure 3.9). On the other hand, the incidence of metastases in the ultrasound-treated tumor-bearing animals was decreased. Indeed, only 4 out of 10 (40%) developed lung metastases and 2 over 10 (20%) developed medullary metastases. Moreover, the number of tumor cell colonies per animal was considerably reduced.

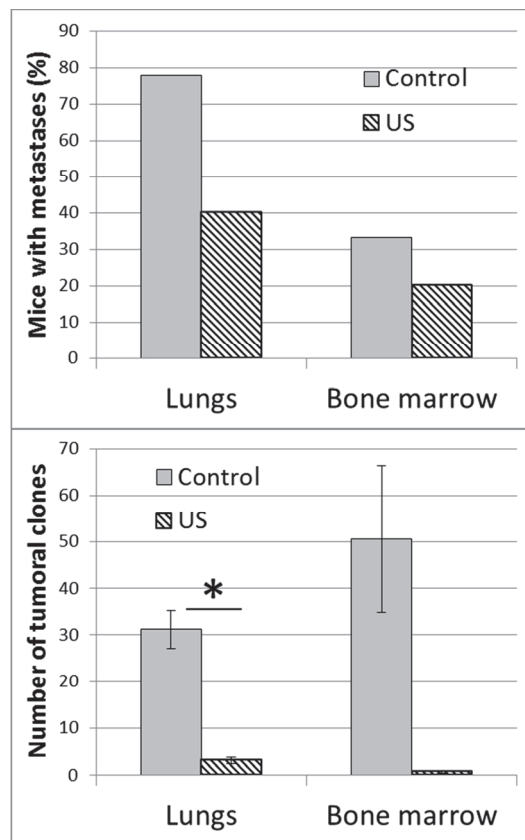


**Figure 3.9: Impact of unseeded inertial cavitation on spontaneous development of metastases in lung and bone marrow from female Balb/c mice bearing 4T1 mammary tumor (9 mice in the control group, 10 in the US group).**

Upper figure: percentage of mice with lung or bone marrow metastases. Lower figure: mean number of tumor cell colonies in the lungs and bone marrow. Error bars represent the standard error, defined as the standard deviation divided by the square root of N (i.e., the number of mice). The symbol \* represent a statistically significant difference  $p < 0.05$  with a Wilcoxon test. The large standard error in the bone marrow case for control group comes from a mouse with a very high number of tumor cell colonies (427).

The size of 4T1 breast tumors into the mammary gland of ultrasound-treated animals was substantially reduced at D22 and D25 (up to 48% reduction), compared to untreated tumor-bearing animals ( $p < 0.01$  with Mann-Whitney statistical test) (Figure 3.10). Immunohistochemical analysis of untreated and ultrasound-treated tumors at D25 is shown in Figure 3.11. Immunostaining of tumors for CD31 (a measure of microvessel density), Ki67 (a measure of tumor cell proliferation) and caspase-3 (a measure of tumor cell death) showed, respectively, that the vascularization and the proliferative and apoptotic indexes were similar regardless of the treatment. Thus, the short treatment exposure to ultrasound (2-s exposure) only transiently inhibited the growth rate of tumors in the mammary gland (Figure 3.10 and Figure 3.11). This transient inhibitory effect of ultrasound on primary tumor growth was however sufficient to decrease the formation of distant metastases in the lungs and bone marrow (Figure 3.9).

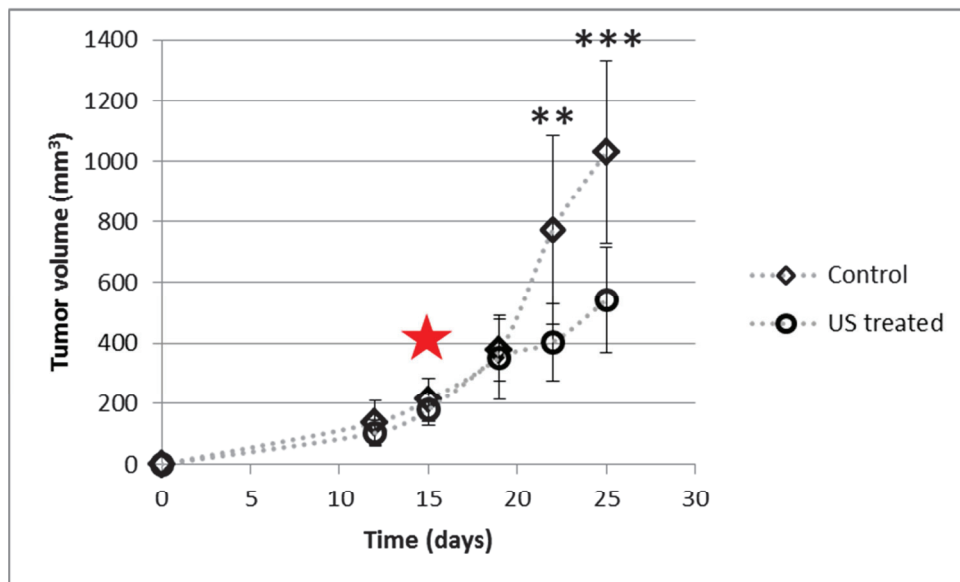
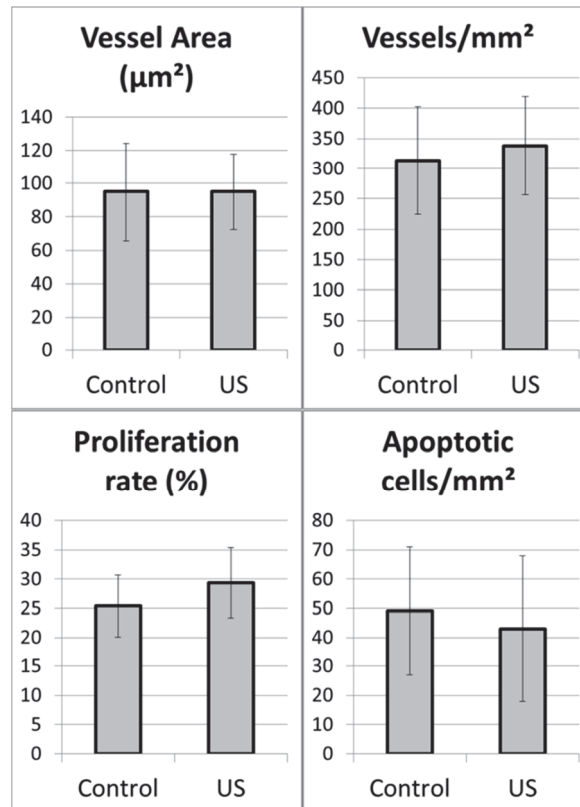


Figure 3.10: Follow up of the growth of 4T1 mammary tumors in female Balb/c mice. US were delivered at D15 (indicated by the star). Tumor volume at each time point corresponds to an average on 10 animals for control and 9 for

the treated group. Errors bars represent the standard deviation. Statistical significance of the difference between the two groups performed using a Wilcoxon test ( $p < 0.01^{**}$ ;  $p < 0.001^{***}$ ).



**Figure 3.11: Immunohistochemical analysis. Data showed no significant difference between the control and the sonicated tumors. Error bars represent the standard deviations.**

## 4 Discussion

This study aimed at evaluating an eventual safety issue of inertial cavitation for drug delivery purposes. The ultrasound setup consisted in short pulses (1% duty cycle) with a limited nonlinear distortion. The focal pressures are 13 MPa for the negative pressure and 20.5 MPa for the positive pressure. The effects on drug integrity and healthy tissues have been assessed, as well as the local effects on sonicated tumors and eventual metastatic spreading. This work focused on safety aspects only. The three major concerns cited above were discarded. However, the actual efficacy of using inertial cavitation for enhancing the delivery of doxorubicin in cancer cells *in vivo* remains to be demonstrated.

Firstly, LC-MS analysis of doxorubicin sample with or without ultrasound exposures showed identical chromatograms. Retention time and molecular weight remained the same. Moreover, no sign of structure modification was observed. Cytotoxicity of the doxorubicin did not appear to be modified by the ultrasound. On one hand, doxorubicin is a relatively small molecule and as the therapeutic arsenal is widening, size distribution of therapeutic agents is widening too and this study does not evaluate the effect of inertial cavitation on bigger structures. On the other hand, this study is representative of the concerns in drug delivery as doxorubicin is one of the most frequently used drugs for cancer therapy.

We have shown that the ultrasound experimental conditions used here only induce slight injuries, mainly on skin. This was attributed to cavitation occurring outside the body, on skin surface, when the targeted zone is very close to the skin. The Figure 3.4 is representative of cavitation events during an ultrasound exposure. The intensity of the cavitation activity varies over the same targeted site and over the entire treatment procedure. These variations are inherent to the fixed-power sonication and the stochastic nature of cavitation. Also, the CI level of the whole exposure shows 4 steps of CI. This is due to the 4 exposure plane in depths which affects the level of the back-scattered signal as well as the cavitation activity. However, the increase of the broadband noise proves that cavitation activity was present in every treated site. Therefore, the entire treatment zone was exposed to inertial cavitation, despite an improvable homogeneity. There is interesting questions regarding this step-shaped cavitation activity across the volume. One can hypothesize that this could be related to the tissues absorption coefficient. The difference in CI between two steps is approximately 3dB. However, a good approximation of attenuation in biological tissues is 0.5 dB/cm/MHz. With the used 1 MHz frequency and the depth difference of 2 mm, the difference due to attenuation should be around 0.1 dB. Taking into account that the center frequency of the received noise is 3.55 MHz (considering a white noise between 0.1 and 7.1 MHz, the recorded bandwidth), the expected difference should be approximately 0.35 dB. A more pertinent hypothesis is that the cavitation activity itself is lower for deeper events. This cannot be explained by the difference of attenuation as we just saw that this one was minimal for this small depth change. The hypothesis of bubbles from the previous plan remaining and helping the cavitation initiation is not valid either because this would also induce a change during the lateral translations, which is not the case. Nevertheless, the beams will be more spatially distorted for deep focal point, changing drastically the focal pressures and interference patterns. As cavitation is very sensitive upon these points, this could explain a less intense and reproducible generation of cavitation. In the present work, tissues were exposed

only once in order to assess local damages. It should be kept in mind that conventional clinical treatment consists in repeated administrations of chemotherapy agents up to 6 cycles with a period of 2 or 3 weeks between each cycle. Ultrasound treatment should then be repeated accordingly. However, immediate (72h after sonication) and long-term (2 weeks after sonication) bio-effects were studied in the present work and only minor and reversible changes were observed on histology at 2 weeks. It can be expected that repeated sonications would not further impact the tissues.

In this study, the metastatic spreading was reduced when applying ultrasound exposure to the primary tumor. The number of tumor cell colonies in the lungs from the ultrasound-treated group dropped by 6-fold compared to control. Thus, under our experimental conditions, inertial cavitation did not enhance the metastatic spreading. These results were in contrast to those reported by Oosterhof<sup>189</sup> and Miller<sup>190</sup>. However, the ultrasonic parameters used here were significantly different. Indeed, even if we used higher negative pressures, other previous studies were based on shock waves with positive peak pressure above 40 MPa<sup>191,192</sup>, or long pulses configurations<sup>193</sup> (millisecond range). The difference with our exposure conditions is therefore in the mechanical stress induced in the tumor. Histopathologic analyses show tissue disruption neither in normal tissues nor in tumor tissues in our case. Indeed, in the present study, short pulsed waves of high amplitude were used, but the confocal configuration allowed cavitation to occur without the formation of a shock wave (Figure 3.1). This reduction of shock wave formation is mostly due to the fact that the emission surface is doubled comparing to a single transducer, so the acoustic intensity is distributed on a wider surface. This allows reducing the nonlinear propagation, responsible (combined with diffraction) for the formation the asymmetry between positive and negative pressure. Additionally, splitting the beam in two separate beams by using a confocal configuration also results in a reduction of

---

<sup>189</sup> Oosterhof et al., "The Influence of High-Energy Shock Waves on the Development of Metastases."

<sup>190</sup> Miller and Dou, "The Potential for Enhancement of Mouse Melanoma Metastasis by Diagnostic and High-Amplitude Ultrasound."

<sup>191</sup> Miller, Dou, and Song, "Lithotripter Shockwave-Induced Enhancement of Mouse Melanoma Lung Metastasis."

<sup>192</sup> Oosterhof et al., "The Influence of High-Energy Shock Waves on the Development of Metastases."

<sup>193</sup> Miller and Dou, "The Potential for Enhancement of Mouse Melanoma Metastasis by Diagnostic and High-Amplitude Ultrasound."

nonlinear propagation. The spatial accuracy of the confocal setup is also much better than with only one transducer due to the crossing of the beams that provides a small focal region. The targeting of the treated area is therefore more accurate. It also hypothesized that the device “traps” the bubbles at the nodes and antinodes of the interference pattern, which might result in fewer bubbles pushed away from the targeted area by the radiation force. Thus, the confocal configuration can induce cavitation activity while limiting the effects on nearby tissues.

We cannot exclude that the impact of the ultrasound treatment varies according the tumor model used. The metastatic spreading was inhibited when applying ultrasound to the breast tumors in the mammary gland. The size of mammary tumors was even reduced. At this stage, it is important to bear in mind that for immunohistochemistry, results were expressed as ratios (number and area of vessels/mm<sup>2</sup>, number of proliferative or apoptotic cells/mm<sup>2</sup>) so the data are normalized. This means that tumor growth kinetics were the same regardless the treatment with or without ultrasound. This phenomenon is well documented in the literature<sup>194</sup>. A longer exposure of primary tumors to ultrasound treatment would have probably been more efficacious than the short exposure at inhibiting mammary tumor growth. Nevertheless, our experimental conditions were effective enough to inhibit metastasis formation, suggesting that ultrasound were killing metastatic cancer cells which escaped from the primary tumor at the time of the exposure of tumor-bearing animals to the treatment. Apart from the formation of a shock wave when a bubble collapses, asymmetric boundary conditions can induce jetting by collapsing bubbles<sup>195</sup>. The resulting stress at the surface of a cell has been shown to be much larger than the elastic modulus of human cells and also larger than the stress induced by the shock wave emitted in the collapse<sup>196</sup>. Thus, one can assume that potential bioeffects of collapsing bubbles will depend on the type of collapse. In healthy human tissues and in tumor tissues, the cell network is dense and homogeneous. The intercellular distance is in the sub-micrometric range<sup>197</sup>. The boundary between blood vessels

---

<sup>194</sup> Croset et al., “TWIST1 Expression in Breast Cancer Cells Facilitates Bone Metastasis Formation.”

<sup>195</sup> Leighton, *The Acoustic Bubble*.

<sup>196</sup> Brujan, Ikeda, and Matsumoto, “Jet Formation and Shock Wave Emission during Collapse of Ultrasound-Induced Cavitation Bubbles and Their Role in the Therapeutic Applications of High-Intensity Focused Ultrasound.”

<sup>197</sup> Young, Woodford, and O'Dowd, *Wheater's Functional Histology*.

however –measuring at least 3.5 micrometers in diameter<sup>198</sup> – and the endothelium or the surface of a cell in the blood flow could favor asymmetric collapse of a bubble and jetting. A different type of bubble collapse can therefore occur depending on the cavitation site.

Migration of cancer cells via the blood vessels is a major mechanism of metastatic spreading in the case of breast tumor<sup>199</sup>, as studied here. We can therefore hypothesize that the cells most likely to proliferate are those closest to the blood vessels and are most likely to be affected by the deleterious effect of inertial cavitation: jetting associated with asymmetric collapse. This would explain the reduction of metastatic spreading while applying ultrasound. Also, this could explain why deep healthy tissues are almost undamaged, contrarily to skin – asymmetric condition water/skin – which undergo moderate reversible damages. However, as written before, no differences were observed on vessel number, apoptosis and proliferation rate on tumors. This can be explained by the relatively long delay between the sonication and the tumor collecting (10 days). Indeed, as damages were shown to be reversible, it is likely that the tumors recovered swiftly after sonication explaining the results obtained at day 25 for the blood vessel density and tumor cell proliferation. Nevertheless, this short exposure to ultrasound was sufficient to reduce the size of primary tumors. Having observed differences in the tumor size between the control and ultrasound-treated groups, whereas growth rates of these tumors (as illustrated by the blood vessel density and proliferation index) were similar, is a proof that a transient inhibitory effect of ultrasound did occur.

Analyzing the safety of *in vivo* inertial cavitation remains subjective. Indeed, benefits for the patient have to be taken into account and this safety study should be looked in light of studies which demonstrate the efficacy of associated ultrasound and chemotherapeutic drugs. Moreover, as most injuries were superficial and reversible, their relevance is subjective and depends on the associated treatment efficacy gain. Finally, as the sonicated zones will be deeper in human and as the acoustic conditions at the focal point will be the same, there will probably be less injuries than in the studied case in which the skin was closer to the focal spot. One has to keep in mind that the rationale to combine doxorubicin with ultrasound is i) to increase the efficacy of the treatment to overcome the acquired drug resistance of the tumor, ii) to decrease the dose in case of sufficient efficacy in order to reduce side effects thus improving the quality of life of patients. Safety aspects are particularly important for this second point. Indeed, there is

---

<sup>198</sup> Cliff, *Blood Vessels*.

<sup>199</sup> Pantel and Brakenhoff, “Dissecting the Metastatic Cascade.”



numerous ways to combine chemotherapy with other treatment modalities. But each one of them presents various drawbacks in terms of quality of life. Studies about safety aspects as the one presented here tend to show that ultrasound is a good candidate for combination with chemotherapeutic drugs because of its minimal invasiveness and undesirable effects. The efficacy of the combination of doxorubicin with unseeded inertial cavitation has not been demonstrated *in vivo* yet and constitute the purpose of the next chapter. However, the present study shows that this could be assessed safely with our ultrasonic setup.

## 5 Conclusion

The safety of unseeded inertial cavitation was evaluated considering damages to healthy tissues, eventual metastatic spreading and molecular degradation of the chemotherapeutic drugs. LC-MS analysis of the sonicated doxorubicin did not permit to show any molecular degradation due to ultrasound exposure and its cytotoxicity remained unchanged. Only slight damages were done to healthy tissues in rat, mostly on skin. Most of the damages were reversible (2 weeks). Metastatic spreading of breast cancer cells to lungs and bone marrow was reduced following short-time exposure of primary tumors to the selected ultrasound conditions. Moreover, the growth rate of breast tumors in the mammary gland was reduced compared to untreated group. The reduction of metastatic spreading was most likely a consequence of the growth reduction of the primary tumors. In the light of these results, unseeded inertial cavitation can be considered safe regarding these three points under our experimental conditions. However, the limitations of this study are the use of small animals and the sonication of shallow tissues only. Also, although several treatment sessions will be performed during preclinical and clinical studies, the present study only investigated the effect of a single exposure. For clinical applications, as tumors would be of bigger size, targets will be deeper, having an influence of beam distortion. Thus, higher power levels will be required to compensate. The safety for clinical applications has to be investigated. Even if this particular condition did not promote metastatic spreading, an effect on tumor growth is undeniable. Further histological analyses and/or blood flow monitoring within the tumor right after sonication could improve our understanding of ultrasound actions and thus potentially improve drug delivery strategies.

## **Chapter 4: Unseeded inertial cavitation for doxorubicin potentiation. Preclinical study on MDA-MB-231 tumors in mice**

### **1 Introduction**

As previously described in this document, doxorubicin (DOX), also known as Adriamycin, is one of the most employed anticancer drug in clinical use. This potent chemotherapy drug is a member of the anthracycline class and has the broadest spectrum of action of its family. DOX is used against many malignancies including solid tumors (breast, endometrium, ovary, thyroid, lung, bladder, stomach and sarcomas of the bone) and haematological malignancies (lymphoma, acute lymphoblastic and myeloblastic leukemia)<sup>200</sup>. Although its antitumor activity is still not completely elucidated, it has been attributed to several mechanisms: intercalation of the planar anthracycline nucleus with the mitochondrial<sup>201</sup> or nuclear DNA double helix, inhibition of topoisomerase II by stabilization of its cleavable complexes and production of Reactive Oxygen Species (ROS). Despite its widespread use, the efficacy of DOX is hampered by major undesired effects such as the development of P-glycoprotein and topoisomerase II resistances in tumor cells and acute or chronic toxicity in healthy tissues. The most serious side effect is a cumulative cardiotoxicity but DOX also triggers hematotoxicity, nausea or vomiting, mouth sores, hair loss and a secondary risk of acute myeloid leukaemia. To overcome these side effects, the development of an efficient and targeted delivery of DOX is required, the aim being to increase the efficacy of chemotherapy while minimizing the therapeutic dose administered to patients. Ultrasound is an ideal candidate for such a purpose as it would potentially overcome the limits of current treatment strategies.

An ultrasonic device based on two confocal transducers has been described in the chapter 2 and 3 of this thesis. In the latter one, it was shown that inertial cavitation produced with the confocal device can be considered safe in the context of drug delivery with our particular conditions. Indeed, the doxorubicin molecules and their cytotoxicity were not altered. The exposure of healthy tissues did not result in severe nor irreversible damages. Finally, the spreading of metastases was

---

<sup>200</sup> Carvalho et al., "Doxorubicin."

<sup>201</sup> Ashley and Poulton, "Mitochondrial DNA Is a Direct Target of Anti-Cancer Anthracycline Drugs."

not enhanced. However, the potential benefit of combining such US exposures to doxorubicin was not evaluated.

The purpose of the present chapter is to assess the practical efficacy of using unseeded inertial cavitation generated by confocal US for the potentiation of doxorubicin *in vivo*. The designed preclinical device, the Cavistation, is used to induce unseeded inertial cavitation in mice. The efficacy of the combined treatment is assessed on the basis of tumor growth. Also, potential damages are assessed with histologic observations. Finally, the uptake of doxorubicin by tumors is evaluated.

## 2 Preclinical efficacy study

### 2.1 Materials and methods

#### 2.1.1 Tumor model

Four week-old female CB17 SCID (Charles River laboratories, L'Arbresle, France) were bred under pathogen-free conditions at an animal facility of Lyon University (Antineo, Lyon, France). Development of MDA-MB231 derived tumors in SCID mice were obtained by subcutaneous injection of  $2 \cdot 10^6$  MDA-MB231 cells.

**Animals were treated in accordance with the European Union guidelines and French laws for laboratory animal care and use.**

#### 2.1.2 Study design

The study consisted of 4 groups of 5 mice, divided randomly. DOX was injected intravenously at the sub-optimal dose of 2 mg/kg. The Table 4.1 summarizes the repartition on the mice in the four groups. The treatments with DOX and/or US were initiated when the diameter of tumors were felt by hand by trained operators. For group 4 (DOX+US), US was applied within 5 minutes of DOX injection, according to the peak distribution of free doxorubicin in MDA-MB231 tumor model<sup>202</sup>. The volume of the tumors was measured using a caliper twice weekly to document the tumor growth. The tumor volumes were then calculated by the following formula:  $V = 4/3 (\pi \times r^3)$ . Here,  $V$  is the tumor volume and  $r$  is the average of maximum and minimum tumor radii. After the fifth treatment session

---

<sup>202</sup> Anders et al., "Pharmacokinetics and Efficacy of PEGylated Liposomal Doxorubicin in an Intracranial Model of Breast Cancer."

(the last one), the tumors were harvested in order to perform histologic observations with Hematoxylin and Eosin (H&E) staining.

<b>Group (5 mice/group)</b>	<b>Doxorubicin* 2 mg/kg. i.v</b>	<b>Ultrasound exposition**</b>	<b>Frequency</b>
<b>1</b>	-	-	-
<b>2</b>	-	+	1/week (w)
<b>3</b>	+	-	1/w
<b>4</b>	+	+	1/w

**Table 4.1: mice repartition in the four groups. \*Doxorubicin 2 mg/ml (Accord Lot P04794). \*\*Ultrasound will be applied just after doxorubicin injection**

## 2.2 Results

### 2.2.1 Macroscopic and histologic observations

No sign of stress or suffering was observed during the five weeks of the experiment, even in the case of animals treated with ultrasound. The macroscopic assessment indicated no ultrasound specific toxicity. Mice of groups 1 and 3 did not present histological damages without ultrasound. Similarly, histology on tumors of mice from groups 2 and 4 did not evidence particular damages one week after the last exposure to ultrasound. However, in the case where is tumor was exposed 5 consecutive weeks and was harvested right after the last one, some mechanical damages can be observed (Figure 4.1). By applying ultrasound only once in mice from group 1 just before euthanasia, it appears that one US treatment only did not induced histological damage. Firstly, this suggests reversible damages induced in the tumor tissues. Secondly, although induced damages are reversible, the tumor tissues are sensitive to repeated exposures.

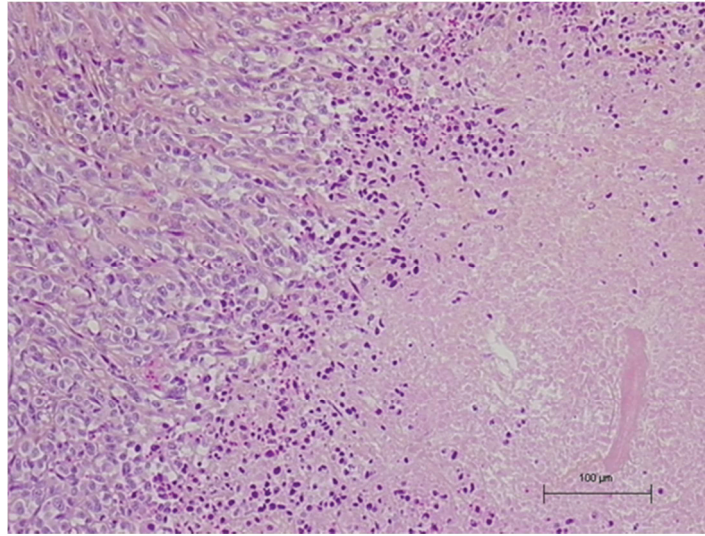


**Figure 4.1: Mechanical damages on a tumor which received five US exposures and harvested right after the last one.**

#### 2.2.2 Efficacy study

The Figure 4.2 represents the average tumor growth in the four different groups. The differences between the four groups are the most important around D18. At this time point, the tumor volume was reduced by 30% by doxorubicin alone (group 2) compared to the control group. Ultrasound alone resulted in a 25% times of tumor volume decrease (group 3) compared to the control group. The addition of US after the doxorubicin injection resulted in an inhibition of tumor growth by approximately 45% compared to doxorubicin alone and 60% compared to the control group.

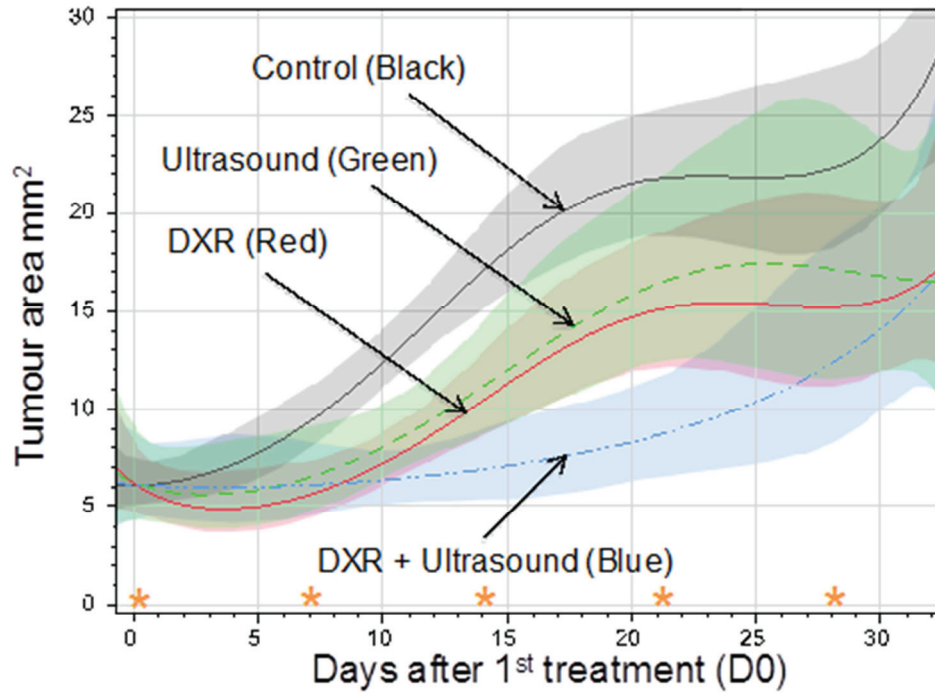


Figure 4.2: Tumor growth of MDA-MB-231 tumors with Doxorubicin administration (2 mg/kg) combined with cavitation treatment. Tumor fold increase is calculated by dividing each tumor size by its size at D0. Error bars represent the standard deviation

### 3 Evaluation of doxorubicin uptake in tumors

As the results were not satisfying, the amounts of doxorubicin in the tumor with or without US were assessed after the last US exposure. This was performed after the last measurement and thus did not influence the first part of the study. Also, as stable cavitation is showing a great potential in various studies described in the first chapter of the present document, it was investigated both the inertial regimen and a different parameter set which induces stable cavitation *ex vivo*. This set of parameters consisted in longer pulses to reach 15% of duty cycle. Moreover, the peak rarefaction pressure was diminished to 7 MPa (55W). These were determined by adjusting the power level in order to obtain a consistent occurrence of the sub-harmonic frequency (550 kHz).

### 3.1 Material and methods

A lethal dose of 30 mg/kg of doxorubicin was injected to the mice before the US treatment. This dose was chosen based on the necessity to have a high quantity of doxorubicin in the tumor so that its fluorescence intensity can be measured by fluorescent microscopy (the usual sub-optimal dose used in the first part of the study is not sufficient to detect and evaluate the doxorubicin intake). Tumors were excised 20 minutes after injection and directly frozen at -80°C in nitrogen. Tumors were then sliced with 20 micrometres thickness and stained with 4',6-diamidino-2-phenylindole (DAPI). The DAPI staining permits to distinguish clearly cells from other material. The slices were then pictured on a Leica SP5X (Leica, Nussloch, Germany) by a qualified operator from the Lyon-Est Centre of Quantitative Imaging (CIQLE, Lyon, France). Images consisted in DAPI images (blue) and the natural fluorescence of doxorubicin in green.

In order to evaluate the fluorescence of the doxorubicin in the tumor, morphologic filters were designed from the DAPI data: the fluorescence value of each pixel is accounted for only if included in a cell. These filters were then applied to each doxorubicin fluorescence image in order to receive only the doxorubicin signal from the cells. The mean intensity value of the non-null points was then calculated and considered as representative of the amount of doxorubicin in the tumor. All the steps of the described process are gathered in Figure 4.3 for clarity purpose.

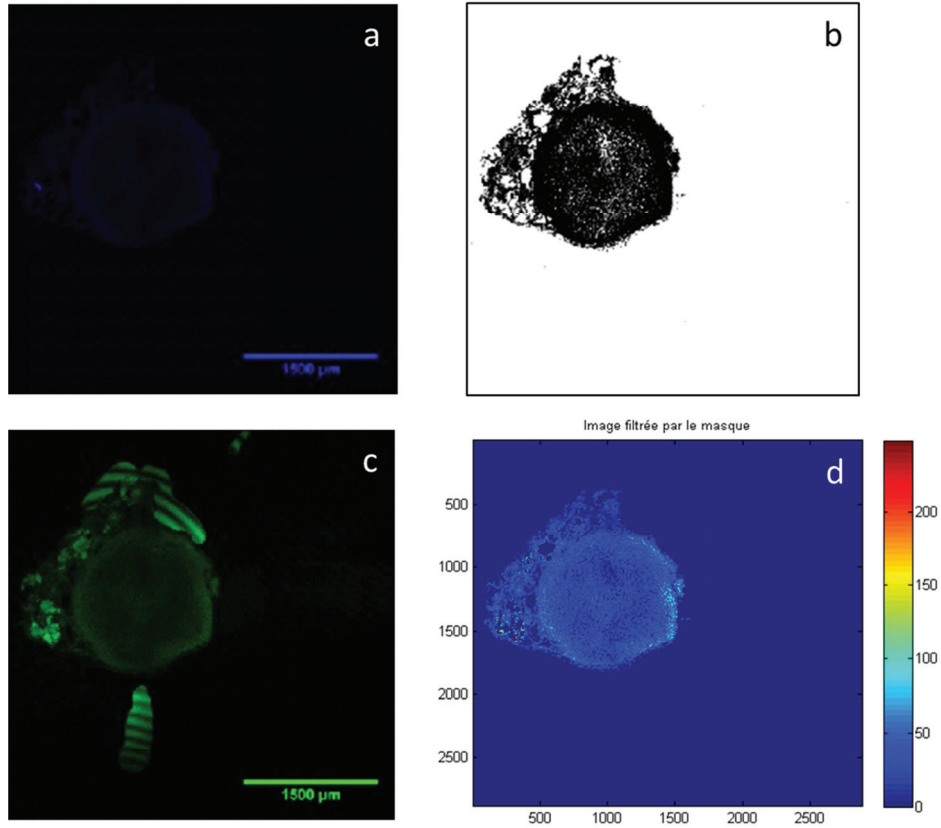


**Figure 4.3: Process steps for measuring the quantity of doxorubicin inside the tumors. From the DAPI data (a), a binary filter is constructed (b). This filtered is applied to the doxorubicin data (c) to keep only the fluorescence intensity where cells are present (d).**

### 3.2 Results

Figure 4.4 presents the means fluorescence intensities in tumors that were treated with doxorubicin only (N=2) and in combination with inertial cavitation (N=3) or stable cavitation (N=3). The group treated by inertial cavitation is only showing a slight difference (not statistically significant). Contrarily, the group treated with the combination of doxorubicin and stable cavitation shows an increase of fluorescence of approximately 40%. This increase is statistically significant ( $p=0.019$  with ANOVA analysis). This result suggests an increase of the uptake of doxorubicin by the tumor via the addition of stable cavitation.



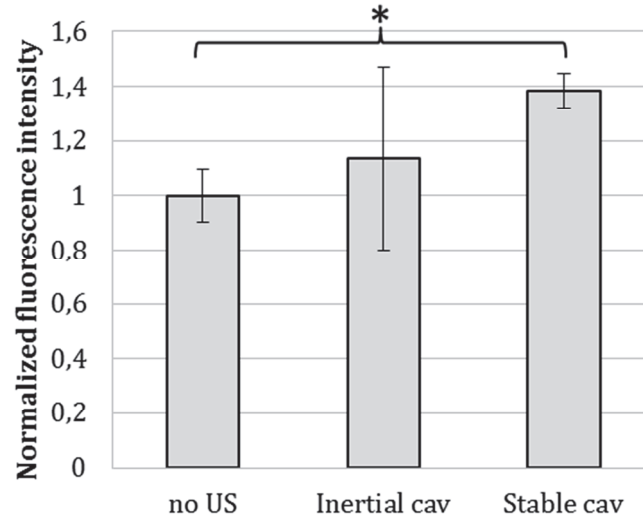


**Figure 4.4: Normalized doxorubicin fluorescence of tumors with no US (N=2), inertial cavitation (N=3) and stable cavitation (N=3). This suggests that stable cavitation increases the uptake of doxorubicin. Errors bars represent the standard deviation. \* denotes for a statistically significant difference ( $p=0.019$ ).**

## 4 Discussion

After developing an acoustic configuration which provides good abilities for cavitation applications and demonstrating the safety of its use for DOX delivery, this study consisted in assessing the therapeutic efficacy of combining DOX with unseeded inertial cavitation *in vivo*. Mice were implanted with MDA-MB231 tumors and exposed to various treatments combinations. At D18 of the study (two days after the second treatment session), the results indicated that doxorubicin administration combined with posterior acoustic cavitation exposure resulted in inhibition of tumors growth by 60% compared to group control (group 1). Compared with group 1, groups 2 (DOX alone) and 3 (US alone), it showed an inhibition of tumor growth of 30% and 25% times, respectively. This difference was statistically significant using a non-parametric Wilcoxon test ( $p<0.02$ ). However, this response to treatment was only temporary and at the end of the study, the tumor growths were identical in DOX and combined DOX+US groups. Secondly, as US itself has an effect on tumor growth, one may consider the inhibitive effect of the combined treatment as a superimposition of the two effects more than a synergetic effect by potentiation. Indeed, two factors ANOVA analyses were unable to confirm the synergetic effect of the interaction of doxorubicin with

our US parameters. It should be noted that the wide dispersion of the tumor volumes within the same group of animals lead to the weakening of statistical analyses and interpretation of these results. There are various factors explaining the wide spreading of the tumor sizes. Amongst them, there is the fact that the tumors are of various sizes and are thus treated at different tumor stages. These stages induce changes in the tumor permeability and so on changes in the treatment efficacy. As the tumors were dispatched in groups so that the mean tumor sizes are optimized, we can nevertheless expect that this source of variability does not have an influence in the conclusions that were drawn. It appears that the benefit is more likely resulting from the addition of both DOX and inertial cavitation anti-tumor effects. In order to evaluate if inertial cavitation actually increased the delivery of doxorubicin to tumor cells, the intracellular uptake of drug was measured after a lethal DOX injection, with or without adding US. In the meantime, *in vitro* experiments conducted on parallel projects provided indications for potential benefits from combination with stable cavitation. It was thus also investigated the drug quantity in the tumor after stable cavitation exposures. Interestingly, this further experiment is suggesting the possibility for stable cavitation to potentiate the uptake of doxorubicin by the tumor. This hypothesis is notably supported by the literature by the formation of pores<sup>203</sup>, endocytosis<sup>204</sup>, opening of biological structures<sup>205</sup>. In other biological structures such as in the brain, it was reported an increase of drug penetration with correlated with the emission of sub-harmonic, indicating stable cavitation<sup>206</sup>. Nevertheless, the result obtained here has to be regarded cautiously. Firstly, the number of sample was small. Moreover, it is not sure if the increased amount of doxorubicin would have resulted in an improved therapeutic outcome. It would have been very interesting to evaluate the actual therapeutic benefit resulting from this drug concentration increase. With was however not possible because of the lethal doxorubicin dose injected and the fact that the tumors were already very close to the defined ethical maximal volume. Further experiments would thus consist in new studies, both *in vitro* and *in vivo* exploring the use of stable cavitation for potentiating doxorubicin. For these studies, attention has to be put on the tumor growth variability.

---

<sup>203</sup> van Wamel et al., "Micromanipulation of Endothelial Cells."

<sup>204</sup> Meijering et al., "Ultrasound and Microbubble-Targeted Delivery of Macromolecules Is Regulated by Induction of Endocytosis and Pore Formation."

<sup>205</sup> Collis et al., "Cavitation Microstreaming and Stress Fields Created by Microbubbles," 2010.

<sup>206</sup> O'Reilly and Hynynen, "Blood-Brain Barrier."

## 5 Conclusion

An *in vivo* experiment was conducted in order to evaluate the efficacy of the combination of doxorubicin and inertial cavitation. Although a temporary improvement was evidenced, no synergetic interaction was shown. The high intra-group variations of the tumor sizes also constituted a limiting factor to the statistical analysis. A second part of the study demonstrated the possibility for stable cavitation conditions to increase the doxorubicin penetration in this particular case. Following experiments will thus focus on stable cavitation with effort to reduce sources of variability.

## Chapter 5: *In vitro* potentiation of doxorubicin by unseeded controlled stable cavitation

### 1 Introduction

Generation of unseeded inertial cavitation *in vivo* was discussed in previous sections of this work. Exposures were performed using a confocal US setup which is well adapted for generating cavitation. These were considered safe for the potentiation of doxorubicin *in vivo*. However, evaluation of the efficacy of the combination of DOX with unseeded inertial cavitation in mice implanted with MDA-MB231 did not result in satisfying results. An improvement was observed but was however attributed to the addition of two effects more than a synergetic interaction. Moreover, the observed improvement was limited in time. However, quantification of DOX inside the tumor zone showed that for US exposures inducing stable cavitation, the uptake was increased. In order to explore the potential of stable cavitation, *in vitro* experiments are conducted. The previous *in vivo* study included MDA-MB231 tumors. The low reproducibility of their growth induced an additional limitation for drawing conclusions on the results as it lowered their statistical strength.

The aim of this study is to investigate whether the combination of DOX and unseeded stable cavitation, can enhance the efficacy of DOX on 4T1 cell death *in vitro*. The advantage of 4T1 murine breast cancer cells is their capacity to be grown *in vivo* and to form mammary carcinomas as a primary tumor in BALB/c mice<sup>207</sup>. They can be used as a syngeneic model to assess the efficacy of US *in vivo*. Furthermore, this cell line is well-characterized and very sensitive to DOX. Additionally, we are already in possession of data concerning the sonication of 4T1 tumors, notably on the potential metastatic spreading. There are thus two advantages (better reproducibility and knowledge on metastatic spreading) in conducting investigations in the 4T1 tumor cells rather than on the MDA-MB231. The purpose of this study was to enhance the effects of DOX on apoptosis-induced cell death rather than causing immediate destruction of cells. We therefore investigated acoustic parameters which avoid the formation of inertial cavitation. The first step of our study was thus to determine ultrasonic settings that are able to induce stable cavitation in a repeatable manner. We can therefore assess a potential synergetic effect between unseeded stable cavitation and DOX. Finally, a

---

<sup>207</sup> Pulaski and Ostrand-Rosenberg, "Mouse 4T1 Breast Tumor Model."

mechanistic study is conducted to investigate the precise mechanisms leading to synergetic interactions.

Heating of the propagation medium is a well-known effect of ultrasound. When the US beam is focused on a very small target, the power deposited per unit area can significantly increase, resulting in considerable heating. This effect is especially observed with continuous wave exposure. Studies have shown that ultrasound-induced heating can cause destruction of tissues by coagulation<sup>208,209</sup>. Moderate hyperthermia was also reported to enhance the penetration of drug in tumor cells, with increases in temperature of 4-5°C (from 37 to 41°C) in cell suspensions exposed to ultrasound<sup>210</sup>. It is therefore important to evaluate the increase in temperature of the propagation medium produced by our ultrasonic settings. A potential synergetic interaction involving free radicals was also explored. For this purpose, specific hydroxyl radical scavengers (L-Histidine and Mannitol) were employed in order to inhibit the effects of ultrasound. Also, electronic microscope observations were performed in order to investigate potential morphologic changes such as membrane opening or organel destruction. Finally, we investigated the use of UCA in order to mimick their acoustic signature in unseeded conditions to potentially increase the treatment efficacy.

## 2 Methods

### 2.1 Reproducible stable cavitation generation

The cavitation device used in this study was developed by the company Caviskills (Vaulx-en-Velin, France) and termed CaviBox®. In this device, ultrasonic waves are generated at an emission frequency of 1,1MHz by two, 50 mm diameter confocal transducers PZ28 (Ferroperm, Kvistgaard, Denmark), with a separation angle of 90° between the two acoustic axes. The focal distance of both transducers is 50 mm. The transducers are inserted in a tank filled with Ablasonic® (EDAP-TMS, Vaulx-en-Velin, France), a cavitation-inhibitor liquid which prevents acoustic cavitation outside the sonicated sample. The cells to be

---

<sup>208</sup> Nomikou and McHale, "Exploiting Ultrasound-Mediated Effects in Delivering Targeted, Site-Specific Cancer Therapy."

<sup>209</sup> Kinoshita and Hynynen, "Key Factors That Affect Sonoporation Efficiency in in Vitro Settings."

<sup>210</sup> Saad and Hahn, "Ultrasound Enhanced Drug Toxicity on Chinese Hamster Ovary Cells in Vitro."

treated are placed in a 2 mL safe-lock micro test tube (Eppendorf, Hamburg, Germany), positioned at the focal zone.

In order to control the levels of stable and inertial cavitation, a home-made hydrophone produced with a PVDF film (25  $\mu\text{m}$  thickness, 10 mm in diameter) in resin (AY103 Araldite+ 10% HY956) is placed between the two focused transducers, directed at the exposed sample. The signal generated by the bubble cloud is recorded. As described in the first chapter, the frequency content of this signal exhibits features which are characteristic of the cavitation regimen. An increased level of broadband noise indicates inertial cavitation. Sub-harmonic (half the emission frequency) indicates stable cavitation. An estimate of the level of inertial or stable cavitation is given by the cavitation index (CI). Stable cavitation index (CIs) is calculated on a small frequency window around the sub-harmonic. In our case, the stable cavitation index CIs was defined as the difference between the maximum level in the 540-560 kHz range and the mean level in the 560-600 kHz range. Inertial index (CI) was calculated as the difference between the average of the entire frequency spectrum and its base level. They must not be interpreted quantitatively as their value are interdependent and vary according to the size of bubbles and subtle changes in their oscillation pattern. It is estimated from preliminary experiments that stable cavitation occurs for a CIs above 3 dB in our experimental setup.

The control system is based on two distinct modes: a high power mode, aimed at creating a population of bubbles in the cell suspension, and a low power mode aimed at maintaining the oscillation of bubbles in a stable cavitation regimen. If the CIs is under the threshold of 3 dB, a high power pulse – termed boosting pulse – is sent to revive the cavitation cloud. The low power mode is then used to maintain the stable oscillation of the created bubbles. The total number of boosting pulses is recorded. This process is summarized in Figure 5.1. In our settings, the low and high intensity pulses correspond to peak negative pressures of -2.95 MPa ( $P_{\text{min}}$ ) and -6.7 MPa ( $P_{\text{max}}$ ) at the focus, respectively.

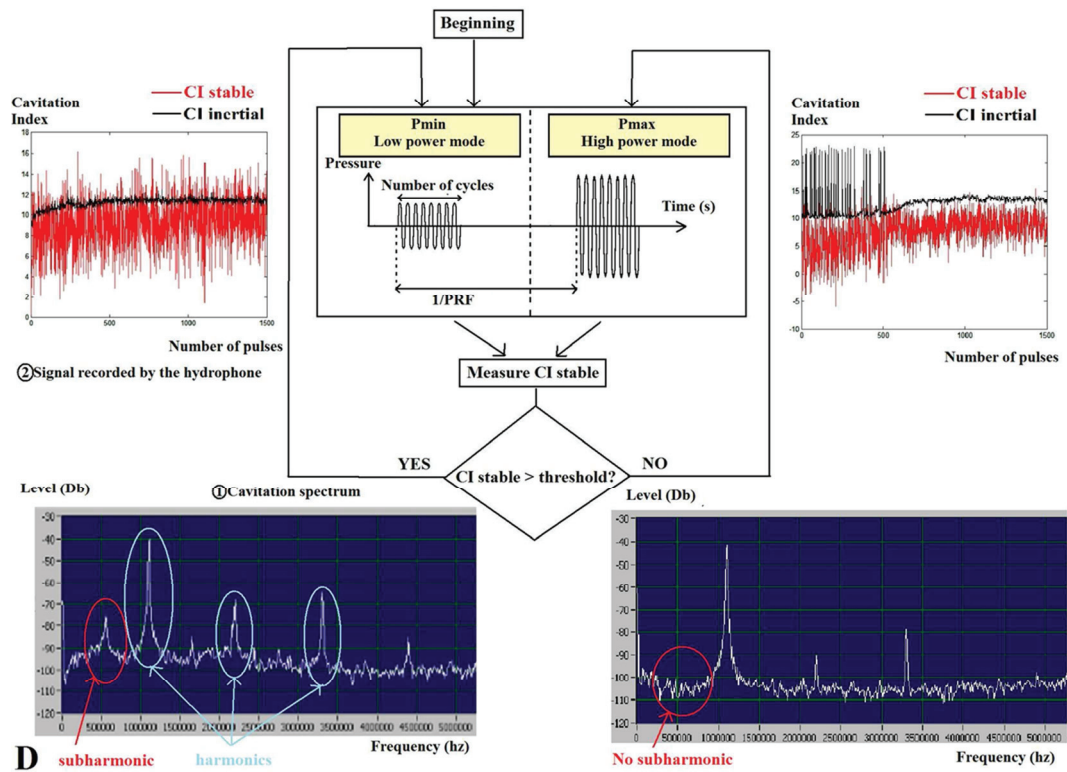


**Figure 5.1: Schematic of the stable cavitation control skim.** The control system is based on the conditional alternation of high power pulses (Pmax) creating bubbles in the cell suspension and low power pulses (Pmin) maintaining the stable oscillation of these bubbles. The level and type of cavitation are given by several indicators on the spectrum of the signal recorded by the hydrophone: occurrence of sub-harmonics indicates stable cavitation and high level of broadband noise (elevation of the global level) indicates inertial cavitation. If the CIs fall below a certain threshold (defined at 3dB in our case), a high power pulse is triggered to revive the cavitation cloud.

Several parameters such as pressure at the focal point, pulse repetition frequency (PRF), the number of cycles in a US pulse and the total exposure time can be modulated in order to induce stable or inertial cavitation in the most repeatable manner while limiting cell mortality in the treated sample. Our objective was to induce a maximum of 20% cell death. Cell death was evaluated in a qualitative manner by microscopic observation using trypan blue coloration (Trypan Blue Solution 0.4%, Life Technologies, Carlsbad, CA). Trypan blue is used as a cell stain to assess cell viability using the dye exclusion test, based upon the concept that viable cells are impermeable to these dyes, while dead cells are permeable and internalize them. PRF was varied from 25 to 125 Hz and the number of cycles from 660 to 6600. The couple PRF = 25 Hz and number of cycles

= 6600, corresponding to a DC = 15%, were found to trigger properly a stable regimen of cavitation. Several exposure times, ranging from 20 to 120 seconds, were tested. Cell death measured in samples exposed to our US conditions was considered acceptable for exposure times lower than 60 seconds. Our US settings were shown to be capable of establishing a constant regimen of stable cavitation. The average number of boosting pulses applied before stabilization of the cavitation phenomenon was  $41.8 \pm 18.4$  over 1500 pulses (2.7%). The average CIs was  $8.05 \pm 3.04$  which confirms the occurrence of stable cavitation. CI was  $11.84 \pm 0.97$ . This value corresponds to a low level of inertial cavitation and is mostly due to the boosting pulses. Thus, this strategy allows for the generation of stable cavitation in a controlled and reproducible manner.

## 2.2 *In vitro* enhanced anti-tumor effect

### 2.2.1 Cell line and culture conditions

4T1 are mammary carcinoma cells, highly tumorigenic and invasive. They can spontaneously metastasize, notably in blood, lymph nodes, bone and lung. As adherent cells and were cultured as a monolayer in T75 culture flasks, in Dulbecco's modified Eagle medium (DMEM) supplemented with 10% Fetal Calf Serum (FCS), 1% L-glutamine and 1% Penicillin-Streptomycin (PS) which corresponds to 100 units/mL of Penicillin and 100  $\mu$ g/mL of Streptomycin. They were maintained in an incubator at 37°C in an atmosphere with 5% CO<sub>2</sub>. Cultures were split 2 to 3 times per week. Cells were not allowed to exceed 90% confluence as overgrowth decreases their viability. All reagents were purchased from Invitrogen Life Technologies. 4T1 cells were tested mycoplasma-free using Mycoalert™ kit (Lonza, Cologne, Germany).

### 2.2.2 Chemicals

Doxorubicin hydrochloride 2mg/mL (Accord Healthcare, Lille, France) was dissolved in a phosphate buffered saline solution (PBS) at a concentration of 20 $\mu$ g/mL, aliquoted in a 5mL tube, and stored at +4°C. The DOX concentration inducing a suboptimal effect was preliminarily evaluated through flow cytometry experiments. A final concentration of 400 ng/mL was chosen for its ability to induce 20% cell death at 48h. For experiments involving hydroxyl radical scavengers, we employed L-Histidine (Fluka) and at 20 mM, Mannitol (Fluka) at 100 mM.



### 2.2.3 DOX delivery by stable cavitation procedure

72 hours prior to treatment, cells were plated at a density of  $1.5 \cdot 10^6$  cells per flask to reach 90 % confluence on the day of the experiment. Cells were trypsinized with 0.25 % trypsin/ 1 mM EDTA (Life Technologies, Cergy-Pontoise, France), centrifuged at 320G during 3 minutes, washed once with 5mL of PBS (Life Technologies) to eliminate traces of FCS (to avoid any complexation between DNA of dead cells and FCS under ultrasound exposure), and then re-suspended in Opti-MEM Reduced-Serum Medium (Life Technologies), at the concentration of 2 million cells per mL. The exact volume of Opti-MEM® was determined after counting the cells using an automated cell counter (Cellometer, Nexcelom Bioscience, Lawrence, MA). Then, 4T1 were put in presence of DOX (400 ng/mL) and/or L-Histidine (20 mmol/L) or Mannitol (100 mmol/L) while in suspension in Opti-MEM® for a total volume of 650  $\mu$ L in 2 mL Eppendorf tubes. As the volume in Eppendorf tubes has a great influence in cavitation set up, electronic pipettes were used to minimize bias due to unequal volumes. Tubes from group 3 (US) and 4 (DOX+US) were then treated with US according to the settings determined earlier using the Cavibox®. After US application, 20  $\mu$ L of cell suspension were collected and used for cell counting. DOX was added in the culture medium to reach the same concentration of drug in the wells as previously. Culture plates were then incubated for 48h and 72h.

### 2.2.4 Cell viability and DOX internalization

Flow cytometry was used to assess cell viability and mean quantity of DOX internalized into sonicated cells. The flow cytometer was a FACS LSR II (BD Biosciences, Franklin Lakes, NJ). Data was analysed with FACS DIVA Software. To assess cell viability, two markers were chosen: DAPI (Sigma-Aldrich, Saint Louis MO, USA) as a necrosis marker and Annexin V APC (Annexin V apoptosis detection kit APC, eBioscience, Paris, France) as an apoptosis marker. DOX is a fluorescent drug whose emission can be used to assess DOX internalization in treated cells. Flow cytometry was performed immediately after sonication (at 1h) and 72h after sonication. At 1h, 300  $\mu$ L of the 650 $\mu$ L Eppendorf tubes were collected and placed in FACS tubes. The remaining 350  $\mu$ L were used for cell counting (20  $\mu$ L) and reseeding (between 60  $\mu$ L and 280  $\mu$ L depending on samples). At 72h, the supernatant in each wells was collected and placed into individual FACS tubes. Wells were washed with 500  $\mu$ L PBS, 300  $\mu$ L of trypsin was added, after which the detached cells were collected and placed into their respective FACS tubes. For both 1h and 72h experiments, cells were then washed twice with 1 mL PBS, , washed with 500  $\mu$ L of Annexin V APC Buffer, marked with Annexin V APC

(Dilution 1/100), put in the dark for 10 minutes and finally marked with DAPI (Dilution 1/500). In some experiments, a third marker (HD2CFDA) was used to assess the production of free radicals. HD2CFDA emits a fluorescent signal when linked to reactive oxygen species (ROS). As the emission frequency of HD2CFDA is closed to that of DOX emission, compensation was performed prior to FACS analysis. Before washing the cells with PBS, 1 mL of HD2CFDA diluted at 1/1000 was added. Cells were then incubated for 30 minutes at 37°C, washed twice with 1 mL PBS, incubated with 1 mL of DMEM at 37°C for 10 minutes (step of fixation of the reactive) and washed twice again with 1 mL PBS.

#### 2.2.5 Cell counting

Cell counting was performed before reseeding and after 72h of culture, using Cellometer (Nexcelom Bioscience, Lawrence, MA). 20 µL of cell suspension were mixed with 20 µL of trypan blue, and the mixture placed into counting plates. Only viable cells were counted. As the Cellometer can often miscount cell aggregates and can only count cell concentrations ranging from  $10^4$  to  $10^6$  cells per mL, automated cell counting was always checked manually. Special attention was placed on samples treated with DOX or US+DOX at 72h, as the concentration was often around  $10^4$  cells per mL and could not be considered as reliable. At 72h, as a result of cell counting, an index of cell growth was performed as the absolute number of cells at 72h divided by the initial number of cells reseeded immediately after sonication. An index inferior to 1 corresponds to inhibition of proliferation and cell death and an index superior to 1 to cell proliferation.

### 2.3 Mechanistic study

To study the parameters involved in a potential therapeutic effect of US, we examined the influence of US on the internalization of DOX in cells, the impact of temperature increase and the role of cavitation.

#### 2.3.1 Analysis of DOX internalization

DOX is a fluorescent drug. The level of fluorescence from DOX inside the cells was recorded immediately after ultrasound exposure using flow cytometry. This measure was then used to determine the mean quantity of DOX internalized in the cells of the sample. The intensity of DOX fluorescence was also assessed after 48h and 72h of culture.

### 2.3.2 Influence of the increase in temperature

The temperature increase during an US exposure is measured by placing a thermocouple in the Eppendorf tube during sonication. In order to avoid perturbations from cavitation as well as the thermocouple artifact, attention was placed to keep the thermocouple as far away as possible from the focal point. The increase in temperature after 60 seconds was measured to be 5°C, rising from 24°C (room temperature) to 29°C.

We recreated this increase in temperature by placing the tubes in a water-bath. We decided to treat one group at 29°C and another group at 37°C which corresponds to body temperature. The changes in temperature were measured using the same method described in the previous paragraph. Tubes were removed from the water bath after a time equal to US exposure time and allowed to cool at room temperature. Groups were split in the following manner :

- Controls (room temperature: 24°C)
- DOX (room temperature: 24°C)
- Temperature: 29°C
- Temperature: 37°C
- Combination of DOX and temperature 29°C
- Combination of DOX and temperature 37°C

Each group contained 4 samples. The concentration of cells and DOX, the parameters observed and the analyses realized are the same as those described in section 2.2.

### 2.3.3 Influence of cavitation

The aim of this experiment was to assess if the effect of ultrasound waves, involving steering of the cells and pressure changes were responsible alone for the therapeutic effects of ultrasound or if the occurrence of cavitation was involved in the process. Two ultrasound settings were used. For both of them, parameters were the same as in section 2.2. However, in the first control group, the setup was changed so that no boosting pulse could initiate cavitation. In the other condition, boosting pulses were used to initiate cavitation. As the proportion of boosting pulses is very low compared to the number of low-power pulses (average of 2.7%), the amount of energy that was deposited in both cases is considered equivalent. Groups were split as follows:

- DOX
- DOX + US without cavitation
- DOX + US with cavitation

Each group contained 5 samples. The absence of stable cavitation was controlled during the experiment by checking the absence of sub-harmonics on the cavitation spectrum and at the end of the experiment by analysing CI. The protocol and materials used to complete this part of the project were the same as those previously described in section 2.2.

#### 2.3.4 Effect of reactive oxygen species

L-Histidine and Mannitol are specific hydroxyl scavengers. Adding these chemicals just before sonication would inhibit the effects of free radicals and would thus have an impact on cell proliferation at 72h<sup>211</sup>. 8 experimental groups, each of them containing 8 samples, were split as follows:

- Controls
- DOX
- L-Histidine or Mannitol
- DOX+L-Histidine or Mannitol
- US
- US+DOX
- US + L-Histidine or Mannitol
- US+DOX+L-Histidine or Mannitol

The protocol and materials used to complete this part of the project were the same as those previously described in section 2.2.

#### 2.3.5 Microscope observations

It may be possible for ultrasound to cause intracellular effects and localize extracellular macromolecules directly into the nucleus<sup>212</sup>. It is suggested that part of these intracellular effects could be due to nuclear pore complex (NPC) opening<sup>213</sup>. US treatment may result in an augmentation of NPC pores and a change in their distribution throughout the nuclear membrane. These ultrasound-induced nuclear effects could be used to potentiate the action of intercalant DNA agents such as DOX. Furthermore, US can affect DNA structure as well as its

---

<sup>211</sup> Yu et al., "The Effect of Free Radical Scavenger and Antioxidant on the Increase in Intracellular Adriamycin Accumulation Induced by Ultrasound."

<sup>212</sup> Furusawa et al., "Effects of Therapeutic Ultrasound on the Nucleus and Genomic DNA."

<sup>213</sup> Vaškovicová et al., "Effects of Therapeutic Ultrasound on the Nuclear Envelope and Nuclear Pore Complexes."

function by single- and double strand breaks<sup>214</sup>. These alterations could lead to cell apoptosis<sup>215</sup>. We thus tried to highlight nuclear pore complexes or DNA damages (by the observation of changes of cell structure due to apoptotic pathways mostly) by using confocal microscopy. The confocal microscope was LEICA TCS-SP5X (CIQLE Centre, Laennec, Lyon). Unsonicated and sonicated cells were fixed for observation with a protocol specific of CIQLE Center, directly after sonication with or without doxorubicin respectively.

## 3 Results

### 3.1 *In vitro* enhanced anti-tumor effect

#### 3.1.1 Cell viability

The anti-tumor effect of the combined doxorubicin/stable cavitation treatment was assessed *in vitro*. Figure 5.2 shows the therapeutic evaluation of cell viability. After sonication (at 1h), only ultrasound has an effect on viability, reducing it to approximately 80% in a repeatable manner in all the experiments (data not shown). However, this immediate mortality did not have any influence on the results at 48h and 72h as the same concentration of cells was reseeded. After 48h and 72h, the proportion of viable cells was very high in both control and US wells. It was respectively of  $97.7 \pm 0.4$  and  $95.0 \pm 1.0$  in controls,  $96.4 \pm 0.9$  and  $94.5 \pm 0.9$  in US group. These results show that there is no delayed mortality due to US. This proportion was slightly decreased in DOX samples after 48h ( $78.4 \pm 6.2$ ) and further dropped after 72h ( $44.9 \pm 10.8$ ). These results are consistent with the mortality rate expected at 48h with a concentration of doxorubicin of 400 ng/mL. In US+DOX group, cell viability dropped more rapidly and was measured to be  $54.6 \pm 11.4\%$  after 48h and  $17.7 \pm 6.0\%$  after 72h. The difference between cell viability in DOX and US+DOX group was found to be highly significant both at 48h ( $p=0.000285$ ) and 72h ( $p=0.000381$ ) using Student tests. In both cases, cells died by apoptosis and nearly no necrotic cells were counted.

The counting of the debris by flow cytometry indicated that samples from the US+DOX group presented a much higher levels of debris at 48h than the other groups. High levels of debris were also observed at 72h in US+DOX group and

---

<sup>214</sup> Kondo and Yoshii, "Effect of Intensity of 1.2 MHz Ultrasound on Change in DNA Synthesis of Irradiated Mouse L Cells."

<sup>215</sup> Hundt et al., "Gene Expression Profiles, Histologic Analysis, and Imaging of Squamous Cell Carcinoma Model Treated with Focused Ultrasound Beams."

more moderately in DOX group. These observations are consistent with the high proportion of cell death among these samples and with the fact that cell death caused by DOX occurs only after 24-48h<sup>216</sup>.

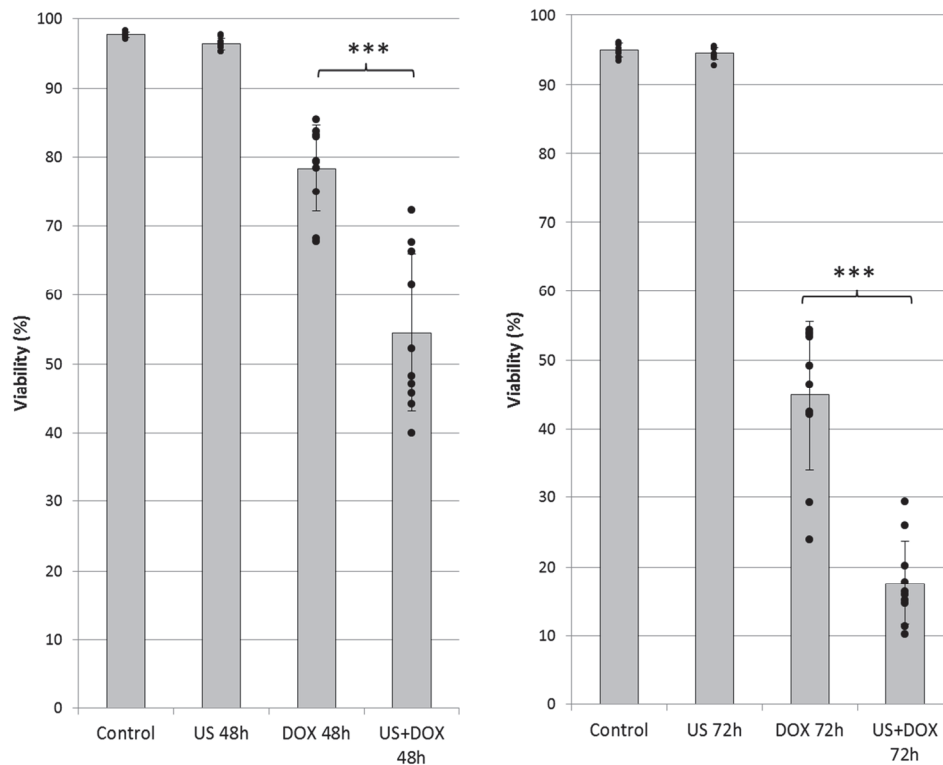


**Figure 5.2: Cell viability at 48h and 72h of cells exposed to DOX alone, controlled stable cavitation or the combination of the two. \*\*\* indicates a statistically significant difference with  $p < 0.001$  using a student test. As ultrasound alone did not involve immediate mortality, this experiment demonstrates the synergy of the combined treatment.**

### 3.1.2 Cell proliferation

Figure 5.3 shows the cell proliferation resulting from exposure to DOX, US and combined treatment. 4T1 cells have a rapid doubling time of 23h. In control samples, a proliferating index of 4 after 48h and 8 after 72h was thus expected. After 48h, cell growth index was  $4.4 \pm 0.7$  which is consistent with expectations but after 72h it was only  $6.5 \pm 1.1$ . One hypothesis is that cells had reached confluence and could not further proliferate in the wells. In US group, cell growth index was  $3.4 \pm 0.6$  after 48h and  $10.7 \pm 3.1$  after 72h. Even if the cell growth index appears to

<sup>216</sup> Al-Ghamdi, "Time and Dose Dependent Study of Doxorubicin Induced DU-145 Cytotoxicity."

be quite low at 48h, it is much higher than that of controls at 72h. These results indicate that cells that did not immediately die after US treatment not only survived, but also proliferated normally. In DOX samples, cell growth index was  $0.85 \pm 0.2$  after 48h and  $0.5 \pm 0.15$  after 72h. These results are consistent with viability data assessed by flow cytometry since there was no proliferation at all in these groups due to a halting of the cell cycle induced by DOX action. In US+DOX samples, the cell growth index was  $0.37 \pm 0.37$  after 48h and  $0.060 \pm 0.047$  after 72h. As the number of viable cells remaining in every well was extremely low, results must be interpreted cautiously. Nevertheless, we could observe that after 48h a huge difference in the viable cell number was observed between groups treated with DOX or with US+DOX. After 72h, this effect was further emphasised since the population of viable cells was divided by two with DOX while almost all the cells had died when treated with US+DOX.

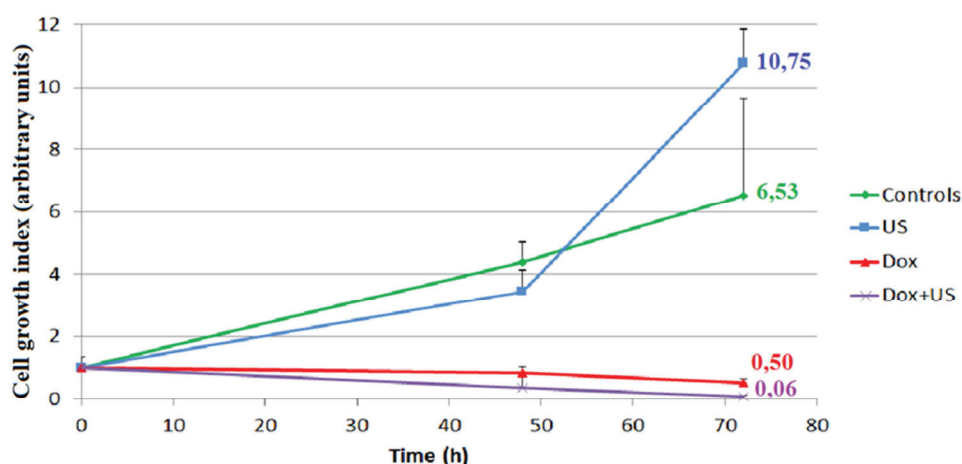


**Figure 5.3: Effect of US, DOX and combined treatment on the 4T1 tumor cell proliferation. Cells were counted at t = 0, 48 and 72h.**

## 3.2 Mechanistic study

### 3.2.1 Effect of temperature

The increase in temperature recreated using the water bath did not exactly reproduce the kinetics of the temperature elevation caused by ultrasound exposure (Figure 5.4). However, since the maximal temperature reached was the same for both US-treated samples and those exposed to a temperature 29°C and that cooling time was longer for US-treated samples, we concluded that if temperature had any effect, it would be particularly evident in samples in the water bath, especially those submitted to a temperature of 37°C.

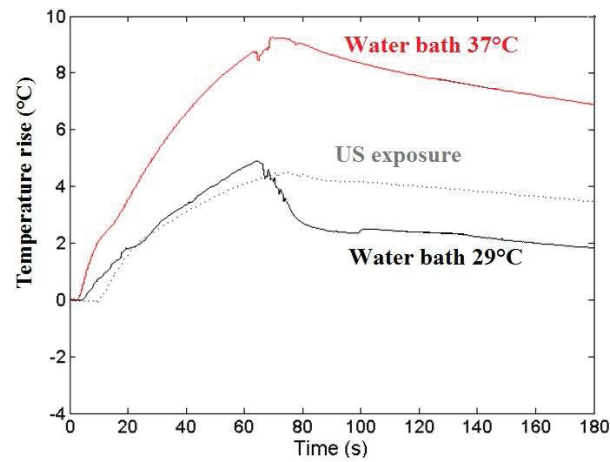


**Figure 5.4: Temperature curves measured with a thermocouple in the Eppendorf tubes when they are submitted to ultrasound exposure (US) or placed in a water bath (T=29 or T=37°C).**

No significant difference in DOX internalization after 1h or in cell death after 48 and 72 h was observed (Figure 5.5 shows only the result at 48h). Thus it is not the temperature elevation due to ultrasound that is responsible for the enhanced efficacy of the combined treatment.

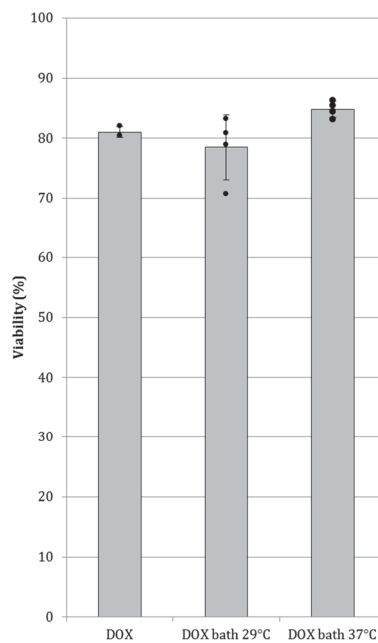


**Figure 5.5: Cell viability 48h after exposure to either DOX alone, smooth US-mimicking heating (bath 29°C) or stronger heating (bath 37°C). There is no statistically significant difference between the three conditions.**



### 3.2.2 Effect of the presence of cavitation

When boosting pulses were blocked, CIs was  $1.81 \pm 2.81$  and CI was  $9.87 \pm 0.22$ . These are both very low levels indicating that neither type of cavitation occurred. When boosting pulses were applied, CIs was  $8.07 \pm 3.19$  and CI was  $12.06 \pm 1.21$ , which is in the range of our usual values. However, evaluation of the inertial cavitation dose of such exposures with a chemical method (reaction of ROS with terephthalic acid) indicated that the dose of inertial cavitation was residual. Thus, the measured CI most likely corresponds to the contributions of the emission signal and sub-harmonic emergence. Figure 5.6 presents the resulting cell viabilities after 48 and 72 hours. No difference in cell viability after 48h or 72h of culture is observed between controls and US without cavitation whereas a therapeutic effect is visible in the presence of cavitation. This experiment proved that cavitation is required for inducing the therapeutic effect observed during the present study.

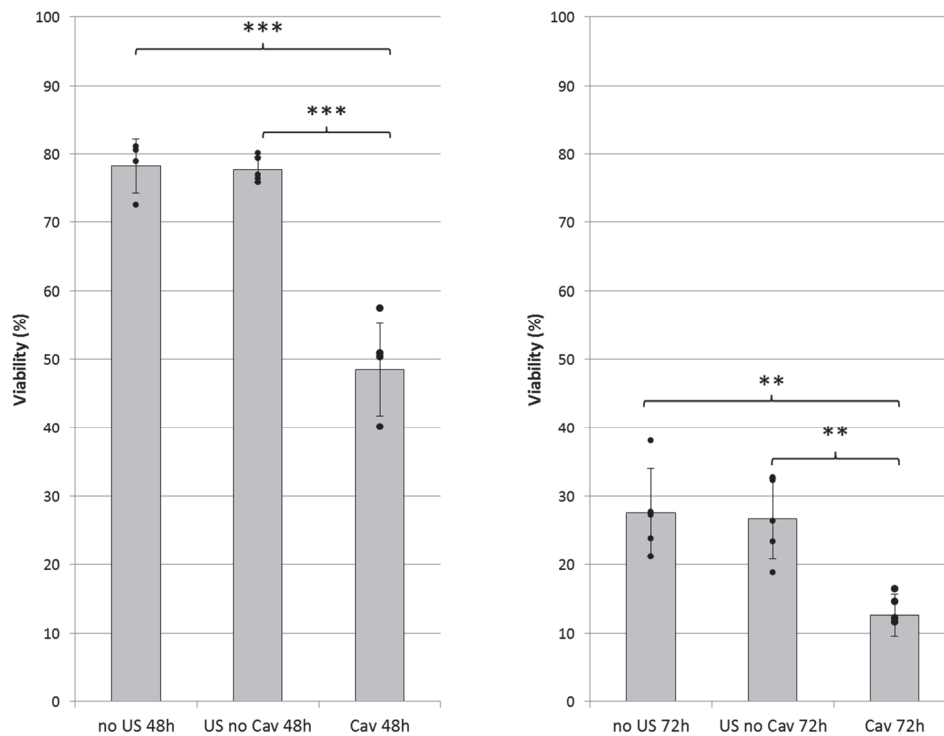


**Figure 5.6: Therapeutic efficacy (viability) at 48h and 72h of DOX alone (no US) and in combination with ultrasound without cavitation (US no Cav) or with controlled stable cavitation (Cav). \*\* and \*\*\* indicate respectively statistically significant differences  $p < 0.01$  and  $p < 0.001$  using a student test. This shows that cavitation is required to induce a beneficial effect.**

### 3.2.3 Effect of reactive oxygen species

4T1 cells were put in presence of hydroxyl scavengers L-Histidine and mannitol to assess the effect of ROS on cell proliferation and US-DOX synergy. Figure 5.7 shows the measured DOX fluorescence 1 hour after sonication as well as the cell viability after 72 hours. There is no significant increase ( $p=0.53$ , Kruskal Wallis) in the fluorescence intensity of DOX between DOX and US+DOX samples at 1h, indicating that US did not enhance the cell internalization of DOX. However, at 72h, a significant increase in DOX and DOX+Histidine samples compared to US+DOX and US+DOX+Histidine samples ( $p=0.002$ , ANOVA 1) is observed. This increase could be explained by a higher number of viable cells in those samples, as cells containing a high dose of DOX in US+DOX and US+DOX+Histidine died due to the US-DOX synergy. The proportion of viable cells 1h after sonication was significantly lower ( $p=0.00001$ , Kruskal Wallis) for sonicated samples which agrees with higher levels of debris. It can be explained by the occurrence of inertial cavitation which leads to cell lysis and important debris. Nevertheless, at 72h, cell viability was very high for both controls ( $93.2\pm0.9\%$ ), histidine ( $93.2\pm0.9\%$ ), US ( $94.6\pm1.7\%$ ) and US+Histidine samples ( $94.9\pm0.7\%$ ), thus showing that there is no US-induced delayed mortality. The cell viability dropped more rapidly in presence of DOX. For DOX and DOX + Histidine samples, the proportion of viable cells was respectively  $70.7\pm4.6\%$  and  $73.7\pm6.6\%$  whereas for US+DOX and US+DOX+Histidine samples, the proportion was respectively  $45.7\pm8.6\%$  and  $48.7\pm11.9\%$ . These results are consistent with higher debris levels for US+DOX and US+DOX+Histidine groups. The difference between cell viability in DOX and US+DOX groups was found to be highly significant ( $p=0.0001$ , Kruskal Wallis).

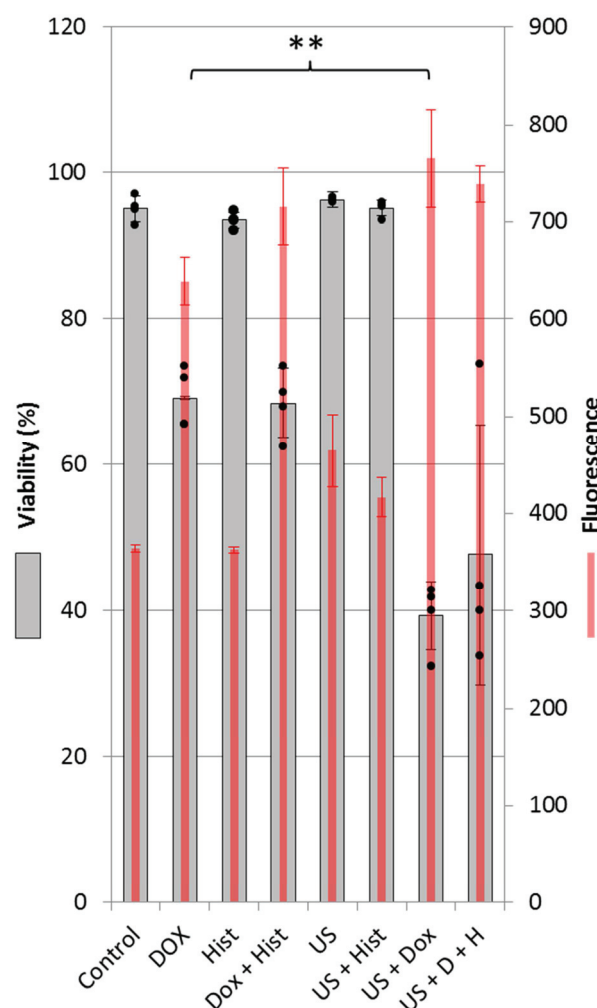


**Figure 5.7: Viability assay using Histidine, a radical scavenger, to assess the effect of ROS in the DOX-US synergetic interaction. However, no inhibition of this effect is observed in presence of Histidine. The superimposed red bars indicate the measured fluorescence of the samples, representative of the doxorubicin penetration. Error bars denote for standard deviation.**

As indicated previously, 4T1 have a rapid doubling time of 23h. The Figure 5.8 shows the cell proliferation 72 hours after sonication. At 72h, the cell growth index was around 12 for controls, histidine, mannitol, US and US+Histidine groups. These values, in combination with the viability results, indicate that the immediate mortality induced by US exposure is a reversible phenomenon. Cell proliferation index was  $0.99 \pm 0.4$ ,  $1.3 \pm 0.8$ ,  $0.5 \pm 0.4$  and  $0.5 \pm 0.6$  for DOX, DOX+Histidine, US+DOX and US+DOX+Histidine samples, respectively (Figure 5.8). These results are consistent with viability data assessed by flow cytometry,

assuming that there was no proliferation at all in these groups due to the inhibition of the cell cycle caused by the action of DOX. Consistent with the results from the previous experiment, cell proliferation index was significantly different between DOX and DOX+Histidine samples and sonicated ones ( $p=0.02$ , Kruskal Wallis). However, this index was not statistically significantly different between DOX+US and DOX+US+Histidine samples. If the synergy between DOX and US was caused by free radicals, inhibiting these ROS would lead to inhibition of the synergy and an increase in cell proliferation as a result, which is not the case in this experiment. In addition, we notice that cell proliferation in DOX+Histidine group is higher than 1, which means that the anti-proliferative effect of DOX was inhibited. We can hypothesize that one of the DOX mechanisms is regulated by free radical production and is thus inhibited by the addition of hydroxyl radical scavenger L-Histidine.

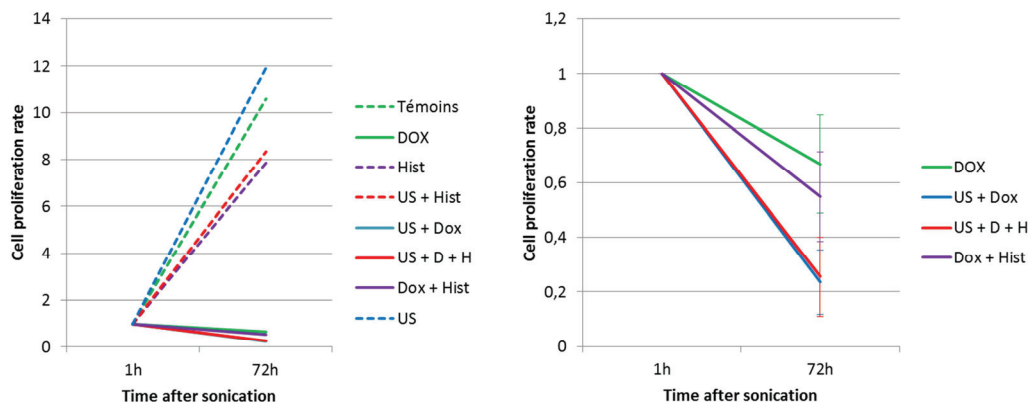


**Figure 5.8: Cell proliferation rate while adding Histidine to block the effect of the ROS. The plot on the right is a zoom on lower part of the plot on the left. Error bars correspond to standard deviation.**

Mannitol, another radical scavenger, has a range of action wider than L-Histidine. However, the same experiments conducted afterward with Mannitol using the same procedure gave exactly the same results (data not shown).

### 3.2.4 Microscope observations

Observation of sonicated 4T1 cells directly after sonication with or without doxorubicin showed no difference between sonicated and unsonicated 4T1 cells. We did not see any morphological difference on the shape of the cell, the cell membrane, the nuclear membrane or the cell organelles between sonicated and unsonicated cells. Moreover, pores can be observed on the cell membranes.

However, these findings are present both in sonicated and unsonicated cells. Example images of these pores are shown on Figure 5.9. The quantity of nuclear pore complexes was the same in all samples ( $\text{NPC} = 24 \pm 2$  for each sample).

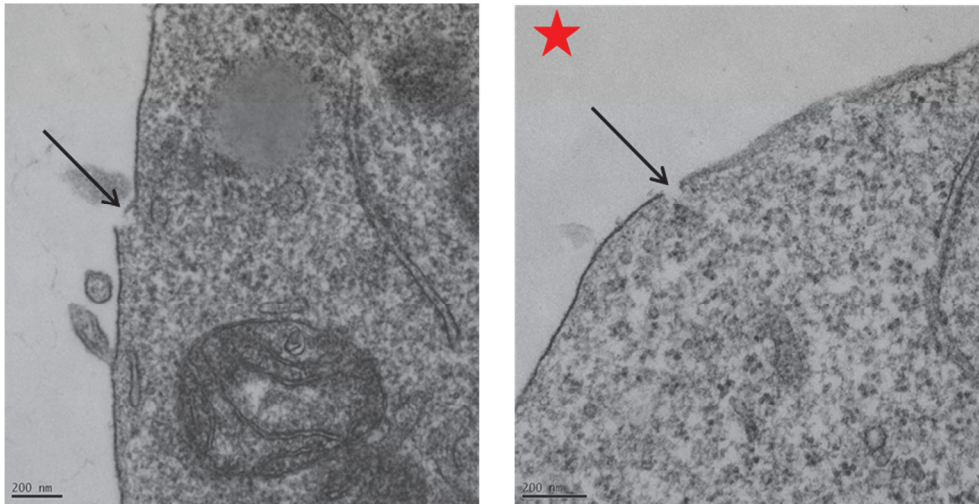


**Figure 5.9: Images examples of pores in the cell membranes in both sonicated and unsonicated cells. The pores are pointed by the black arrows. The red star denotes for the cell that received ultrasound.**

## 4 Discussion

The aim of this study was to evaluate the effect of US on the potentiation of DOX-induced cell death in murine 4T1 mammary tumor cells *in vitro*, using the confocal device called Cavibox®.

Firstly, we designed a strategy to generate stable cavitation in a controlled and reproducible manner. We determined optimized US parameters to induce stable cavitation. These parameters (PRF of 25 Hz, 6600-cycles pulses, 60 seconds of exposure) were shown to be capable of establishing a regimen of stable cavitation in exposed samples, requiring approximately 2.7% of boosting pulses to maintain cavitation all along the exposure. We also studied a potential synergetic effect of DOX and US. We showed that the action of US combined to that of DOX had both a higher and a faster therapeutic effect on tumor cells. These results appear to support a potential synergy. These experiments showed that ultrasound did not induce delayed cell mortality. Indeed, cells that were exposed to US proliferate the same way as those in the control group.

Finally, these experiments further highlighted the mechanisms of action of US. We proved that, for the same amount of energy deposited in the exposed

sample, no therapeutic effect was visible in the absence of cavitation. Therefore, cavitation was a key factor for the potentiation of DOX in 4T1 cells *in vitro*. We also showed that temperature elevations caused by US exposure had no effect in our *in vitro* experiments, which were maintained at room temperature.

But the most important and intriguing point comes from the absence of DOX internalization after US treatment. Indeed, the starting hypothesis was that US-induced cavitation would enhance the intracellular delivery of drugs by transiently increasing the cell membrane permeability. The duration of this increased permeability, termed temporal window, has been studied in 4T1 cells and estimated to be 3h.<sup>217</sup>

To explain our observations, we worked on the kinetics of DOX. DOX is a small molecule (molecular weight: 532g.mol<sup>-1</sup>). Its transport across cell membranes takes place by simple Fickian diffusion<sup>218</sup>. The equilibrium between intracellular and extracellular concentration of DOX is rapidly obtained. However, it was estimated that in our experimental conditions cells were in presence of DOX for approximately one hour and a half before flow cytometry analysis. One potential explanation is that at the time of flow cytometry analysis the equilibrium was already reached. In literature, no information is given on the time between addition of the drug and internalization analysis. It was hypothesized that the appearance of transient pores due to US exposure facilitated the passage of the drug into the cells, thus reaching equilibrium in a much faster manner. As a result, if the measurements of DOX internalization were to be performed during this period of reaching equilibrium, more drug would be counted in cells exposed to US than in the other samples. This hypothesis was weakened by an experiment held by another team working on the Cavibox®. In this experiment, suspension-growing K562 lymphoma cells were treated with DOX+US using slightly different ultrasound settings (PRF of 250Hz, 660-cycle pulses, exposure of 45s). Flow cytometry analysis was performed immediately after US exposure and 1 h after. An increase of 30% in DOX internalization was observed in both cases.

Based on these observations, we can speculate that the increase in membrane permeability might be dependent on the cell line. This hypothesis could be tested by applying our ultrasonic settings on the K562 cell line and analysing if there is still an increase in DOX internalization. In that case, the absence of an increased DOX internalization would not be due to US settings but

---

<sup>217</sup> Lammertink et al., "Duration of Ultrasound-Mediated Enhanced Plasma Membrane Permeability."

<sup>218</sup> Dalmark and Storm, "A Fickian Diffusion Transport Process with Features of Transport Catalysis. Doxorubicin Transport in Human Red Blood Cells."

to the cells. Also, it has to be considered that US exposures were performed in Eppendorf tubes that are not totally acoustically transparent. Thus, a standing wave pattern is occurring in the tube. It is possible that this has an influence on the efficacy of the device. No experiment with particular acoustically transparent material was performed. Indeed, this device is routinely used on several parallels studies in other laboratories. Thus, the use of standard consumable permits a better reciprocity between the different studies.

However, even without an increase in DOX internalization, a therapeutic effect was observed. Some mechanisms have been proposed and described in the literature to explain the efficacy of US in combination with chemotherapy. In this theory, either US would enhance the cytotoxic activity of drugs and be a chemosensitizer<sup>219</sup>, or chemotherapy would enhance the effects of US and be a sonosensitizer<sup>220</sup>. In both cases, their combination results in the kind of synergetic therapeutic effect explored in sonodynamic therapy.

Therapeutic action would be the result of combined cellular stress induced by both agents. As these combined effects exceed the threshold of repair of cell damage, apoptosis is induced<sup>221</sup>. The specific action of US has a wide range of effects on cells at different levels. They can physically destabilize cell membrane. The simple effect of bubble microstreaming triggering a regimen of stable cavitation can induce cellular stress even without creating pores in the membrane. US can also disturb the cell cytoskeleton by acting on microtubules. In the latter, the interesting fact is that the effect of US on cytoskeleton does not only potentiate drugs that target microtubules but also drugs aiming at the nucleus<sup>222</sup>. Another strong mechanism is the generation of ROS-derived radicals induced by US exposure which would initiate a chain peroxidation of cell membrane lipids<sup>223</sup>. ROS are often produced by chemotherapy drugs, including DOX<sup>224</sup>.

Some simple experiments could be performed to further elucidate the specific mechanism involved in the combined action of US exposure and DOX. The kinetics of action can be studied by simply adding DOX either before or after US

---

<sup>219</sup> Yu et al., "Ultrasound."

<sup>220</sup> Rosenthal, Sostaric, and Riesz, "Sonodynamic Therapy—a Review of the Synergistic Effects of Drugs and Ultrasound."

<sup>221</sup> Trendowski, "The Promise of Sonodynamic Therapy."

<sup>222</sup> Ibid.

<sup>223</sup> Rosenthal, Sostaric, and Riesz, "Sonodynamic Therapy—a Review of the Synergistic Effects of Drugs and Ultrasound."

<sup>224</sup> Carvalho et al., "Doxorubicin."



exposure. If no synergetic effect is found when DOX is added after US exposure, US would rather act as a chemosensitizer. The production of ROS induced by US can also be assessed by using radical scavengers. Our team worked on this project and it appears that even in a regimen of stable cavitation, some ROS are produced due to a residual level of inertial cavitation. However, experiments showed that the radical scavengers were not able to suppress the synergetic interaction between stable cavitation and doxorubicin. It is thus quite surprising that cavitation potentiates the doxorubicin by neither higher internalization nor sonodynamic interaction based on ROS. One interesting hypothesis could be found in the double-strand breaks of DNA that could be induced by mechanical consequences of cavitation<sup>225</sup>. This would add to the cells a dual stress on its DNA (doxorubicin intercalation and double-strand breaks by ultrasound) which might induce the cell death.

Mechanisms of US-induced effects are far from being fully elucidated and this research, although very interesting, could rapidly turn out as time-consuming. Our priority now is to bridge the gap between *in vitro* and *in vivo* experiments to confirm the potentiation of US+DOX combination in a murine model of 4T1 mammary tumors. Limitations include adaptation of US settings from cells in a plastic tube to *in vivo* tissues, a medium with very different properties. Whereas in Eppendorf tubes stirring of the cell medium practically ensures the passage of most cells through the focal point of the US beam, this phenomenon would be absent in tissues. The solution is to scan the tumor area in order to deposit the same energy in every part of the tumor. Exposure time and speed of tumor scanning would need to be determined beforehand. Another important issue to address is the adjustment of the DOX concentrations used in our *in vitro experiments* to the quantity of DOX injected in mice and thus the effective quantity of DOX that will reach the tumor.

## 5 Conclusion

In this study, we designed an efficient strategy to produce stable cavitation in a controlled and reproducible manner. The created stable cavitation regimen was demonstrated to induce a synergetic effect with doxorubicin on viability and proliferation of 4T1 tumor cells *in vitro*. The underlying mechanism was investigated. The quantity of internalized doxorubicin was not increased. Neither US-induced temperature elevations, nor generation of ROS had any influence on

---

<sup>225</sup> Furusawa et al., "Effects of Therapeutic Ultrasound on the Nucleus and Genomic DNA."



the enhanced efficacy of the treatment. Nevertheless, we demonstrated that cavitation is necessary to produce this effect. Observations with an electronic transmission microscope did not reveal any morphological changes caused by our ultrasound parameters.

# **Chapter 6: Unseeded controlled stable cavitation for potentiation of doxorubicin. Preclinical study on 4T1 tumor in mice**

## **1 Introduction**

Previous experiments permitted to show the synergetic effect between doxorubicin and acoustic exposures inducing stable cavitation *in vitro* on 4T1 tumor cells. The aim of the present study is to investigate whether this combination of DOX and US, particularly stable acoustic cavitation, can enhance the efficacy of DOX on 4T1 cell death *in vivo*. 4T1 murine breast cancer can be grown *in vivo* and to form mammary carcinomas as a primary tumor in BALB/c mice<sup>226</sup> that can be used for *in vivo* efficacy study. Furthermore, this cell line is well-characterized and very sensitive to DOX. The follow-up of four groups of mice (vehicle, US alone, DOX alone, DOX + US) over a few weeks with weekly treatments permits to assess i) the reproducibility of stable cavitation induction *in vivo*, ii) the actual efficacy of the combined treatment on tumor growth, iii) the survival rate and iv) the impact of repeated US exposures on metastatic spreading.

## **2 Methods**

### **2.1 Cell culture conditions**

4T1 tumor cells were grown as monolayer at 37°C in a humidified atmosphere (5% CO<sub>2</sub>, 95% air). The culture medium was RPMI 1640 containing 2mM L-glutamine (Lonza, Verviers, Belgium) supplemented with 10% fetal bovine serum (Lonza). The cells are adherent to plastic flasks. For experimental use, tumor cells were detached from the culture flask by a 5-minute treatment with trypsin-versene (Lonza), in Hanks' medium without calcium or magnesium (Lonza) and neutralized by addition of complete culture medium. The cells were counted in a hemocytometer and their viability was assessed by 0.25% trypan blue exclusion assay.

---

<sup>226</sup> Pulaski and Ostrand-Rosenberg, "Mouse 4T1 Breast Tumor Model."

## 2.2 Use of Animals

### 2.2.1 Animals

Forty two healthy female Balb/C (BALB/cByJ) mice, of matching age and weight (approximately 20g), were obtained from CHARLES RIVER (L'Arbresles). Animals were maintained in SPF health status according to the FELASA guidelines. Animal housing and experimental procedures were realized according to the French and European Regulations and NRC Guide for the Care and Use of Laboratory Animals. Animal facility is authorized by the French authorities (Agreement N° B 21 231 011 EA). All procedures using animals were submitted to the Animal Care and Use Committee of Oncodesign (Oncomet) agreed by French authorities (CNREEA agreement N° 91). Animals were individually identified with ear tags/RFID transponder. Each cage was labeled with a specific code.

### 2.2.2 Induction of 4T1 tumors in animals

Mice were anaesthetized with gaseous Isoflurane (Aerrane, Baxter SAS, France) and a 5-mm incision was made in the skin over the lateral thorax to expose the upper mammary fat pad (MFP). One hundred thousand ( $1.10^5$ ) 4T1 breast cells suspended in a volume of 50  $\mu$ L RPMI 1640 medium were injected into the MFP tissue by means of a tuberculin syringe taking care to avoid the subcutaneous space. After tumor cells injection, the syringe was removed and the thoracic surface was gently dabbed with a 95% ethanol-dampened cotton-swab to kill tumor cells that may leak from the injection site. The skin of mice was closed with 4-0 crinence sutures. The day of tumor implantation was considered as D0.

### 2.2.3 Euthanasia

Each animal was euthanized as it reached a defined critical ethic endpoint. These endpoints were such as signs of suffering, tumor ulceration or interfering with ambulation or nutrition, tumor exceeding 10% of the normal body weight, 20% body weight loss, neurologic signs (circling, paralysis...), poor body condition... Euthanasia of animals was performed by gas anesthesia over-dosage (Isoflurane) followed by cervical dislocation, performed by a highly skilled and trained technician. Methods used are recommended for mice and rats by European directive 2010/63/CE and the procedure describing euthanasia methods was approved by IACUC.

#### 2.2.4 Doxorubicin administration

The days of administration to mice, Doxorubicin (DOXO-cell, cell pharm) was diluted in NaCl 0.9% to 0.8 mg/mL. Based on Oncodesign historical data, the dose of 8 mg/kg is chosen because well tolerated and expected to show moderate antitumor efficacy in this tumor model. Doxorubicin and its vehicle were administered by intravenous (IV) injection at a volume of 10 mL/kg/inj (i.e for one mouse weighing 20 g, 200  $\mu$ L of test substance will be injected) according to the most recent body weight of mice.

### 2.3 Ultrasound conditions

#### 2.3.1 Ultrasound apparatus

The same preclinical ultrasound apparatus as before, termed Cavistation was used (Figure 6.1). The operating frequency was modified to 1.1 MHz. The emission signal consisted in 1650-cycle pulses with a PRF of 100 Hz (DC of 15%). This signal was generated with LabVIEW and powered by a 1 kW amplifier (E&I, Rochester, NY). The stable cavitation activity was monitored with an in-house PVDF hydrophone attached in the water tank allowing adapting the signal amplitude in order to control the stable cavitation regimen. This control is based on two pressure levels as presented in the previous chapter. Firstly, a high pressure regimen aims at initiating the cavitation cloud. Then, a lower pressure level maintains the cavitation activity in a stable regimen. These two pressure levels were determined in a parametric study phase, detailed hereafter. The cavitation activity was evaluated using the frequency content of the signal reflected on the cavitation cloud recorded by the hydrophone. As describe in Chapter 5, the stable cavitation index CIs is defined as the difference between the maximum level in the 540-560 kHz range and the mean level in the 560-600 kHz range. This characterizes the emergence of the subharmonic emitted by the bubbles oscillating in the stable regimen. The inertial cavitation index is the average difference between the levels in the 0.1-7.1 MHz range compared to this level when US is turned off. This characterizes accurately the inertial cavitation activity because of the broadband noise produced by collapsing bubbles.

#### 2.3.2 *Ex vivo* parametric study for stable cavitation generation

In order to use a set of parameters that leads to favorable conditions for a generation of stable cavitation, an *ex vivo* parametric study was conducted. In a first place, a large collection of settings was roughly investigated on the basis of

the regulation rate (the proportion of low amplitude pulses regarding to high amplitude ones). Then, additional exposures are performed around the parameters set that provide the most promising regulation rate. The explored parameters were the pulse repetition frequency (PRF of 25, 50, 100 and 250 Hz) and the couple of high/low pressures. These are respectively determined by  $A_{min}/A_{max}$  which corresponds to the amplitude instruction between 0 and 1 for the software to create the signal, before amplification. One should note that in the number of cycles in each pulse is modified according to the PRF so that the duty cycle is 15%. The exposures were performed in beef, which is less homogeneous than chicken breast, in order to create an unfavorable environment.

### 2.3.3 *In vivo* ultrasound exposure

As before, US was applied by putting the mice over the dedicated hole on the top of the Cavistation. US imaging permitted the localization of the tumor and the treatment planning. The US transducers induced cavitation in the labeled zone by successive continuous exposure lines over the 3D tumor volume, starting from the most distal plan. The energy deposition dose depending on the cavitation occurrence, the US dose is defined as the time of exposure to stable cavitation per  $\text{mm}^3$ . As the ultrasound scanning speed was 1 mm/s and the size of the cavitation was estimated at  $2 \times 2 \times 2 \text{ mm}^3$ , the dose used in this study was  $0.25 \text{ s/mm}^3$ . As an example, the total cavitation time for a tumor of  $400 \text{ mm}^3$  was 100 seconds. One should note that this time does not account for the displacements with US off between the scanned lines.

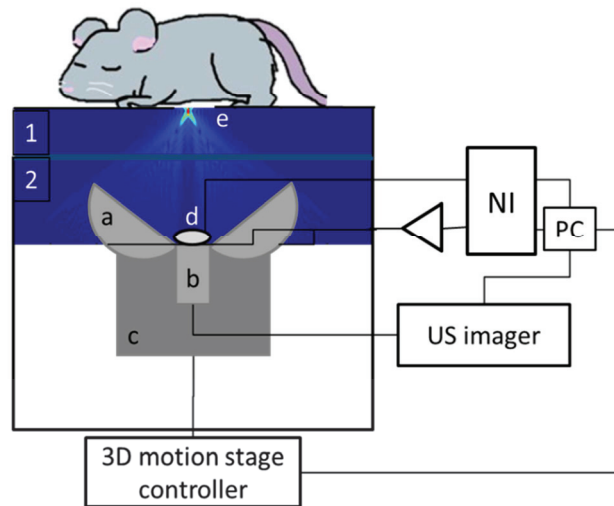


**Figure 6.1: Schematic view of the ultrasonic apparatus used for US treatments. The tank 2 is filled with degassed water. The tank 1 is filled with a**

cavitation-preventing liquid (Ablasonic, EDAP-Technomed, Vaulx-en-Velin). The two water tanks 1 and 2 are separated by a thick silicone membrane. Device composed of two independently driven piezoceramic transducers (a), an imaging probe (b) and a 3D motion stage controller (c). The animal is placed on a plastic plate and the zone of interest is sonicated through a hole in that plate (e). A computer controls the whole procedure with an in-house software. A PVDF hydrophone attached to the ultrasonic head permits to monitor the inertial cavitation activity (d)

## 2.4 Experimental design and treatments

### 2.4.1 Treatment schedule

At the time the study started, the mean volume of the tumors was 114 mm<sup>3</sup>. 32 animals out of 42 were randomized according to their individual tumor volume into 4 groups of 8 using Vivo manager<sup>®</sup> software (Biosystemes, Couternon, France). The schedule consisted in a one treatment per week during three weeks. The treatment schedule is summarized in the table below:

Group	N	Treatment	Dose	Adm. Route	Treatment schedule
1	8	Vehicle (NaCl)	-	IV	1/week, 3 weeks
2	8	DOX	8 mg/kg/inj	IV	1/week, 3 weeks
3	8	HIFU	0.25 s/mm <sup>3</sup>	-	1/week, 3 weeks
4	8	US+DOX	DOX: 8 mg/kg/inj US: 0.25 s/mm <sup>3</sup>	IV	1/week, 3 weeks

**Table 2: Treatment design. The study consists of 4 groups of 8 mice each.**

In group 4, doxorubicin was injected first, and US started 30 minutes after injection to maximize the quantity of DOX present in the tumor during the exposure, according to the literature data<sup>227</sup>. The time between injection and US

<sup>227</sup> Laginha et al., "Determination of Doxorubicin Levels in Whole Tumor and Tumor Nuclei in Murine Breast Cancer Tumors."

was measured for each mouse and differed of 1 min 40s from the fixed delay in the worst case.

#### 2.4.2 Clinical monitoring

All study data, including animal body weight measurements, tumor volume, clinical and mortality records, and treatment was scheduled and recorded on Vivo Manager® database (Biosystemes, Dijon, France). The viability and behavior were recorded every day. Body weights were measured twice a week. The length and width of the tumor were measured twice a week by the same trained technician with calipers and the volume of the tumor was estimated by the formula:

$$Tumor\ Volume = \frac{width^2 \times length}{2}$$

### 2.5 Evaluation of metastatic spreading

When injected into Balb/c mice, 4T1 spontaneously produces highly metastatic tumors that can metastasize to the lung, liver, lymph nodes and brain while the primary tumor is growing *in situ*. At sacrifice, for all mice in the study, lungs were collected, blotted dry using blotting paper, weighed using a high precision scale (Mettler, Toledo, precision: 2 mg), and the level of lung invasion was macroscopically evaluated by counting the number of metastases.

**Animals were treated in accordance with the European Union guidelines and French laws for laboratory animal care and use.**

## 3 Results

### 3.1 *Ex vivo* parametric study for stable cavitation

Figure 6.2 presents the stable cavitation regulation rates for the first step of the parametric study. Two sets of parameters were noticeably more adapted to stable cavitation regulation, one for 50 Hz of PRF and the other at 100 Hz. For numerical processing reasons the PRF of 100 Hz was more adapted to our device.

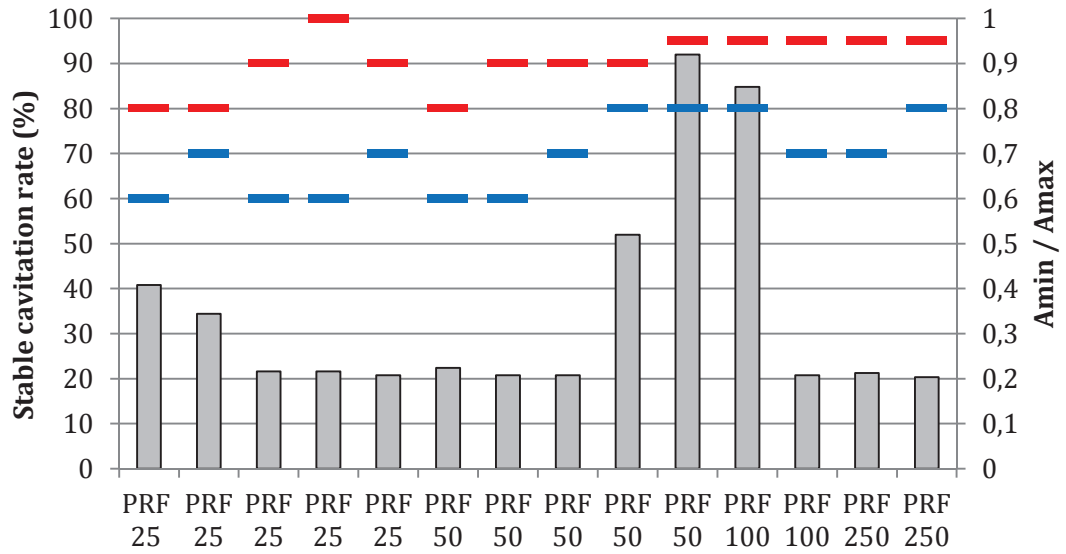


**Figure 6.2: First step of the parametric study for determining a set of parameters for efficient stable cavitation generation and regulation. Grey bars are indicating the regulation rates, defined as the proportion of low amplitude pulses aiming at just maintaining the bubble in an oscillatory motion. Blue and red bars are respectively indicating the level of low and high amplitude pulses.**

It was then performed a more detailed study around this specific condition repeated on various powers and with exposures on three different samples (Figure 6.3). This experiment permitted to obtain the amplitudes set that provide the higher stable cavitation regulation rate. Thus, we set  $A_{min} = 0.5$  and  $A_{max} = 0.85$  which correspond respectively to peak rarefaction pressures of 7 and 13 MPa. This set of parameters allows expecting a rate of around 85% of low amplitude pulses.



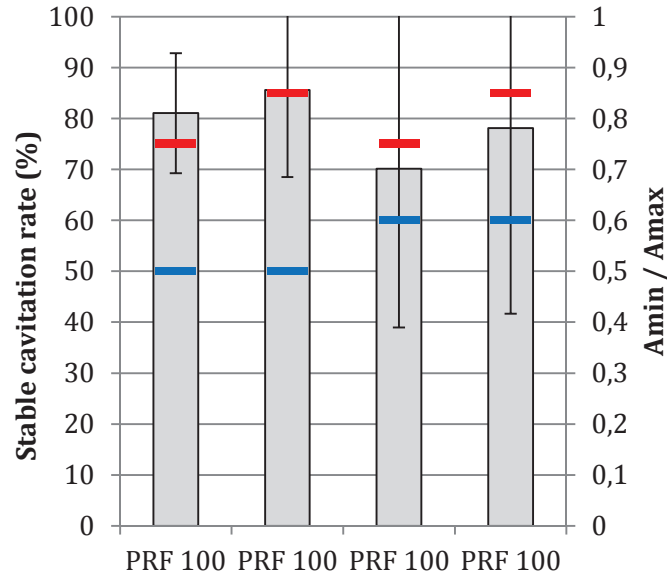


**Figure 6.3: Second step of the parametric study for determining a set of parameters for efficient stable cavitation generation and regulation. Grey bars are indicating the regulation rates, defined as the proportion of low amplitude pulses aiming at just maintaining the bubble in an oscillatory motion. Blue and red bars are respectively indicating the level of low and high amplitude pulses. Exposures were repeated on three different samples. Standard deviations of the resulting regulation rates are indicated by the error bars.**

### 3.2 Control of stable cavitation

As the backscattered signal from the bubbles was recorded, the reproducibility of cavitation exposures of the tumors can be assessed. The Figure 6.4 summarizes both the stable and the inertial cavitation activities during the three treatment sessions. The stable cavitation index remains in the vicinity of 7dB, indicating a significant emergence of the half-subharmonic. The inertial cavitation indexes were also almost constant, around 5dB. One should note that the inertial cavitation represents an elevation of the overall frequency spectrum. Thus, it is impacted by the emitted signal, as well as the presence of the subharmonic. We can consider this inertial cavitation activity as residual. The stable cavitation rate (percentage of low pressure pulses) shows that around 80% of the pulses were on low pressure mode. This proves a good efficacy of the stable cavitation control skim. Observed echo images during the ultrasound exposures (Figure 6.5) assessed the occurrence of cavitation inside the tumor volume. However, this kind of cloud was not observable all along the treatments. This can

be either because cavitation was not occurring in the right place, or because stable cavitation does not create enough reflection to be visible on echo images.

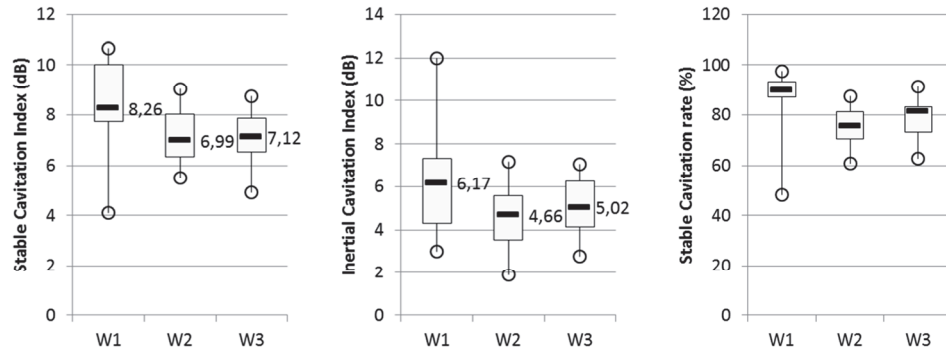


**Figure 6.4: Measurement of the stable cavitation indexes (CIs), inertial cavitation indexes (CI) and stable cavitation rate in each US-treated group during the three treatments. Bold bars are the median values, dots are the extreme values and boxes are delimited by the first and third quartile.**

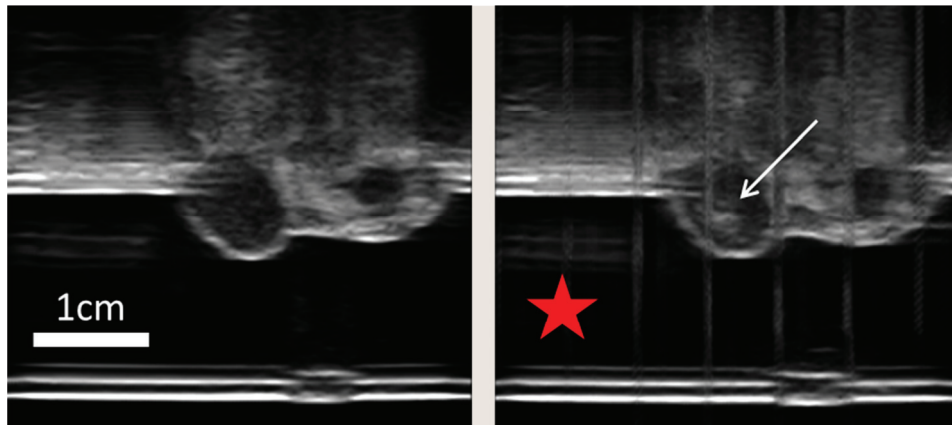


**Figure 6.5: Observation of the cavitation cloud on echo images. Left: echo image of the tumor. Right: Echo image of the tumor during the ultrasound exposure (symbolized by the red star). The white arrow indicates the location of the bubble cloud.**

### 3.3 Growth inhibition

The tumor size were measured twice a week and treated on days 10, 17 and 24. The Figure 6.6 summarizes the follow up of each group growth factor (ie. Each tumor size is normalized by its size at D10, the randomization day). Results

show that the applied ultrasonic exposure conditions did not impact the tumor growth either alone or associated with the doxorubicin treatment.

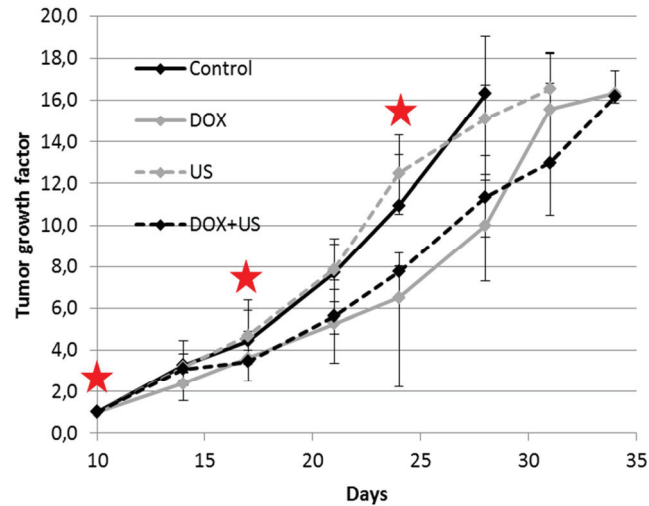


**Figure 6.6: Follow up of the mean tumor growth factors in each group. Red stars are indicating the days of treatments.**

### 3.4 Survival study

The mice were euthanized once they reach any ethical endpoint. The survival score measures the number of mice which is still under the ethical thresholds. The Figure 6.7 presents the survival score from D10 (first treatment) to D37, when the last mouse was euthanized. Ultrasound did not impact the survival score either alone or in combination with the doxorubicin treatment.

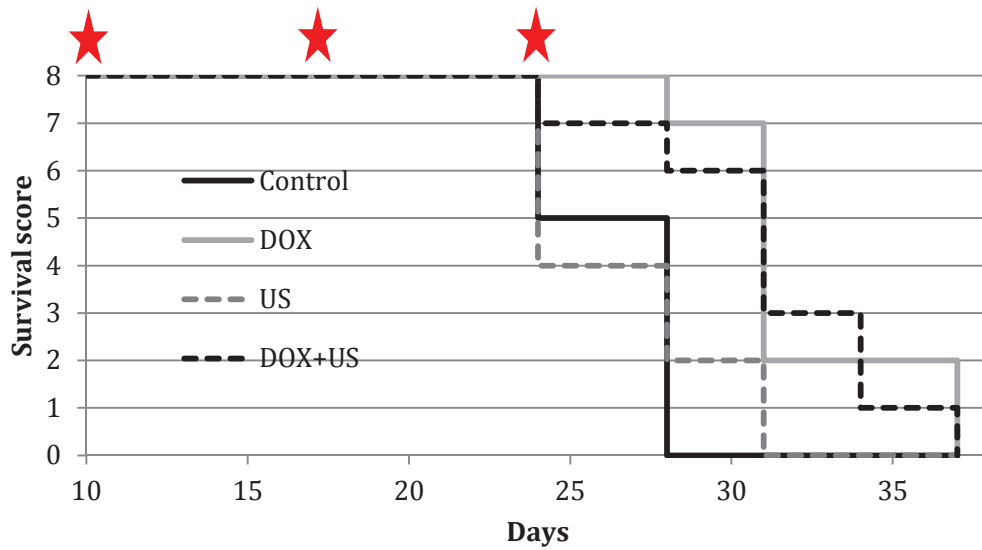


**Figure 6.7: Survival study.** The mice were euthanized when they reach an ethical endpoint, generally tumor size exceeding 1500 mm<sup>3</sup>. Red stars denote for the days of US exposure.

### 3.5 Metastatic spreading

After euthanasia, lungs were excised and lung metastases were counted macroscopically in order to assess the metastatic spreading. The Figure 6.8 presents the metastatic spreading among the four different groups. There is no statistically significant difference between US-treated groups and the others ( $p=0.19$ ). At first sight, it seems that the combination of ultrasound and doxorubicin increases the metastatic spreading. However, the two-way ANOVA analysis reveals that there is no significant interaction increasing the metastatic spreading ( $p=0.61$ ).

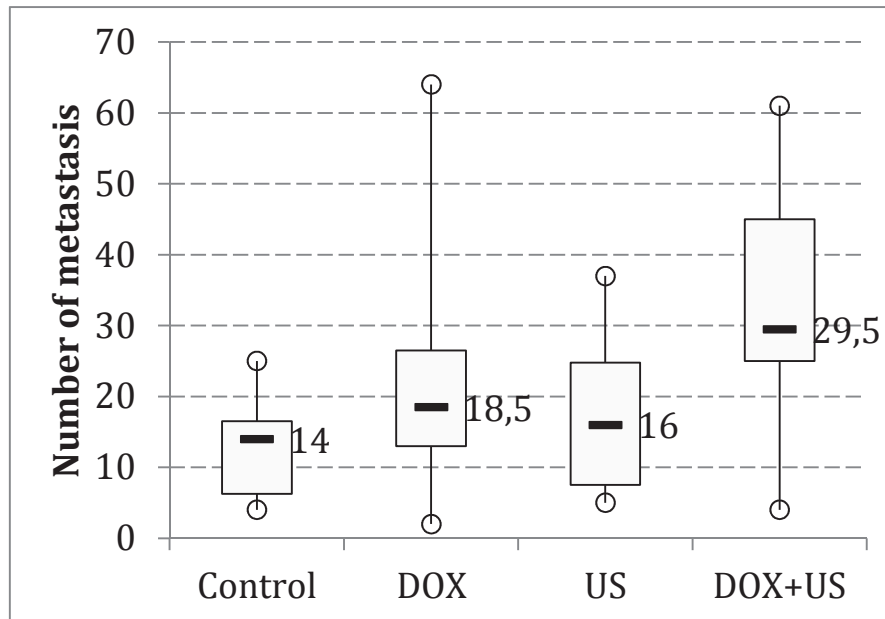


**Figure 6.8: Metastasis counting at sacrifice for the four treatment groups. Bold bars are the median values, dots are the extreme values and boxes are delimited by the first and third quartile.**

## 4 Discussion

Mice were implanted with orthotopic 4T1 mammary tumors and treated weekly either with vehicle, DOX, US or DOX+US during three weeks. US exposures consisted in a controlled alternation between high pressure and low pressure respectively to initiate and maintain a cloud of stable cavitation. The cavitation activity was measured using an integrated hydrophone. The tumor growth was measured as well as the survival rate and the metastatic spreading in the lungs after euthanasia.

The results obtained *in vitro* which have shown a decrease of the tumor cells proliferation after 72h could not be reproduced *in vivo*. Indeed, no benefit from adding US to DOX could be observed. The cavitation regimen was comparable to that obtained *in vitro*. Indeed, the spectral analysis of the emission recorded by the integrated hydrophone indicated a strong emergence of the half sub-harmonic. This emission was characteristic of bubbles oscillating in a stable manner. This emergence, calculated as the stable cavitation index was obtained for each mouse and for each treatment. Comparing all of them, it appears that the half-subharmonic was consistent (approximately 7dB) and was obtained with a high reproducibility (80% of the time in low-pressure mode). This is quite consistent to what was expected from the preliminary parametric study (85% of

the time in low-pressure mode). Moreover, inertial cavitation was not significant (5dB on inertial cavitation index, which can be considered as residual for this index). *In vitro* to *in vivo* transition is complicated and two main assumptions can be made to explain the failure to obtain any synergetic effect:

- A fundamental difference is the fact that *in vitro* cells were exposed to a strong streaming due to ultrasound. This permitted to sonicate a high volume during a large amount of time without inducing strong temperature elevations. *In vivo*, the temperature rise was steep and was a limitation in the exposure time. This was not an issue in inertial cavitation applications because of the very low duty cycle (1%) but with the 15% DC used here, the temperature elevation was evaluated to be of 2-3°C. If a longer exposure time is needed to have an effect on the DOX-US combination, the exposure parameters have to be changed to reduce the duty cycle. By doing so, stable cavitation might be harder to reach as the parameters were optimized for cavitation control. Thus a convenient strategy would be to use nucleation agents to lower the power and thus be able to maintain cavitation activity in the tumor during a larger amount of time. On one hand, this sends back to their main limitations described earlier. Notably, their low extravasation will come out on cavitation only close to the tumor vasculature.
- Considering that cavitation is occurring in the right way at the right location, the *in vivo* context implies a different physiology. As sought in our previous *in vitro* experiment presented in chapter 5, the precise nature of the DOX-US interaction is still unknown. It is thus not possible to assess whether this process is occurring *in vivo*. We can therefore emit two hypotheses. Firstly, the mechanism responsible for the *in vitro* synergy would not be induced *in vivo*. From the acoustic point of view, this would mean different mechanical constraints induced by cavitation. This is highly conceivable considering the different nature of the media. Secondly, considering that the same interaction as *in vitro* would have occurred *in vivo*, the lack of therapeutic effect would be due to improper cavitation induction (as the DOX is obviously effective for the DOX group). As it was properly controlled temporally, this is evidencing the need for an efficient spatial stable cavitation monitoring. Thus, the pursuing of the mechanistic study *in vitro* would increase the knowledge on the action of US on cells and may lead to a strategy to induce the same action *in vivo*. Also, an efficient method of spatial monitoring of stable cavitation should be included to the treatment apparatus in order to discard any doubt regarding this point.

A previous study assessed the safety of using unseeded inertial cavitation *in vivo* in the context of drug delivery<sup>228</sup>. In that particular study, ultrasonic conditions are different from the ones used here: pulses were shorter, PRF was higher as well as the reached pressures. The metastatic spreading was assessed, showing that inertial cavitation exposures did not promote it. However, a limitation was the fact that tumor were only exposed one time to cavitation. In the present study we evaluated the metastatic spreading after three US exposures. As there is no statistical difference between the US groups and the control and DOX groups, we can assume that the US parameters used here did not promote the metastatic spreading.

As in the previous *in vivo* efficacy study, the variability of the tumor growth is quite high and may have disturbed the analysis of the data. This high variability can come from the fact that because of the size distribution of tumor, particularly during the first treatment. An ideal solution would be treating every animal when their tumor is reaching the same volume. However, this constitutes an important constraint in terms of facilities availability and material transportation.

## 5 Conclusion

Antitumor effect of the combination of doxorubicin with stable cavitation was assessed *in vivo* on 4T1 tumors in Balb/c mice. No benefit of the doxorubicin with stable cavitation was evidenced. However, stable cavitation was obtained *in vivo* with a high reproducibility and it was shown that the repeated exposures did not promote metastatic spreading in the lung.

---

<sup>228</sup> Lafond et al., "Unseeded Inertial Cavitation for Enhancing the Delivery of Chemotherapies," 2016.

## Chapter 7: Development of a hydrophone-based method for cavitation localization

### 1 Introduction

In the context of clinical applications, the complete characterization of the cavitation activity includes also the cavitation localization. In this area, various methods use ultrafast echo-imaging<sup>229</sup> to locate the cloud in the uncorrelated area. Also, qualitative evaluation of cavitation presence can be performed by visualizing the hyper-echoic zone created by the bubbles<sup>230</sup>. Passive acoustic mapping is an analogue technique to beamforming that is able to reconstruct the cavitation field from the acoustic signal received on an echo-imaging probe<sup>231,232</sup>. However, these methods come with limitations. Notably, for passive cavitation mapping, the broadband frequency of the echo-imager has to be chosen carefully for the localization and the characterization of stable cavitation. Also, this requires important post-processing time preventing real-time modalities or very efficient calculation power in back-up. The cost of such equipment (ultra-fast imager, numerical apparatus to enable real-time beamforming of fast events) is prohibitive for the development of financially competitive clinical devices. If one wants to observe the cavitation cloud with the echo of the imaging pulse on the water/gas interface the cavitation activity has to be relatively intense, discarding stable cavitation from the events that could be imaged with this technique. Moreover, this does not allow for a characterization of the cavitation activity.

The anti-tumor effects obtained by cavitation-related techniques are promising<sup>233,234</sup>. However, the path toward clinical transfer of such a technique

---

<sup>229</sup> Prieur et al., "Observation of a Cavitation Cloud in Tissue Using Correlation between Ultrafast Ultrasound Images."

<sup>230</sup> Lafond et al., "Unseeded Inertial Cavitation for Enhancing the Delivery of Chemotherapies," January 1, 2016.

<sup>231</sup> Crake et al., "Passive Acoustic Mapping of Magnetic Microbubbles for Cavitation Enhancement and Localization."

<sup>232</sup> Arvanitis, Clement, and McDannold, "Transcranial Assessment and Visualization of Acoustic Cavitation."

<sup>233</sup> Mitragotri, "Healing Sound."

<sup>234</sup> Umemura, Kawabata, and Sasaki, "In Vitro and in Vivo Enhancement of Sonodynamically Active Cavitation by Second-Harmonic Superimposition."



requires proper monitoring, notably of the cavitation phenomenon. We propose to apply a source localization algorithm to cavitation monitoring and characterization. In the context of cavitation-related therapy it is expected to increase the reliability level cavitation applications, giving it more credit for clinical transfer. Also, the technique may be used as a characterization tool to optimize the efficacy of cavitation-based treatments. Concretely, we propose to explore a localization technique for cavitation localization, and estimate the reliability toward high-speed camera observations. In order to overcome the cited limitations, we intend to use a PVDF hydrophones network to localize the bubble cloud, considered as a simple acoustic source. To localize a source from receptors information, a minimum of three hydrophones are needed. The cavitation signal tends to be very unstable, and not stationary. Moreover the beginning of the signal does not correspond to the beginning of the cavitation event because of the direct waves from the emitters. Delays information is therefore extracted using maximum of inter-correlations. Also, as seen before, the cavitation cloud shows specific acoustic features such as the sub-harmonic emission. We therefore propose to reduce the frequency of interest around the sub-harmonic frequency during the data processing. By doing so, only the sound emitted by the oscillating bubbles should be taken into account.

## 2 Material and Methods

### 2.1 Ultrasonic apparatus

Two focused transducers of diameter 50 mm and with a 50 mm curvature radius, separated by a 90° angle and operating at 1.1 MHz were mounted in a manner to match their respective focus. The impedance of the parallel transducers couple was adjusted to 50 ohms to match the amplifier output. The system was placed in a tank filled with partially-degassed water (4mg/L of oxygen concentration). A single 2750-cycle pulse was generated by a digital waveform generator at a 1.4 Vrms voltage. The signal was then amplified with a 1kW RF power amplifier 1140LA (E&I, Rochester, NY). The negative pressure at the focal point was estimated to be 13 MPa. At the time of US emission, a trigger signal was sent to both the recording oscilloscope and the high-speed camera. Three in-house built PVDF hydrophones were mounted on the US setup, oriented toward the focal zone, in the same plan (Figure 7.1). The relative positions of the three hydrophones were measured using a scale picture parallel to the hydrophone plan. Signals received by the hydrophones were recorded at the trigger signal

using an oscilloscope at the sampling frequency of 100 MHz. In the meantime, the cavitation activity was observed with the high-speed camera as described below.

## 2.2 High-speed camera observations

A high-speed camera was placed perpendicularly to the plane of the three hydrophones. A red laser light was facing the camera, passing through the acoustic focal zone. This focal zone was found using a needle hydrophone. Then, the focus of the camera was adjusted to observe clearly the edge of the hydrophone. An area of 1x1.2 cm was observed. Speed recording was set to 32 kfps and 102 images were recorded. A delay of 33  $\mu$ s with the trigger signal was applied in order to observe the focal zone from the time when acoustic beams started to reach it. The 3.2 ms recorded period of time (102 images / 32 kfps) permitted to observe the 2.5 ms during those the wave is present in the focal zone (2750 cycles / 1.1 MHz). In the meantime, signals received by the hydrophones were recorded as described above. From the processed images, the positions of the clouds were estimated in a blind manner (without knowing the position of the source localized by the hydrophone) by three independent operators. The relative errors between the positions localized with the proposed method and the visually estimated cloud position were compared.

## 2.3 Acoustical localization of the cavitation cloud

A classic method for source localization is triangulation. The localization of the cavitation cloud is deduced from the delays obtained between three receptors with known positions. In our case, the receptors are PVDF hydrophones. The signals recorded during the US pulse on the digital oscilloscope were imported into Matlab software (MathWorks, Natick, MA). Then, the delays between the hydrophones were calculated by finding the delay maximizing the inter-correlation between the recorded signals. The calculated position was finally superimposed to the images from the camera. The positions calculated with this method were compared to the positions of the clouds visually estimated. The mean discrepancy was calculated. The method was firstly applied using the signals with full frequency bandwidth. Then, the post-processing operation was repeated after keeping only the broadband of 200 kHz around the sub-harmonic frequency (550 kHz).

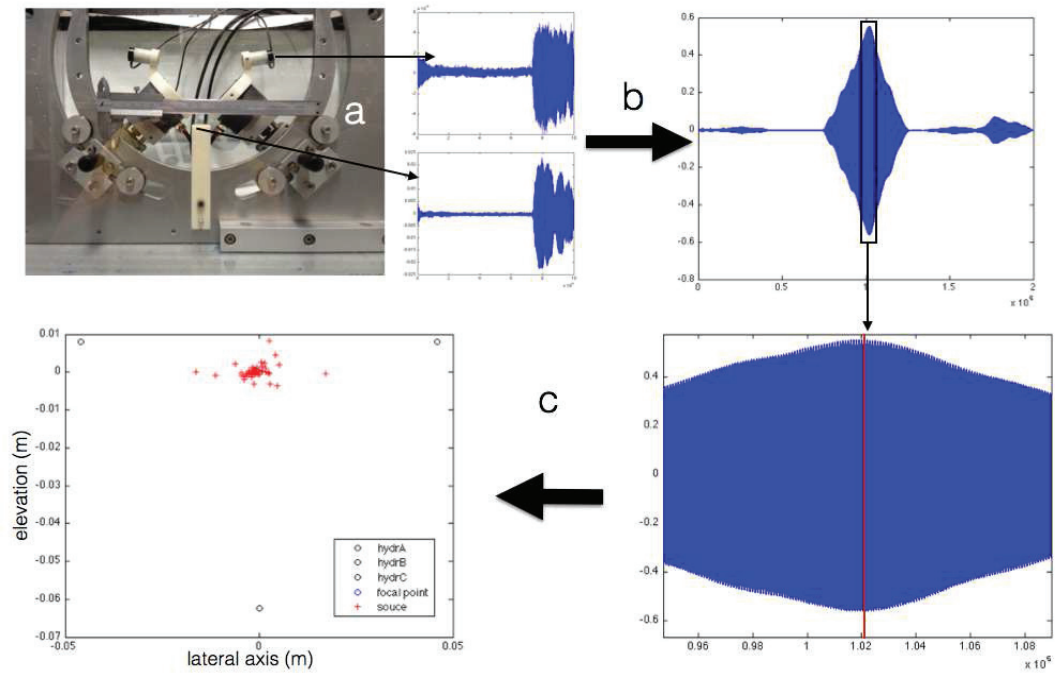


**Figure 7.1: Principle of the localization process. a) Noise emitted by the cavitation cloud is recorded by three hydrophones. b) The intercorrelations between the hydrophones are calculated and the maximum is searched. c) From the time position of the maximum corresponding to delays between the hydrophones, the source of the noise (cloud) can be localized.**

### 3 Results

Figure 7.2 presents the 60th images of the cavitation events with the superimposed positions calculated with the localization technique for each one of 8 independent pulses. The position of the cavitation cloud is calculated with a discrepancy of  $3.1 \pm 1.8$  mm in the case of the full frequency bandwidth. By processing the data only in the 200 kHz frequency band around the 550 kHz sub-harmonic, the accuracy is improved to  $1.4 \pm 0.8$  mm. The circles represent the spatial distance corresponding to the spreading of the intercorrelations (2/3 of the maximum value). The size does not correlate with the intensity of the cavitation activity. The Figure 7.3 presents the discrepancies observed as well as the mean discrepancy. The mean discrepancy indicates that there is no systematic error on the calculated cavitation localization.

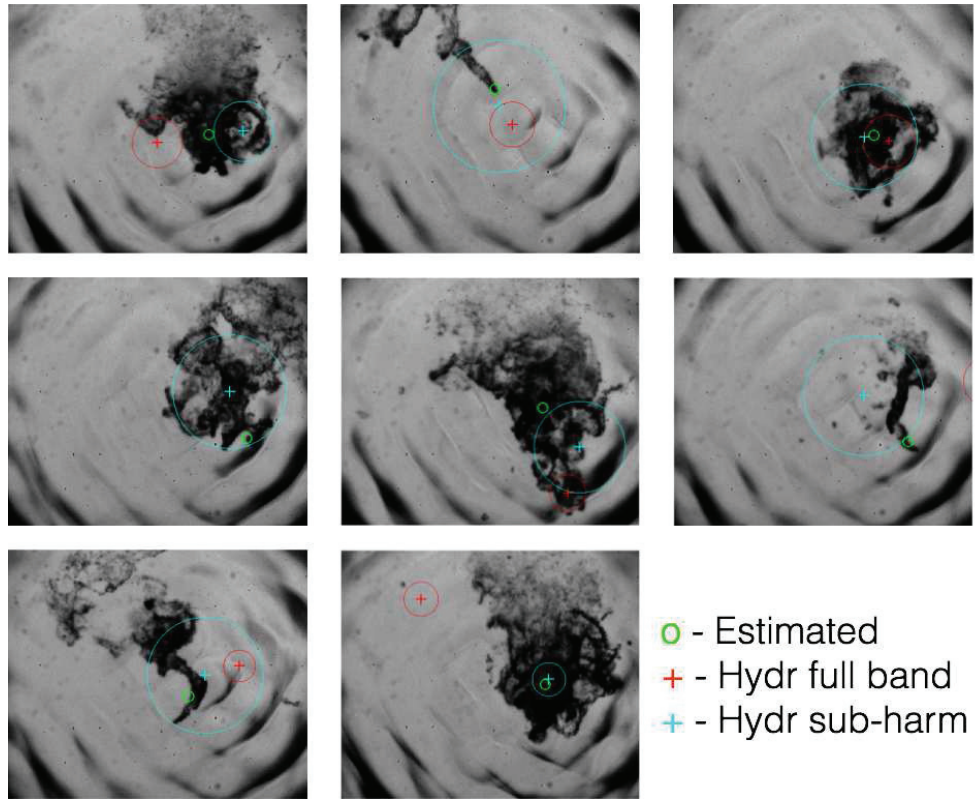


Figure 7.2: Comparisons between the calculated positions for the two frequency contents and the camera observations of the cavitation clouds for 8 independent pulses. Green circle represents the position of the focal point, the red and blue crosses are the calculated positions of the cavitation cloud for the full and reduced frequency bandwidth, respectively.

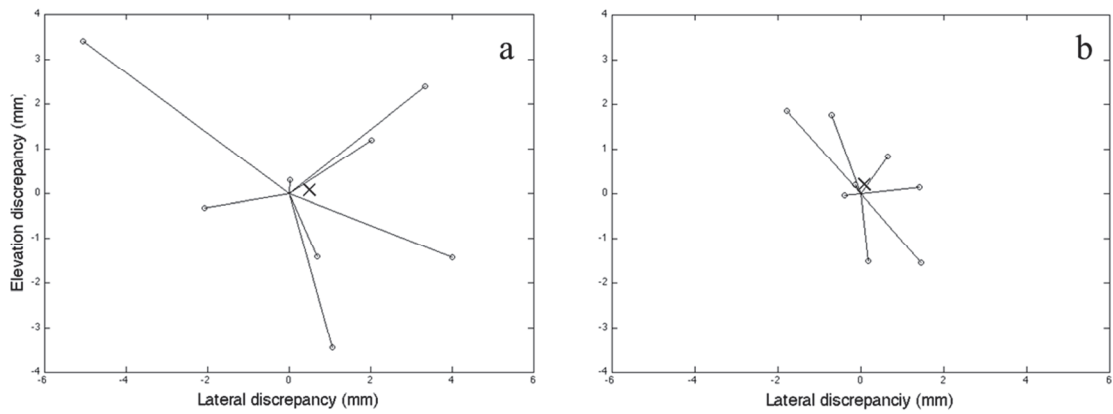


Figure 7.3: Representation of the discrepancies between the calculated and the observed positions of the cavitation cloud taking into account the full frequency bandwidth (a) or the sub-harmonic-filtered signals (b). Circles denote for single events. Crosses denote for the averaged error over the 8 events.

## 4 Discussion

A method of cavitation localization based on a three hydrophones network was explored. Localizations performed with this method were compared with high-speed observation in water. A major step of the developed method consists in calculating the delays between hydrophones. Indeed, a method based on time of arrival cannot apply to our case because of the direct waves: the hydrophones are receiving a part of the beams that create the cavitation cloud. However, as the cloud is not creating from the beginning of the pulse, the cavitation event does not correspond to the time of arrival that could be detected using the hydrophone signals. However, the delay information can be deduced from the inter-correlation between the three signals. By calculating these inter-correlations using the full frequency bandwidth or only a 200 kHz band around the 550 kHz sub-harmonic, the accuracy of the measured position was  $3.1 \pm 1.8$  mm and  $1.4 \pm 0.8$  mm, respectively. The use of the narrowed bandwidth provides a good improvement to the proposed method. Also, it can be seen on the images that the calculated position is always inside or very close to the cavitation cloud. We can therefore consider this method is accurate. However, narrowing further the frequency band resulted in an inaccurate localization. As an example, using a 100 kHz-wide frequency band resulted in accuracy comparable to that obtained with the full frequency band. This comes from the fact that inter-correlation of harmonic signals results in periodic functions. Thus, multiple lobes can appear, resulting in mistakes during the detection of the maximum. The correct estimation of the delay is permitted by the ideal proportion between cavitation noise and harmonic component to allow sufficient signal/noise ratio without a too prominent harmonic component. Another processing based on the inter-correlation of the signals deconvolved by the sub-harmonic frequency was evaluated. Although this method is known to improve correlation maps in elastography, this method gave results that were of intermediate accuracy between our non-filtered technique and the sub-harmonic-filtered one.

The technique developed in the last part of this thesis successfully achieved the first objective to localize efficiently a cavitation cloud in water. However, developments remain to be explored to improve the relevance and the promises of this technique. Concerning the accuracy of the system as presented here, different hydrophone positioning configurations have to be tried to investigate the presence of a potential optimal position for cavitation localization. Moreover, the overall device's bulk should be reduced to provide easier translation toward various kinds of applications, including its integration in *in vivo* experimental devices. Another way to reduce that bulk is to reduce the size of the hydrophones.

This would also permit to improve the accuracy. Indeed, the first hypothesis which was made in this method was that the positions of the hydrophones are known and punctual. Actually, as the hydrophones used here were about 8 mm of diameter, this might include errors in the source position calculation process.

In addition to an increased accuracy, future developments could consist in widening the range of modalities. Firstly, as the cavitation noise is recorded, it is relatively straightforward to use it as a cavitation activity quantifier. Then, this information can be included in a power regulation loop in order to control the intensity of the cavitation activity. Secondly, by arranging the hydrophone network in a different way, the algorithm can be adapted to 3D localization with a minimal added processing time. This would lead to a very time-efficient 3D cavitation imaging technique. The numerical cost of the technique can either be lightened by performing the appropriate filtering using analogic filters or by using narrow-band hydrophones with a bandwidth that fits the frequency of interest. In this study, the position of the cloud was calculated only once during the pulse. However, it might be possible to perform sweeping intercorrelations in order to track the cavitation cloud within the pulse duration. Nevertheless, this stays would stay a device for passive monitoring of the cavitation location. The final step for this technique would be the implementation on a dynamic-focus ultrasound device that could that compensates dynamically the difference between the target location and the measured one. This would permit to control spatially and in real time the position of the cavitation cloud during a US treatment.

After developing a versatile technique for full cavitation monitoring and analysis, this tool could be used *in vitro* to study the chemical reactions occurring during sonodynamic therapy in order to identify the corresponding cavitation characteristics (stable/inertial regime, intensity of the activity, size of the cavitation cloud...). The purpose of this step is to establish criteria permitting comparison between ultrasound exposure conditions and their ability to induce efficient sonodynamic effects. US parameters could therefore be improved on this basis. Also, the reliability of the developed method has to be evaluated *in vivo*. Indeed, it is still unclear how the heterogeneities will impact the accuracy of the cavitation localization.

## 5 Conclusion

An efficient, cheap and fast processing method based on the delays between three hydrophones was explored for cavitation localization. Delays were calculated using the detection of the maximum of inter-correlation. By filtering the

hydrophone signals around 550 kHz to increase the contribution of the sub-harmonic frequency; the average accuracy was  $1.4 \pm 0.8$  mm. The accuracy with the full frequency spectrum was  $3.1 \pm 1.8$  mm. No systematic discrepancy was observed. The obtained results as well as the possibilities that could be explored in the future give credit to this technique as a versatile tool for cavitation position monitoring, a major step for clinical transfer in our application as well as all those related to cavitation.



## Conclusion

This work investigated the possibility for ultrasonic cavitation to enhance the anti-tumor effect of chemotherapy, notably doxorubicin. Particularly, a synergetic effect was sought in combination to cavitation generated without adding nucleation agents. Preliminary experiments indicated a potential *in vivo* efficacy of this combination. The initial goal of this thesis was therefore to validate the concept as well as going further toward clinics, notably regarding safety concerns. Unfortunately, the performed experiments did not permit to validate the concept. The work was therefore reoriented and can finally be broken down in two parts: technical developments on cavitation generation and monitoring on one side and bioeffects of unseeded cavitation and efficacy studies on the other.

The first technical development that was performed was the realization of a simulator that permits to model the pressure fields generated with confocal transducers. Given the high intensity regimen involved by unseeded cavitation generation constraint, nonlinear effects were taken into account. The results obtained using this simulator permitted to prove the potential of this configuration for cavitation applications. Although not presented in this document, the simulator was notably use to design the geometry of a clinical apparatus. Its necessity to reach deep targets implied a high level of nonlinearity and the amount of energy that was needed to reach a target rarefaction pressure was significantly reduced. The second technical point occurred after the decision to use stable cavitation instead of inertial. Stable cavitation is ironically a very unsteady phenomenon. Fixed power ultrasound exposure failed to generate repeatable stable cavitation that gave consistent results from one experiment to another, if not one from sample to the next. Thus, a control loop based on two power regimen was designed. The high-amplitude mode permitted to initiate a bubble cloud. Then, the low-amplitude mode sustained the stable cavitation activity. These two modes were activated in regard to the cavitation noise measured in real-time with a passive cavitation detector. This strategy permitted to obtain consistent and repeatable stable cavitation exposures both *in vitro* and *in vivo*. Finally, the third technical development was on the localization of cavitation. This is of course of the utmost importance in a clinical context but also in a preclinical study as it would clearly assess the correct delivery of ultrasound energy and thus avoid a possible uncertainty in case of failure as it was the case in our study. The developed method was based on a three hydrophones network,



measuring the delays between those by inter-correlations in a frequency bandwidth that is specific to stable cavitation. This method showed a good accuracy and was the object of a patent application.

Various effects of cavitation were assessed along the studies presented here. The safety of unseeded inertial cavitation was assessed on different scales. At the molecular scale, it was shown that no modification of the doxorubicin was occurring. At the tissue scale, only moderate reversible effects were observed in various tissues types. A surprising result was on the metastasis spreading evaluation. Indeed, although the literature reports either the absence of change or a dramatic metastatic spreading depending on the ultrasound parameters and the tumor model, ours resulted in a decrease of the metastatic spreading. The suggested hypothesis was that our particular device, limiting the nonlinear distortion, permits to induce cavitation that remains quite gentle in homogeneous conditions (such as in tissues) but inducing a significant stress in asymmetric conditions such in blood-epithelium interfaces, where the tumor cells are the most likely to proliferate from. The effect on cavitation was also assessed on efficacy both *in vitro* and *in vivo*. In the first preclinical study, using inertial cavitation, no potentiation of the doxorubicin was demonstrated. However, the analysis of the doxorubicin quantity in the tumor suggested a potential enhancement of the drug retention using stable cavitation. Nevertheless, the following *in vitro* experiments did not support the hypothesis of enhanced drug penetration in cells. Still, a strong synergetic effect was observed between doxorubicin and our ultrasound exposure. Although the conducted mechanistic studies failed to evidence the precise mechanism by which the synergy is operating, it was shown that stable cavitation was necessary to trigger it. The last *in vivo* experiment was conducted in order to assess whether the synergy operating *in vitro* is also occurring in an *in vivo* context. However, no improvement on the doxorubicin efficacy was observed when combining it with stable cavitation exposures.

One would notice that the obtained results are not satisfying from a preclinical point of view in comparison with the initial expectations. However, each one of these difficulties brought opportunities for technical developments. Notably, the stable cavitation regulation strategy and the cavitation localization methods are providing new perspectives. Indeed, stable cavitation has shown a great potential in various therapeutic applications such as brain blood barrier opening. However, its use is generally limited a fixed acoustic intensity value and the stable cavitation monitoring by assessing the presence of sub-harmonic. The control of this activity is however lacking. In a drug delivery context, we showed the potential for the use

of stable cavitation *in vitro*. Although this result did not translate *in vivo*, further insights into the synergetic mechanisms that were operating could lead to successful preclinical studies in the future. Questions about safety and proper monitoring of cavitation exposures are frequently asked. Even if the work conducted in this thesis did not permitted to validate the preclinical proof of concept, answers to these challenges were partly brought. Although they have to be very specific to the application and ultrasound parameters, key safety points were assessed for our context. The cavitation localization technique is efficient and could be applied in our future drug delivery studies. More importantly, this method is not specific to the particular application described in this thesis but could benefit to every cavitation-based applications.

On the basis of the limitations encountered, future work would consist in elucidating the mechanisms of the synergetic effect observed *in vitro* and try to reproduce it in an *in vivo* context. With the cavitation generation apparatus and strategy as well as the characterization and localization techniques that were developed here, there is a potential for the development of efficient and reliable devices for various types of cavitation applications. Another step that could be considered is the mimicking of the ultrasound contrast agents dynamics based on their acoustic response in order to reproduce their bioeffects in an unseeded environment.



## References

- Adams, Monica L., Afsaneh Lavasanifar, and Glen S. Kwon. "Amphiphilic Block Copolymers for Drug Delivery." *Journal of Pharmaceutical Sciences* 92, no. 7 (July 2003): 1343–55. doi:10.1002/jps.10397.
- Ahmed, Salma E., Ana M. Martins, and Ghaleb A. Hussein. "The Use of Ultrasound to Release Chemotherapeutic Drugs from Micelles and Liposomes." *Journal of Drug Targeting* 23, no. 1 (2015): 16–42.
- Al-Ghamdi, Saeed S. "Time and Dose Dependent Study of Doxorubicin Induced DU-145 Cytotoxicity." *Drug Metabolism Letters* 2, no. 1 (2008): 47–50.
- Al-Ghazal, S. K., L. Fallowfield, and R. W. Blamey. "Comparison of Psychological Aspects and Patient Satisfaction Following Breast Conserving Surgery, Simple Mastectomy and Breast Reconstruction." *European Journal of Cancer* 36, no. 15 (October 2000): 1938–43. doi:10.1016/S0959-8049(00)00197-0.
- Anders, Carey K., Barbara Adamo, Olga Karginova, Allison M. Deal, Sumit Rawal, David Darr, Allison Schorzman, et al. "Pharmacokinetics and Efficacy of PEGylated Liposomal Doxorubicin in an Intracranial Model of Breast Cancer." *PLoS One* 8, no. 5 (2013): e61359.
- Arvanitis, Costas D., Gregory T. Clement, and Nathan McDannold. "Transcranial Assessment and Visualization of Acoustic Cavitation: Modeling and Experimental Validation." *IEEE Transactions on Medical Imaging* 34, no. 6 (June 2015): 1270–81. doi:10.1109/TMI.2014.2383835.
- Arvanitis, Costas D., Margaret S. Livingstone, Natalia Vykhodtseva, and Nathan McDannold. "Controlled Ultrasound-Induced Blood-Brain Barrier Disruption Using Passive Acoustic Emissions Monitoring." *PLoS ONE* 7, no. 9 (September 24, 2012): e45783. doi:10.1371/journal.pone.0045783.
- Ashley, Neil, and Joanna Poulton. "Mitochondrial DNA Is a Direct Target of Anti-Cancer Anthracycline Drugs." *Biochemical and Biophysical Research Communications* 378, no. 3 (2009): 450–455.
- Bailey, M. R., V. A. Khokhlova, O. A. Sapozhnikov, S. G. Kargl, and L. A. Crum. "Physical Mechanisms of the Therapeutic Effect of Ultrasound (a Review)." *Acoustical Physics* 49, no. 4 (2003): 369–388.
- Bessonova, O.V., V.A. Khokhlova, M.R. Bailey, M.S. Canney, and L.A. Crum. "FOCUSING OF HIGH POWER ULTRASOUND BEAMS AND LIMITING VALUES OF SHOCK WAVE PARAMETERS." *Acoustical Physics* 55, no. 4–5 (July 21, 2009): 463–76. doi:10.1134/S1063771009040034.
- Bohmer, M. R., C. H. T. Chlon, B. I. Raju, C. T. Chin, T. Shevchenko, and A. L. Klibanov. "Focused Ultrasound and Microbubbles for Enhanced Extravasation." *Journal of Controlled Release: Official Journal of the Controlled Release Society* 148, no. 1 (November 20, 2010): 18–24. doi:10.1016/j.jconrel.2010.06.012.
- Boucher, Y., L. T. Baxter, and R. K. Jain. "Interstitial Pressure Gradients in Tissue-Isolated and Subcutaneous Tumors: Implications for Therapy." *Cancer Research* 50, no. 15 (August 1, 1990): 4478–84.
- Bray, Freddie, Jian-Song Ren, Eric Masuyer, and Jacques Ferlay. "Global Estimates of Cancer Prevalence for 27 Sites in the Adult Population in 2008." *International Journal of Cancer* 132, no. 5 (March 1, 2013): 1133–45. doi:10.1002/ijc.27711.
- Brujan, E. A., T. Ikeda, and Y. Matsumoto. "Jet Formation and Shock Wave Emission during Collapse of Ultrasound-Induced Cavitation Bubbles and Their Role in the Therapeutic Applications of High-Intensity Focused Ultrasound." *Physics in Medicine and Biology* 50, no. 20 (2005): 4797.
- Byun, Ki-Taek, Ki Young Kim, and Ho-Young Kwak. "Sonoluminescence Characteristics from Micron and Submicron Bubbles." *Journal of the Korean Physical Society* 47, no. 6 (2005): 1010–22.

- Camarena, Francisco, Silvia Adrián-Martínez, Noé Jiménez, and Víctor Sánchez-Morcillo. "Nonlinear Focal Shift beyond the Geometrical Focus in Moderately Focused Acoustic Beams." *The Journal of the Acoustical Society of America* 134, no. 2 (August 1, 2013): 1463–72. doi:10.1121/1.4812865.
- Canney, Michael S., Vera A. Khokhlova, Olga V. Bessonova, Michael R. Bailey, and Lawrence A. Crum. "Shock-Induced Heating and Millisecond Boiling in Gels and Tissue Due to High Intensity Focused Ultrasound." *Ultrasound in Medicine & Biology* 36, no. 2 (February 2010): 250–67. doi:10.1016/j.ultrasmedbio.2009.09.010.
- Carvalho, Cristina, Renato X. Santos, Susana Cardoso, Sonia Correia, Paulo J. Oliveira, Maria S. Santos, and Paula I. Moreira. "Doxorubicin: The Good, the Bad and the Ugly Effect." *Current Medicinal Chemistry* 16, no. 25 (2009): 3267–3285.
- Chapelon, Jean-Yves, Olivier Rouvière, Sébastien Crouzet, and Albert Gelet. "Prostate Focused Ultrasound Therapy." *Advances in Experimental Medicine and Biology* 880 (2016): 21–41. doi:10.1007/978-3-319-22536-4\_2.
- Chaussy, Christian, Ch Chaussy, and others. *Extracorporeal Shock Wave Lithotripsy: Technical Concept, Experimental Research, and Clinical Application*. S Karger Ag, 1986.
- Chen, Jiayan, Chi Zhang, Fei Li, Liping Xu, Hongcheng Zhu, Shui Wang, Xiaolan Liu, et al. "A Meta-Analysis of Clinical Trials Assessing the Effect of Radiofrequency Ablation for Breast Cancer." *OncoTargets and Therapy* 9 (March 23, 2016): 1759–66. doi:10.2147/OTT.S97828.
- Chen, Wen-Shiang, Ping-Mo Ma, Hao-Li Liu, Chih-Kuang Yeh, Min-Shin Chen, and Chein-Wei Chang. "A Novel Method for Estimating the Focal Size of Two Confocal High-Intensity Focused Ultrasound Transducers." *The Journal of the Acoustical Society of America* 117 (2005): 3740.
- Chettab, Kamel, Stéphanie Roux, Doriane Mathé, Emeline Cros-Perrial, Maxime Lafond, Cyril Lafon, Charles Dumontet, and Jean-Louis Mestas. "Spatial and Temporal Control of Cavitation Allows High In Vitro Transfection Efficiency in the Absence of Transfection Reagents or Contrast Agents." *PloS One* 10, no. 8 (2015): e0134247.
- Christopher, P. Ted, and Kevin J. Parker. "New Approaches to the Linear Propagation of Acoustic Fields." *The Journal of the Acoustical Society of America* 90 (1991): 507.
- Chu, Katrina F., and Damian E. Dupuy. "Thermal Ablation of Tumours: Biological Mechanisms and Advances in Therapy." *Nature Reviews Cancer* 14, no. 3 (2014): 199–208.
- Ciuti, Piero, Nikolai V. Dezhkunov, Alberto Francescutto, Anatoly I. Kulak, and Glauco Iernetti. "Cavitation Activity Stimulation by Low Frequency Field Pulses." *Ultrasonics Sonochemistry* 7, no. 4 (2000): 213–216.
- Clarke, P. R., and C. R. Hill. "Physical and Chemical Aspects of Ultrasonic Disruption of Cells." *The Journal of the Acoustical Society of America* 47, no. 2B (1970): 649–653.
- Cliff, Walter John. *Blood Vessels*. CUP Archive, 1976.
- Collis, James, Richard Manasseh, Petar Liovic, Paul Tho, Andrew Ooi, Karolina Petkovic-Duran, and Yonggang Zhu. "Cavitation Microstreaming and Stress Fields Created by Microbubbles." *Ultrasonics* 50, no. 2 (2010): 273–279.
- Coussios, Constantin C., and Ronald A. Roy. "Applications of Acoustics and Cavitation to Noninvasive Therapy and Drug Delivery." *Annual Review of Fluid Mechanics* 40, no. 1 (2008): 395–420. doi:10.1146/annurev.fluid.40.111406.102116.
- Crake, Calum, Marie de Saint Victor, Joshua Owen, Christian Coviello, Jamie Collin, Constantin-C. Coussios, and Eleanor Stride. "Passive Acoustic Mapping of Magnetic Microbubbles for Cavitation Enhancement and Localization." *Physics in Medicine and Biology* 60, no. 2 (January 21, 2015): 785–806. doi:10.1088/0031-9155/60/2/785.
- Croset, Martine, Delphine Goehrig, Agnieszka Frackowiak, Edith Bonnelye, Stéphane Ansieau, Alain Puisieux, and Philippe Clézardin. "TWIST1 Expression in Breast Cancer Cells Facilitates Bone Metastasis Formation." *Journal of Bone and Mineral Research* 29, no. 8 (August 1, 2014): 1886–99. doi:10.1002/jbmr.2215.
- Crum, Lawrence A. "Bjerknes Forces on Bubbles in a Stationary Sound Field." *The Journal of the Acoustical Society of America* 57 (1975): 1363.

- Dalmark, Mads, and H. H. Storm. "A Fickian Diffusion Transport Process with Features of Transport Catalysis. Doxorubicin Transport in Human Red Blood Cells." *The Journal of General Physiology* 78, no. 4 (1981): 349–364.
- De Cock, Ine, Elisa Zagato, Kevin Braeckmans, Ying Luan, Nico de Jong, Stefaan C. De Smedt, and Ine Lentacker. "Ultrasound and Microbubble Mediated Drug Delivery: Acoustic Pressure as Determinant for Uptake via Membrane Pores or Endocytosis." *Journal of Controlled Release* 197 (January 10, 2015): 20–28. doi:10.1016/j.jconrel.2014.10.031.
- Delalande, A., S. Kotopoulis, T. Rovers, C. Pichon, and M. Postema. "Sonoporation at a Low Mechanical Index." *Bubble Science, Engineering & Technology* 3, no. 1 (May 1, 2011): 3–12. doi:10.1179/1758897911Y.0000000001.
- Deng, Cheri X., Fred Sieling, Hua Pan, and Jianmin Cui. "Ultrasound-Induced Cell Membrane Porosity." *Ultrasound in Medicine and Biology* 30, no. 4 (April 1, 2004): 519–26. doi:10.1016/j.ultrasmedbio.2004.01.005.
- Desjouy, C., M. Fouqueray, C. W. Lo, P. Muleki Seya, J. L. Lee, J. C. Bera, W. S. Chen, and C. Inserra. "Counterbalancing the Use of Ultrasound Contrast Agents by a Cavitation-Regulated System." *Ultrasonics Sonochemistry* 26 (September 2015): 163–68. doi:10.1016/j.ultsonch.2014.12.017.
- Dhalla, Naranjan S., Rana M. Temsah, and Thomas Netticadan. "Role of Oxidative Stress in Cardiovascular Diseases." *Journal of Hypertension* 18, no. 6 (2000): 655–673.
- Diederich, Chris J. "Thermal Ablation and High-Temperature Thermal Therapy: Overview of Technology and Clinical Implementation." *International Journal of Hyperthermia* 21, no. 8 (2005): 745–753.
- Eggen, Siv, Mercy Afadzi, Esben A. Nilssen, Solveig Bjørnum Haugstad, Bjørn Angelsen, and Catharina de L. Davies. "Ultrasound Improves the Uptake and Distribution of Liposomal Doxorubicin in Prostate Cancer Xenografts." *Ultrasound in Medicine & Biology* 39, no. 7 (2013): 1255–1266.
- Eggen, Siv, Stein-Martin Fagerland, Yrr Mørch, Rune Hansen, Kishia Søvik, Sigrid Berg, Håkon Furu, et al. "Ultrasound-Enhanced Drug Delivery in Prostate Cancer Xenografts by Nanoparticles Stabilizing Microbubbles." *Journal of Controlled Release* 187 (2014): 39–49.
- Escoffre, J. M., J. Piron, A. Novell, and A. Bouakaz. "Doxorubicin Delivery into Tumor Cells with Ultrasound and Microbubbles." *Molecular Pharmaceuticals* 8, no. 3 (2011): 799–806.
- Escoffre, J.-M., A. Novell, M. de Smet, and A. Bouakaz. "Focused Ultrasound Mediated Drug Delivery from Temperature-Sensitive Liposomes: In-Vitro Characterization and Validation." *Physics in Medicine and Biology* 58, no. 22 (November 21, 2013): 8135–51. doi:10.1088/0031-9155/58/22/8135.
- Everbach, E. Carr, Inder Raj S. Makin, Mitra Azadniv, and Richard S. Meltzer. "Correlation of Ultrasound-Induced Hemolysis with Cavitation Detector Output in Vitro." *Ultrasound in Medicine and Biology* 23, no. 4 (January 1, 1997): 619–24. doi:10.1016/S0301-5629(97)00039-2.
- Evjen, Tove J., Eirik Hagtvet, Alexei Moussatov, Sibylla Røgnvaldsson, Jean-Louis Mestas, R. Andrew Fowler, Cyril Lafon, and Esben A. Nilssen. "< I> In Vivo</i> Monitoring of Liposomal Release in Tumours Following Ultrasound Stimulation." *European Journal of Pharmaceutics and Biopharmaceutics* 84, no. 3 (2013): 526–531.
- Fan, Zhenzhen, Haiyan Liu, Michael Mayer, and Cheri X. Deng. "Spatiotemporally Controlled Single Cell Sonoporation." *Proceedings of the National Academy of Sciences* 109, no. 41 (October 9, 2012): 16486–91. doi:10.1073/pnas.1208198109.
- FDA, US. "Guidance for Industry and FDA Staff Information for Manufacturers Seeking Marketing Clearance of Diagnostic Ultrasound Systems and Transducers." *Document Issued on September 9* (2008).
- Feril, Loreto B., Takashi Kondo, Zheng-Guo Cui, Yoshiaki Tabuchi, Qing-Li Zhao, Hidetaka Ando, Takuro Misaki, Hideki Yoshikawa, and Shin-ichiro Umemura. "Apoptosis Induced by the Sonomechanical Effects of Low Intensity Pulsed Ultrasound in a Human Leukemia Cell Line." *Cancer Letters* 221, no. 2 (2005): 145–152.



- Ferlay, J., E. Steliarova-Foucher, J. Lortet-Tieulent, S. Rosso, J. W. W. Coebergh, H. Comber, D. Forman, and F. Bray. "Cancer Incidence and Mortality Patterns in Europe: Estimates for 40 Countries in 2012." *European Journal of Cancer* 49, no. 6 (April 2013): 1374–1403. doi:10.1016/j.ejca.2012.12.027.
- Ferrara, Katherine W. "Driving Delivery Vehicles with Ultrasound." *Advanced Drug Delivery Reviews*, Ultrasound in Drug and Gene Delivery, 60, no. 10 (June 30, 2008): 1097–1102. doi:10.1016/j.addr.2008.03.002.
- Fleisher, Lee A., Joshua A. Beckman, Kenneth A. Brown, Hugh Calkins, Elliott L. Chaikof, Kirsten E. Fleischmann, William K. Freeman, et al. "ACC/AHA 2007 Guidelines on Perioperative Cardiovascular Evaluation and Care for Noncardiac SurgeryA Report of the American College of Cardiology/American Heart Association Task Force on Practice Guidelines (Writing Committee to Revise the 2002 Guidelines on Perioperative Cardiovascular Evaluation for Noncardiac Surgery) Developed in Collaboration With the American Society of Echocardiography, American Society of Nuclear Cardiology, Heart Rhythm Society, Society of Cardiovascular Anesthesiologists, Society for Cardiovascular Angiography and Interventions, Society for Vascular Medicine and Biology, and Society for Vascular Surgery." *Journal of the American College of Cardiology* 50, no. 17 (October 23, 2007): e159–242. doi:10.1016/j.jacc.2007.09.003.
- Fornage, Bruno D., and Rosa F. Hwang. "Current Status of Imaging-Guided Percutaneous Ablation of Breast Cancer." *AJR. American Journal of Roentgenology* 203, no. 2 (August 2014): 442–48. doi:10.2214/AJR.13.11600.
- Frenkel, Victor, Amena Etherington, Maiya Greene, Jade Quijano, Jianwu Xie, Finie Hunter, Sergio Dromi, and King CP Li. "Delivery of Liposomal Doxorubicin (Doxil) in a Breast Cancer Tumor Model: Investigation of Potential Enhancement by Pulsed-High Intensity Focused Ultrasound Exposure." *Academic Radiology* 13, no. 4 (2006): 469–479.
- Furusawa, Yukihiro, Mariame A. Hassan, Qing-Li Zhao, Ryohei Ogawa, Yoshiaki Tabuchi, and Takashi Kondo. "Effects of Therapeutic Ultrasound on the Nucleus and Genomic DNA." *Ultrasonics Sonochemistry* 21, no. 6 (2014): 2061–2068.
- Gaitan, D. Felipe, Lawrence A. Crum, Charles C. Church, and Ronald A. Roy. "Sonoluminescence and Bubble Dynamics for a Single, Stable, Cavitation Bubble." *The Journal of the Acoustical Society of America* 91, no. 6 (1992): 3166–3183.
- Gamarra, Fernando, Fritz Spelsberg, Gerhard EH Kuhnle, and Alwin E. Goetz. "High-Energy Shock Waves Induce Blood Flow Reduction in Tumors." *Cancer Research* 53, no. 7 (1993): 1590–1595.
- Gelet, A., J. Y. Chapelon, R. Bouvier, O. Rouviere, Y. Lasne, D. Lyonnet, and J. M. Dubernard. "Transrectal High-Intensity Focused Ultrasound: Minimally Invasive Therapy of Localized Prostate Cancer." *Journal of Endourology* 14, no. 6 (2000): 519–528.
- Ghoshal, Goutam, Stanley Swat, and Michael L. Oelze. "Synergistic Effects of Ultrasound-Activated Microbubbles and Doxorubicin on Short-Term Survival of Mouse Mammary Tumor Cells." *Ultrasonic Imaging* 34, no. 1 (January 2012): 15–22.
- Goertz, David E. "An Overview of the Influence of Therapeutic Ultrasound Exposures on the Vasculature: High Intensity Ultrasound and Microbubble-Mediated Bioeffects." *International Journal of Hyperthermia* 31, no. 2 (February 17, 2015): 134–44. doi:10.3109/02656736.2015.1009179.
- Goldberg, S. Nahum, G. Scott Gazelle, and Peter R. Mueller. "Thermal Ablation Therapy for Focal Malignancy: A Unified Approach to Underlying Principles, Techniques, and Diagnostic Imaging Guidance." *American Journal of Roentgenology* 174, no. 2 (2000): 323–331.
- Graham, Susan, James Kwan, Rachel Myers, Christian Coviello, Robert Carlisle, and Constantin Coussios. "Ultrasound-Mediated Drug Release from Nanoscale Liposomes Using Nanoscale Cavitation Nuclei." *The Journal of the Acoustical Society of America* 138, no. 3 (2015): 1846–1846.
- Gyöngy, Miklós, and Constantin-C. Coussios. "Passive Spatial Mapping of Inertial Cavitation during HIFU Exposure." *IEEE Transactions on Bio-Medical Engineering* 57, no. 1 (January 2010): 48–56. doi:10.1109/TBME.2009.2026907.

- Hachimine, Ken, Hirotomo Shibaguchi, Motomu Kuroki, Hiromi Yamada, Tetsushi Kinugasa, Yoshinori Nakae, Ryuji Asano, et al. "Sonodynamic Therapy of Cancer Using a Novel Porphyrin Derivative, DCPH-P-Na(I), Which Is Devoid of Photosensitivity." *Cancer Science* 98, no. 6 (June 1, 2007): 916–20. doi:10.1111/j.1349-7006.2007.00468.x.
- Hallow, Daniel M., Anuj D. Mahajan, Todd E. McCutchen, and Mark R. Prausnitz. "Measurement and Correlation of Acoustic Cavitation with Cellular Bioeffects." *Ultrasound in Medicine & Biology* 32, no. 7 (2006): 1111–1122.
- Hassan, Mariame A., Yukihiro Furusawa, Masami Minemura, Natalya Rapoport, Toshiro Sugiyama, and Takashi Kondo. "Ultrasound-Induced New Cellular Mechanism Involved in Drug Resistance," 2012. <http://dx.plos.org/10.1371/journal.pone.0048291>.
- He, Yonghong, Da Xing, Shici Tan, Yonghong Tang, and Ken-ichi Ueda. "In Vivo Sonoluminescence Imaging with the Assistance of FCLA." *Physics in Medicine and Biology* 47, no. 9 (2002): 1535.
- Hiraoka, Wakako, Hidemi Honda, Loreto B. Feril, Nobuki Kudo, and Takashi Kondo. "Comparison between Sonodynamic Effect and Photodynamic Effect with Photosensitizers on Free Radical Formation and Cell Killing." *Ultrasonics Sonochemistry* 13, no. 6 (2006): 535–542.
- Holland, Christy K., and Robert E. Apfel. "Thresholds for Transient Cavitation Produced by Pulsed Ultrasound in a Controlled Nuclei Environment." *The Journal of the Acoustical Society of America* 88 (1990): 2059.
- Hoshi, S., S. Orikasa, M. Kuwahara, K. Suzuki, K. Yoshikawa, S. Saitoh, C. Ohyama, M. Satoh, S. Kawamura, and M. Nose. "High Energy Underwater Shock Wave Treatment on Implanted Urinary Bladder Cancer in Rabbits." *The Journal of Urology* 146, no. 2 (1991): 439–443.
- Hoshi, Senji, Seiichi Orikasa, Masa-aki Kuwahara, Ken-ichi Suzuki, Syuuichi Shirai, Kazuyuki Yoshikawa, and Masato Nose. "Shock Wave and THP-Adriamycin for Treatment of Rabbit's Bladder Cancer." *Cancer Science* 83, no. 3 (March 1, 1992): 248–50. doi:10.1111/j.1349-7006.1992.tb00095.x.
- Hu, Xiaowen, Azadeh Kheirloom, Lisa M. Mahakian, Julie R. Beegle, Dustin E. Kruse, Kit S. Lam, and Katherine W. Ferrara. "Insonation of Targeted Microbubbles Produces Regions of Reduced Blood Flow within Tumor Vasculature." *Investigative Radiology* 47, no. 7 (July 2012): 398–405. doi:10.1097/RLI.0b013e31824bd237.
- Huang, Xiaoyi, Fang Yuan, Meihua Liang, Hui-Wen Lo, Mari L. Shinohara, Cary Robertson, and Pei Zhong. "M-HIFU Inhibits Tumor Growth, Suppresses STAT3 Activity and Enhances Tumor Specific Immunity in a Transplant Tumor Model of Prostate Cancer." *PloS One* 7, no. 7 (2012): e41632.
- Hundt, Walter, Esther L. Yuh, Mark D. Bednarski, and Samira Guccione. "Gene Expression Profiles, Histologic Analysis, and Imaging of Squamous Cell Carcinoma Model Treated with Focused Ultrasound Beams." *American Journal of Roentgenology* 189, no. 3 (2007): 726–736.
- Husseini, Ghaleb A., and William G. Pitt. "Micelles and Nanoparticles for Ultrasonic Drug and Gene Delivery." *Advanced Drug Delivery Reviews* 60, no. 10 (June 30, 2008): 1137–52. doi:10.1016/j.addr.2008.03.008.
- Husseini, Ghaleb A., William G. Pitt, and Ana M. Martins. "Ultrasonically Triggered Drug Delivery: Breaking the Barrier." *Colloids and Surfaces B: Biointerfaces* 123 (November 1, 2014): 364–86. doi:10.1016/j.colsurfb.2014.07.051.
- Hwang, Joo Ha, Juan Tu, Andrew A. Brayman, Thomas J. Matula, and Lawrence A. Crum. "Correlation between Inertial Cavitation Dose and Endothelial Cell Damage in Vivo." *Ultrasound in Medicine and Biology* 32, no. 10 (October 2006): 1611–19. doi:10.1016/j.ultrasmedbio.2006.07.016.
- Iernetti, G., P. Ciuti, N. V. Dezhkunov, M. Reali, A. Francescutto, and G. K. Johri. "Enhancement of High-Frequency Acoustic Cavitation Effects by a Low-Frequency Stimulation." *Ultrasonics Sonochemistry* 4, no. 3 (1997): 263–268.
- Jain, R. K. "Delivery of Molecular and Cellular Medicine to Solid Tumors." *Advanced Drug Delivery Reviews* 46, no. 1–3 (March 1, 2001): 149–68.



- Juffermans, Lynda J. M., Annemieke van Dijk, Cees A. M. Jongenelen, Benjamin Drukarch, Arie Reijerkerk, Helga E. de Vries, Otto Kamp, and René J. P. Musters. "Ultrasound and Microbubble-Induced Intra- and Intercellular Bioeffects in Primary Endothelial Cells." *Ultrasound in Medicine and Biology* 35, no. 11 (November 1, 2009): 1917–27. doi:10.1016/j.ultrasmedbio.2009.06.1091.
- Kinoshita, Manabu, and Kullervo Hynynen. "Key Factors That Affect Sonoporation Efficiency in in Vitro Settings: The Importance of Standing Wave in Sonoporation." *Biochemical and Biophysical Research Communications* 359, no. 4 (2007): 860–865.
- Koch, Sandra, Peter Pohl, Ulrich Cobet, and Nikolai G. Rainov. "Ultrasound Enhancement of Liposome-Mediated Cell Transfection Is Caused by Cavitation Effects." *Ultrasound in Medicine & Biology* 26, no. 5 (2000): 897–903.
- Kondo, Takashi, and Giichi Yoshii. "Effect of Intensity of 1.2 MHz Ultrasound on Change in DNA Synthesis of Irradiated Mouse L Cells." *Ultrasound in Medicine & Biology* 11, no. 1 (1985): 113–119.
- Kripfgans, Oliver D., J. Brian Fowlkes, Douglas L. Miller, O. Petter Eldevik, and Paul L. Carson. "Acoustic Droplet Vaporization for Therapeutic and Diagnostic Applications." *Ultrasound in Medicine & Biology* 26, no. 7 (September 2000): 1177–89. doi:10.1016/S0301-5629(00)00262-3.
- Kripfgans, Oliver D., Catherine M. Orifici, Paul L. Carson, Kimberly A. Ives, O. Petter Eldevik, and J. Brian Fowlkes. "Acoustic Droplet Vaporization for Temporal and Spatial Control of Tissue Occlusion: A Kidney Study." *IEEE Transactions on Ultrasonics, Ferroelectrics, and Frequency Control* 52, no. 7 (July 2005): 1101–10.
- Kuznetsov, V. P. "Equations of Nonlinear Acoustics." *Sov. Phys. Acoust* 16, no. 4 (1971): 467–470.
- Lafon, Cyril, Lucie Somaglino, Guillaume Bouchoux, Jean Martial Mari, Sabrina Chesnais, Jacqueline Ngo, Jean-Louis Mestas, Sigrid L. Fossheim, Esben A. Nilssen, and Jean-Yves Chapelon. "Feasibility Study of Cavitation-Induced Liposomal Doxorubicin Release in an AT2 Dunning Rat Tumor Model." *Journal of Drug Targeting* 20, no. 8 (2012): 691–702.
- Lafond, Maxime, Jean-Louis Mestas, Fabrice Prieur, Kamel Chettab, Sandra Geraci, Philippe Clézardin, and Cyril Lafon. "Unseeded Inertial Cavitation for Enhancing the Delivery of Chemotherapies: A Safety Study." *Ultrasound in Medicine & Biology* 42, no. 1 (2016): 220–231.
- Laginha, Kimberley M., Sylvia Verwoert, Gregory J. R. Charrois, and Theresa M. Allen. "Determination of Doxorubicin Levels in Whole Tumor and Tumor Nuclei in Murine Breast Cancer Tumors." *Clinical Cancer Research* 11, no. 19 (October 1, 2005): 6944–49. doi:10.1158/1078-0432.CCR-05-0343.
- Lammertink, Bart, Roel Deckers, Gert Storm, Chrit Moonen, and Clemens Bos. "Duration of Ultrasound-Mediated Enhanced Plasma Membrane Permeability." *International Journal of Pharmaceutics*, Particulate Systems in Nanomedicine Selected papers from a 2014 EWPS Workshop, 482, no. 1–2 (March 30, 2015): 92–98. doi:10.1016/j.ijpharm.2014.12.013.
- Leighton, T. *The Acoustic Bubble*. Academic press, 1994. [http://books.google.fr/books?hl=fr&lr=&id=tR-8SNimBuEC&oi=fnd&pg=PP1&dq=acoustic+bubble&ots=gWxtvs\\_kPm&sig=KKKYTzMifqz6wuZIZ4Rr3eRm5cg](http://books.google.fr/books?hl=fr&lr=&id=tR-8SNimBuEC&oi=fnd&pg=PP1&dq=acoustic+bubble&ots=gWxtvs_kPm&sig=KKKYTzMifqz6wuZIZ4Rr3eRm5cg).
- Lentacker, Ine, Ine De Cock, R. Deckers, S. C. De Smedt, and C. T. W. Moonen. "Understanding Ultrasound Induced Sonoporation: Definitions and Underlying Mechanisms." *Advanced Drug Delivery Reviews* 72 (2014): 49–64.
- Lin, Chung-Yin, Tzu-Ming Liu, Chao-Yu Chen, Yen-Lin Huang, Wei-Kai Huang, Chi-Kuang Sun, Fu-Hsiung Chang, and Win-Li Lin. "Quantitative and Qualitative Investigation into the Impact of Focused Ultrasound with Microbubbles on the Triggered Release of Nanoparticles from Vasculature in Mouse Tumors." *Journal of Controlled Release: Official Journal of the Controlled Release Society* 146, no. 3 (September 15, 2010): 291–98. doi:10.1016/j.jconrel.2010.05.033.

- Livraghi, Tito, Luigi Solbiati, M. Franca Meloni, G. Scott Gazelle, Elkan F. Halpern, and S. Nahum Goldberg. "Treatment of Focal Liver Tumors with Percutaneous Radio-Frequency Ablation: Complications Encountered in a Multicenter Study 1." *Radiology* 226, no. 2 (2003): 441–451.
- Lokerse, Wouter JM, Esther CM Kneepkens, Timo LM ten Hagen, Alexander MM Eggermont, Holger Grüll, and Gerben A. Koning. "In Depth Study on Thermosensitive Liposomes: Optimizing Formulations for Tumor Specific Therapy and in Vitro to in Vivo Relations." *Biomaterials* 82 (2016): 138–150.
- Mahmud, Abdullah, Xiao-Bing Xiong, Hamidreza Montazeri Aliabadi, and Afsaneh Lavasanifar. "Polymeric Micelles for Drug Targeting." *Journal of Drug Targeting* 15, no. 9 (January 1, 2007): 553–84. doi:10.1080/10611860701538586.
- Marmottant, Philippe, and Sascha Hilgenfeldt. "Controlled Vesicle Deformation and Lysis by Single Oscillating Bubbles." *Nature* 423, no. 6936 (May 8, 2003): 153–56. doi:10.1038/nature01613.
- Martins, Susana, Bruno Sarmento, Domingos C. Ferreira, and Eliana B. Souto. "Lipid-Based Colloidal Carriers for Peptide and Protein Delivery-Liposomes versus Lipid Nanoparticles." *International Journal of Nanomedicine* 2, no. 4 (2007): 595.
- Marty, Benjamin, Benoit Larrat, Maxime Van Landeghem, Caroline Robic, Philippe Robert, Marc Port, Denis Le Bihan, et al. "Dynamic Study of Blood-Brain Barrier Closure after Its Disruption Using Ultrasound: A Quantitative Analysis." *Journal of Cerebral Blood Flow and Metabolism: Official Journal of the International Society of Cerebral Blood Flow and Metabolism* 32, no. 10 (October 2012): 1948–58. doi:10.1038/jcbfm.2012.100.
- Matsunaga, Terry O., Paul S. Sheeran, Samantha Luois, Jason E. Streeter, Lee B. Mullin, Bhaskar Banerjee, and Paul A. Dayton. "Phase-Change Nanoparticles Using Highly Volatile Perfluorocarbons: Toward a Platform for Extravascular Ultrasound Imaging." *Theranostics* 2, no. 12 (2012): 1185–98. doi:10.7150/thno.4846.
- Maxwell, Adam D., Charles A. Cain, Alexander P. Duryea, Lingqian Yuan, Hitinder S. Gurm, and Zhen Xu. "Noninvasive Thrombolysis Using Pulsed Ultrasound Cavitation Therapy–histotripsy." *Ultrasound in Medicine & Biology* 35, no. 12 (2009): 1982–1994.
- Maxwell, Adam D., Tzu-Yin Wang, Charles A. Cain, J. Brian Fowlkes, Oleg A. Sapozhnikov, Michael R. Bailey, and Zhen Xu. "Cavitation Clouds Created by Shock Scattering from Bubbles during Histotripsy." *The Journal of the Acoustical Society of America* 130 (2011): 1888.
- Maxwell, Adam, Oleg Sapozhnikov, Michael Bailey, Lawrence Crum, Zhen Xu, Brian Fowlkes, Charles Cain, and Vera Khokhlova. "Disintegration of Tissue Using High Intensity Focused Ultrasound: Two Approaches That Utilize Shock Waves." *Acoustics Today* 8, no. 4 (2012): 24–37.
- McHale, Anthony P., John F. Callan, Nikolitsa Nomikou, Colin Fowley, and Bridgeen Callan. "Sonodynamic Therapy: Concept, Mechanism and Application to Cancer Treatment." In *Therapeutic Ultrasound*, 429–450. Springer, 2016. [http://link.springer.com/chapter/10.1007/978-3-319-22536-4\\_22](http://link.springer.com/chapter/10.1007/978-3-319-22536-4_22).
- Medina-Franco, Heriberto, Santos Soto-Germes, José L. Ulloa-Gómez, Cecilia Romero-Trejo, Norma Uribe, Carlos A. Ramirez-Alvarado, and Carlos Robles-Vidal. "Radiofrequency Ablation of Invasive Breast Carcinomas: A Phase II Trial." *Annals of Surgical Oncology* 15, no. 6 (June 2008): 1689–95. doi:10.1245/s10434-008-9875-4.
- Meijering, Bernadet DM, Lynda JM Juffermans, Annemieke van Wamel, Rob H. Henning, Inge S. Zuhorn, Marcia Emmer, Amanda MG Versteilen, et al. "Ultrasound and Microbubble-Targeted Delivery of Macromolecules Is Regulated by Induction of Endocytosis and Pore Formation." *Circulation Research* 104, no. 5 (2009): 679–687.
- Mestas, Jean-Louis, R. Andrew Fowler, Tove J. Evjen, Lucie Somaglino, Alexei Moussatov, Jacqueline Ngo, Sabrina Chesnais, et al. "Therapeutic Efficacy of the Combination of Doxorubicin-Loaded Liposomes with Inertial Cavitation Generated by Confocal Ultrasound in AT2 Dunning Rat Tumour Model." *Journal of Drug Targeting*, no. 22 (2014): 688–97.

- Mestas, Jean-Louis, Noémie Grandjean, Lina Reslan, Jean-Christophe Béra, Charles Dumontet, and Cyril Lafon. "In-vitro and in-vivo siRNA transfection by an ultrasonic confocal device." In *Acoustics 2012 Nantes*, edited by Société Française d'Acoustique. Nantes, France, 2012. <http://hal.archives-ouvertes.fr/hal-00810881>.
- Miller, Douglas L., and Chunyan Dou. "The Potential for Enhancement of Mouse Melanoma Metastasis by Diagnostic and High-Amplitude Ultrasound." *Ultrasound in Medicine & Biology* 32, no. 7 (2006): 1097–1101.
- Miller, Douglas L., Chunyan Dou, and Jianming Song. "Lithotripter Shockwave-Induced Enhancement of Mouse Melanoma Lung Metastasis: Dependence on Cavitation Nucleation." *Journal of Endourology* 18, no. 9 (2004): 925–929.
- Minchinton, Andrew I., and Ian F. Tannock. "Drug Penetration in Solid Tumours." *Nature Reviews. Cancer* 6, no. 8 (August 2006): 583–92. doi:10.1038/nrc1893.
- MIŠÍK, VLADIMÍR, and Peter Riesz. "Free Radical Intermediates in Sonodynamic Therapy." *Annals of the New York Academy of Sciences* 899, no. 1 (2000): 335–348.
- Mitragotri, Samir. "Healing Sound: The Use of Ultrasound in Drug Delivery and Other Therapeutic Applications." *Nature Reviews Drug Discovery* 4, no. 3 (March 2005): 255–60. doi:10.1038/nrd1662.
- Miyoshi, Norio, Takashi Igarashi, and Peter Riesz. "Evidence against Singlet Oxygen Formation by Sonolysis of Aqueous Oxygen-Saturated Solutions of Hematoporphyrin and Rose Bengal: The Mechanism of Sonodynamic Therapy." *Ultrasonics Sonochemistry* 7, no. 3 (2000): 121–124.
- Mo, Steven, Constantin-C. Coussios, Len Seymour, and Robert Carlisle. "Ultrasound-Enhanced Drug Delivery for Cancer." *Expert Opinion on Drug Delivery* 9, no. 12 (2012): 1525–1538.
- Molema, Grietje, Dirk KF Meijer, and Lou FMH de Leij. "Tumor Vasculature Targeted Therapies: Getting the Players Organized." *Biochemical Pharmacology* 55, no. 12 (1998): 1939–1945.
- Morton, K. I., G. R. Ter Haar, I. J. Stratford, and C. R. Hill. "Subharmonic Emission as an Indicator of Ultrasonically-Induced Biological Damage." *Ultrasound in Medicine & Biology* 9, no. 6 (November 1983): 629–33. doi:10.1016/0301-5629(83)90008-X.
- Moussatov, Alexei, Cyril Lafon, Jean-Louis Mestas, Sabine Chesnais, Jaqueline Ngo, Lucie Somaglino, and Jean-Yves Chapelon. "Stabilisation of Cavitation Zone for Therapeutic Applications." *10ème Congrès Fran\ccais d'Acoustique*, 2010. <http://hal.archives-ouvertes.fr/hal-00551185/>.
- Nejad, S. Moosavi, Hamid Hosseini, Hidenori Akiyama, and Katsuro Tachibana. "Reparable Cell Sonoporation in Suspension: Theranostic Potential of Microbubble." *Theranostics* 6, no. 4 (2016): 446–55. doi:10.7150/thno.13518.
- Nguyen, Daniel P., Stefanie Hnilicka, Bernhard Kiss, Roland Seiler, George N. Thalmann, and Beat Roth. "Optimization of Extracorporeal Shock Wave Lithotripsy Delivery Rates Achieves Excellent Outcomes for Ureteral Stones: Results of a Prospective Randomized Trial." *The Journal of Urology* 194, no. 2 (August 2015): 418–23. doi:10.1016/j.juro.2015.01.110.
- Nishikawa, Hiroki, and Yukio Osaki. "Comparison of High-Intensity Focused Ultrasound Therapy and Radiofrequency Ablation for Recurrent Hepatocellular Carcinoma." *Hepatobiliary Surgery and Nutrition* 2, no. 3 (2013): 168–170.
- Niu, Lizhi, Liang Zhou, and Kecheng Xu. "Cryosurgery of Breast Cancer." *Gland Surgery* 1, no. 2 (August 2012): 111–18. doi:10.3978/j.issn.2227-684X.2012.08.01.
- Nixdorff, U., A. Schmidt, T. Morant, N. Stilianakis, J.-U. Voigt, F. A. Flachskampf, W. G. Daniel, and C. D. Garlichs. "Dose-Dependent Disintegration of Human Endothelial Monolayers by Contrast Echocardiography." *Life Sciences* 77, no. 13 (August 12, 2005): 1493–1501. doi:10.1016/j.lfs.2005.04.011.
- Nomikou, Nikolitsa, Colin Fowley, Niall M. Byrne, Bridgeen McCaughan, Anthony P. McHale, and John F. Callan. "Microbubble-sonosensitiser Conjugates as Therapeutics in Sonodynamic Therapy." *Chemical Communications* 48, no. 67 (July 25, 2012): 8332–34. doi:10.1039/C2CC33913G.

- Nomikou, Nikolitsa, and Anthony P. McHale. "Exploiting Ultrasound-Mediated Effects in Delivering Targeted, Site-Specific Cancer Therapy." *Cancer Letters* 296, no. 2 (2010): 133–143.
- Novell, Anthony, Chantal Al Sabbagh, Jean-Michel Escoffre, Cédric Gaillard, Nicolas Tsapis, Elias Fattal, and Ayache Bouakaz. "Focused Ultrasound Influence on Calcein-Loaded Thermosensitive Stealth Liposomes." *International Journal of Hyperthermia* 31, no. 4 (May 19, 2015): 349–58. doi:10.3109/02656736.2014.1000393.
- Oosterhof, G. O. N., E. B. Cornel, GAHJ Smits, F. M. J. Debruyne, and J. A. Schalken. "The Influence of High-Energy Shock Waves on the Development of Metastases." *Ultrasound in Medicine & Biology* 22, no. 3 (1996): 339–344.
- O'Reilly, Meaghan A., and Kullervo Hynynen. "Blood-Brain Barrier: Real-Time Feedback-Controlled Focused Ultrasound Disruption by Using an Acoustic Emissions-based Controller." *Radiology* 263, no. 1 (2012): 96–106.
- Pantel, Klaus, and Ruud H. Brakenhoff. "Dissecting the Metastatic Cascade." *Nature Reviews Cancer* 4, no. 6 (2004): 448–456.
- Park, Juyoung, Zhenzhen Fan, Ronald E. Kumon, Mohamed E. H. El-Sayed, and Cheri X. Deng. "MODULATION OF INTRACELLULAR CA<sup>2+</sup> CONCENTRATION IN BRAIN MICROVASCULAR ENDOTHELIAL CELLS IN VITRO BY ACOUSTIC CAVITATION." *Ultrasound in Medicine & Biology* 36, no. 7 (July 2010): 1176–87. doi:10.1016/j.ultrasmedbio.2010.04.006.
- PDQ Adult Treatment Editorial Board. "Breast Cancer Treatment (PDQ®): Patient Version." In *PDQ Cancer Information Summaries*. Bethesda (MD): National Cancer Institute (US), 2002. <http://www.ncbi.nlm.nih.gov/books/NBK65969/>.
- Pichardo, S., A. Gelet, L. Curiel, S. Chesnais, and J.-Y. Chapelon. "New Integrated Imaging High Intensity Focused Ultrasound Probe for Transrectal Prostate Cancer Treatment." *Ultrasound in Medicine & Biology* 34, no. 7 (2008): 1105–1116.
- Pitt, William G., Ghaleb A. Hussein, and Bryant J. Staples. "Ultrasonic Drug Delivery - A General Review." *Expert Opinion on Drug Delivery* 1, no. 1 (November 2004): 37–56. doi:10.1517/17425247.1.1.37.
- Ponchon, Thierry, Alan N. Barkun, Bertrand Pujol, Jean Louis Mestas, and René Lambert. "Gallstone Disappearance after Extracorporeal Lithotripsy and Oral Bile Acid Dissolution." *Gastroenterology* 97, no. 2 (1989): 457–463.
- Postema, Michiel, Annemieke van Wamel, Folkert J. ten Cate, and Nico de Jong. "High-Speed Photography during Ultrasound Illustrates Potential Therapeutic Applications of Microbubbles." *Medical Physics* 32, no. 12 (December 1, 2005): 3707–11. doi:10.1118/1.2133718.
- Prieur, Fabrice, Ali Zorgani, Stefan Catheline, Remi Souchon, Jean-Louis Mestas, Maxime Lafond, and Cyril Lafon. "Observation of a Cavitation Cloud in Tissue Using Correlation between Ultrafast Ultrasound Images." *Ultrasonics, Ferroelectrics, and Frequency Control, IEEE Transactions on* 62, no. 7 (2015): 1256–1264.
- Pulaski, Beth A., and Suzanne Ostrand-Rosenberg. "Mouse 4T1 Breast Tumor Model." *Current Protocols in Immunology*, 2001, 20–2.
- Qin, Jiale, Tzu-Yin Wang, and Jürgen K. Willmann. "Sonoporation: Applications for Cancer Therapy." In *Therapeutic Ultrasound*, 263–291. Springer, 2016. [http://link.springer.com/chapter/10.1007/978-3-319-22536-4\\_15](http://link.springer.com/chapter/10.1007/978-3-319-22536-4_15).
- Qiu, Yuanyuan, Yi Luo, Yanli Zhang, Weicheng Cui, Dong Zhang, Junru Wu, Junfeng Zhang, and Juan Tu. "The Correlation between Acoustic Cavitation and Sonoporation Involved in Ultrasound-Mediated DNA Transfection with Polyethylenimine (PEI) in Vitro." *Journal of Controlled Release* 145, no. 1 (July 1, 2010): 40–48. doi:10.1016/j.jconrel.2010.04.010.
- Rapoport, Natalya. "Drug-Loaded Perfluorocarbon Nanodroplets for Ultrasound-Mediated Drug Delivery." In *Therapeutic Ultrasound*, edited by Jean-Michel Escoffre and Ayache Bouakaz, 221–41. *Advances in Experimental Medicine and Biology* 880. Springer International Publishing, 2016. [http://link.springer.com/chapter/10.1007/978-3-319-22536-4\\_13](http://link.springer.com/chapter/10.1007/978-3-319-22536-4_13).



- Rapoport, Natalya Y., Anne M. Kennedy, Jill E. Shea, Courtney L. Scaife, and Kweon-Ho Nam. "Controlled and Targeted Tumor Chemotherapy by Ultrasound-Activated Nanoemulsions/microbubbles." *Journal of Controlled Release: Official Journal of the Controlled Release Society* 138, no. 3 (September 15, 2009): 268–76. doi:10.1016/j.jconrel.2009.05.026.
- Rawat, Manju, Deependra Singh, S. Saraf, and Swarnlata Saraf. "Nanocarriers: Promising Vehicle for Bioactive Drugs." *Biological and Pharmaceutical Bulletin* 29, no. 9 (2006): 1790–1798.
- Razavi, Arash, David Clement, R. Andrew Fowler, Alain Birer, Françoise Chavrier, Jean-louis Mestas, Fabrice Romano, Jean-Yves Chapelon, Aurélie Béglé, and Cyril Lafon. "Contribution of Inertial Cavitation in the Enhancement of In Vitro Transscleral Drug Delivery." *Ultrasound in Medicine & Biology* 40, no. 6 (June 2014): 1216–27. doi:10.1016/j.ultrasmedbio.2013.12.032.
- Reznik, Nikita, Ross Williams, and Peter N. Burns. "Investigation of Vaporized Submicron Perfluorocarbon Droplets as an Ultrasound Contrast Agent." *Ultrasound in Medicine & Biology* 37, no. 8 (August 2011): 1271–79. doi:10.1016/j.ultrasmedbio.2011.05.001.
- Riesz, Peter, and Takashi Kondo. "Free Radical Formation Induced by Ultrasound and Its Biological Implications." *Free Radical Biology and Medicine* 13, no. 3 (1992): 247–270.
- Rizzitelli, S., P. Giustetto, D. Faletto, D. Delli Castelli, S. Aime, and E. Terreno. "The Release of Doxorubicin from Liposomes Monitored by MRI and Triggered by a Combination of US Stimuli Led to a Complete Tumor Regression in a Breast Cancer Mouse Model." *Journal of Controlled Release* 230 (May 28, 2016): 57–63. doi:10.1016/j.jconrel.2016.03.040.
- Rizzitelli, Silvia, Pierangela Giustetto, Cinzia Boffa, Daniela Delli Castelli, Juan Carlos Cutrin, Silvio Aime, and Enzo Terreno. "In Vivo MRI Visualization of Release from Liposomes Triggered by Local Application of Pulsed Low-Intensity Non-Focused Ultrasound." *Nanomedicine: Nanotechnology, Biology and Medicine* 10, no. 5 (July 1, 2014): e901–4. doi:10.1016/j.nano.2014.03.012.
- Roberts, William W., Timothy L. Hall, Kimberly Ives, J. Stuart Wolf Jr, J. Brian Fowlkes, and Charles A. Cain. "Pulsed Cavitation Ultrasound: A Noninvasive Technology for Controlled Tissue Ablation (Histotripsy) in the Rabbit Kidney." *The Journal of Urology* 175, no. 2 (2006): 734–738.
- Rooney, J.A. "Shear as a Mechanism for Sonically Induced Biological Effects." *Journal of the Acoustical Society of America* 52, no. 6B (1972): 1718–24. doi:10.1121/1.1913306.
- Rosenthal, Ionel, Joe Z. Sostaric, and Peter Riesz. "Sonodynamic Therapy—a Review of the Synergistic Effects of Drugs and Ultrasound." *Ultrasonics Sonochemistry* 11, no. 6 (2004): 349–363.
- Saad, A. H., and G. M. Hahn. "Ultrasound Enhanced Drug Toxicity on Chinese Hamster Ovary Cells in Vitro." *Cancer Research* 49, no. 21 (November 1, 1989): 5931–34.
- Sabel, Michael S., Matthew A. Nehs, Gang Su, Kathleen P. Lowler, James L. M. Ferrara, and Alfred E. Chang. "Immunologic Response to Cryoablation of Breast Cancer." *Breast Cancer Research and Treatment* 90, no. 1 (March 2005): 97–104. doi:10.1007/s10549-004-3289-1.
- Sabraoui, Abbas, Claude Inserra, Bruno Gilles, Jean-Christophe Béra, and Jean-Louis Mestas. "Feedback Loop Process to Control Acoustic Cavitation." *Ultrasonics Sonochemistry* 18, no. 2 (2011): 589–594.
- Saksena, T. K., and W. L. Nyborg. "Sonoluminescence from Stable Cavitation." *The Journal of Chemical Physics* 53, no. 5 (1970): 1722–1734.
- Sapozhnikov, Oleg A., and Michael R. Bailey. "Radiation Force of an Arbitrary Acoustic Beam on an Elastic Sphere in a Fluid." *The Journal of the Acoustical Society of America* 133, no. 2 (February 1, 2013): 661–76. doi:10.1121/1.4773924.
- Sazgarnia, Ameneh, Ahmad Shanei, Naser Tayyebi Meibodi, Hossein Eshghi, and Hooriyeh Nassirli. "A Novel Nanosonosensitizer for Sonodynamic Therapy in Vivo Study on a Colon Tumor Model." *Journal of Ultrasound in Medicine* 30, no. 10 (2011): 1321–1329.

- Schroeder, Avi, Joseph Kost, and Yechezkel Barenholz. "Ultrasound, Liposomes, and Drug Delivery: Principles for Using Ultrasound to Control the Release of Drugs from Liposomes." *Chemistry and Physics of Lipids* 162, no. 1 (2009): 1–16.
- Sheikov, Nickolai, Nathan McDannold, Natalia Vykhodtseva, Ferenc Jolesz, and Kullervo Hynynen. "Cellular Mechanisms of the Blood-Brain Barrier Opening Induced by Ultrasound in Presence of Microbubbles." *Ultrasound in Medicine & Biology* 30, no. 7 (July 2004): 979–89. doi:10.1016/j.ultrasmedbio.2004.04.010.
- Somaglino, Lucie, Guillaume Bouchoux, Jean-Louis Mestas, and Cyril Lafon. "Validation of an Acoustic Cavitation Dose with Hydroxyl Radical Production Generated by Inertial Cavitation in Pulsed Mode: Application to in Vitro Drug Release from Liposomes." *Ultrasonics Sonochemistry* 18, no. 2 (March 2011): 577–88. doi:10.1016/j.ultsonch.2010.07.009.
- Staples, Bryant J. "Pharmacokinetics of Ultrasonically-Released, Micelle-Encapsulated Doxorubicin in the Rat Model and Its Effect on Tumor Growth," 2007. <http://scholarsarchive.byu.edu/etd/900/>.
- Sugita, Nami, Ken-ichi Kawabata, Kazuaki Sasaki, Isao Sakata, and Shin-ichiro Umemura. "Synthesis of Amphiphilic Derivatives of Rose Bengal and Their Tumor Accumulation." *Bioconjugate Chemistry* 18, no. 3 (May 1, 2007): 866–73. doi:10.1021/bc060189p.
- Ta, Terence, Elizabeth Bartolak-Suki, Eun-Joo Park, Kavon M. Karrobi, Nathan J. McDannold, and Tyrone M. Porter. "Localized Delivery of Doxorubicin in Vivo from Polymer-Modified Thermosensitive Liposomes with MR-Guided Focused Ultrasound-Mediated Heating." *Journal of Controlled Release: Official Journal of the Controlled Release Society* 194 (November 28, 2014): 71–81. doi:10.1016/j.jconrel.2014.08.013.
- Ta, Terence, and Tyrone M. Porter. "Thermosensitive Liposomes for Localized Delivery and Triggered Release of Chemotherapy." *Journal of Controlled Release* 169, no. 1 (2013): 112–125.
- Tang, Wei, Quanhong Liu, Xiaobing Wang, Na Mi, Pan Wang, and Jing Zhang. "Membrane Fluidity Altering and Enzyme Inactivating in Sarcoma 180 Cells Post the Exposure to Sonoactivated Hematoporphyrin in Vitro." *Ultrasonics* 48, no. 1 (2008): 66–73.
- Tarkowski, Radoslaw, and Marek Rzaca. "Cryosurgery in the Treatment of Women with Breast Cancer—a Review." *Gland Surgery* 3, no. 2 (May 2014): 88–93. doi:10.3978/j.issn.2227-684X.2014.03.04.
- Tavakkoli, Jahangir, Dominique Cathignol, Rémi Souchon, and Oleg A. Sapozhnikov. "Modeling of Pulsed Finite-Amplitude Focused Sound Beams in Time Domain." *The Journal of the Acoustical Society of America* 104 (1998): 2061.
- Torres, Elena, Francesco Mainini, Roberta Napolitano, Franco Fedeli, Roberta Cavalli, Silvio Aime, and Enzo Terreno. "Improved Paramagnetic Liposomes for MRI Visualization of pH Triggered Release." *Journal of Controlled Release* 154, no. 2 (September 5, 2011): 196–202. doi:10.1016/j.jconrel.2011.05.017.
- Trendowski, Matthew. "The Promise of Sonodynamic Therapy." *Cancer and Metastasis Reviews* 33, no. 1 (December 18, 2013): 143–60. doi:10.1007/s10555-013-9461-5.
- Ugarenko, Michal, Chee-Kai Chan, Abraham Nudelman, Ada Rephaeli, Suzanne M. Cutts, and Don R. Phillips. "Development of Pluronic Micelle-Encapsulated Doxorubicin and Formaldehyde-Releasing Prodrugs for Localized Anticancer Chemotherapy." *Oncology Research Featuring Preclinical and Clinical Cancer Therapeutics* 17, no. 7 (January 1, 2009): 283–99. doi:10.3727/096504009787721212.
- Umemura, Shin-ichiro, Ken-ichi Kawabata, and Kazuaki Sasaki. "In Vitro and in Vivo Enhancement of Sonodynamically Active Cavitation by Second-Harmonic Superimposition." *The Journal of the Acoustical Society of America* 101, no. 1 (1997): 569–577.
- Umemura, Shin-ichiro, Nagahiko Yumita, Ryuichiro Nishigaki, and Koshiro Umemura. "Mechanism of Cell Damage by Ultrasound in Combination with Hematoporphyrin." *Japanese Journal of Cancer Research* 81, no. 9 (1990): 962–966.

- Umemura, Shin-ichiro, Nagahiko Yumita, Koshiro Umemura, and Ryuichiro Nishigaki. "Sonodynamically Induced Effect of Rose Bengal on Isolated Sarcoma 180 Cells." *Cancer Chemotherapy and Pharmacology* 43, no. 5 (March 1999): 389–93. doi:10.1007/s002800050912.
- Un, Keita, Shigeru Kawakami, Yuriko Higuchi, Ryo Suzuki, Kazuo Maruyama, Fumiyoshi Yamashita, and Mitsuru Hashida. "Involvement of Activated Transcriptional Process in Efficient Gene Transfection Using Unmodified and Mannose-Modified Bubble Lipoplexes with Ultrasound Exposure." *Journal of Controlled Release* 156, no. 3 (2011): 355–363.
- Van Esser, S., G. Stapper, P. J. Van Diest, MAAJ van den Bosch, JHGM Klaessens, WP Th M. Mali, IHM Borel Rinkes, and R. van Hillegersberg. "Ultrasound-Guided Laser-Induced Thermal Therapy for Small Palpable Invasive Breast Carcinomas: A Feasibility Study." *Annals of Surgical Oncology* 16, no. 8 (2009): 2259–2263.
- Van Wamel, Annemieke, Klazina Kooiman, Miranda Harteveld, Marcia Emmer, Folkert J. Ten Cate, Michel Versluis, and Nico De Jong. "Vibrating Microbubbles Poking Individual Cells: Drug Transfer into Cells via Sonoporation." *Journal of Controlled Release* 112, no. 2 (2006): 149–155.
- Varslot, Trond, and Gunnar Taraldsen. "Computer Simulation of Forward Wave Propagation in Soft Tissue." *Ultrasonics, Ferroelectrics and Frequency Control, IEEE Transactions on* 52, no. 9 (2005): 1473–1482.
- Vaškovicová, Naděžda, Zdena Druckmüllerová, Roman Janisch, Jiřina Škorpíková, and Vojtěch Mornstein. "Effects of Therapeutic Ultrasound on the Nuclear Envelope and Nuclear Pore Complexes." *Journal of Applied Biomedicine* 11, no. 4 (2013): 235–42. doi:10.2478/v10136-012-0042-7.
- Wamel, Annemieke van, Ayache Bouakaz, Michel Versluis, and Nico de Jong. "Micromanipulation of Endothelial Cells: Ultrasound-Microbubble-Cell Interaction." *Ultrasound in Medicine & Biology* 30, no. 9 (2004): 1255–1258.
- Wang, Tzu-Yin, Zhen Xu, Timothy L. Hall, J. Brian Fowlkes, and Charles A. Cain. "An Efficient Treatment Strategy for Histotripsy by Removing Cavitation Memory." *Ultrasound in Medicine & Biology* 38, no. 5 (2012): 753–766.
- Wang, Xiaohuai, Thomas J. Lewis, and Doug Mitchell. "The Tumoricidal Effect of Sonodynamic Therapy (SDT) on S-180 Sarcoma in Mice." *Integrative Cancer Therapies* 7, no. 2 (2008): 96–102.
- Ward, Mark, Junru Wu, and Jen-Fu Chiu. "Ultrasound-Induced Cell Lysis and Sonoporation Enhanced by Contrast Agents." *The Journal of the Acoustical Society of America* 105, no. 5 (1999): 2951–2957.
- Westervelt, Peter J. "Parametric Acoustic Array." *The Journal of the Acoustical Society of America* 35 (1963): 535.
- Williams, Earl G. *Fourier Acoustics: Sound Radiation and Nearfield Acoustical Holography*. Access Online via Elsevier, 1999.
- Wu, Junru. "Theoretical Study on Shear Stress Generated by Microstreaming Surrounding Contrast Agents Attached to Living Cells." *Ultrasound in Medicine & Biology* 28, no. 1 (2002): 125–129.
- Wu, Junru, and Wesley L. Nyborg. "Ultrasound, Cavitation Bubbles and Their Interaction with Cells." *Advanced Drug Delivery Reviews, Ultrasound in Drug and Gene Delivery*, 60, no. 10 (June 30, 2008): 1103–16. doi:10.1016/j.addr.2008.03.009.
- Xu, Zhen, Mekhala Raghavan, Timothy L. Hall, Ching-Wei Chang, M.-A. Mycek, J. Brian Fowlkes, and Charles A. Cain. "High Speed Imaging of Bubble Clouds Generated in Pulsed Ultrasound Cavitation Therapy-Histotripsy." *Ultrasonics, Ferroelectrics and Frequency Control, IEEE Transactions on* 54, no. 10 (2007): 2091–2101.
- Yang, Fang, Ning Gu, Di Chen, Xiaoyu Xi, Dong Zhang, Yixin Li, and Junru Wu. "Experimental Study on Cell Self-Sealing during Sonoporation." *Journal of Controlled Release* 131, no. 3 (November 12, 2008): 205–10. doi:10.1016/j.jconrel.2008.07.038.
- Yang, Kyu-Hyun, Javad Parvizi, Shyu-Jye Wang, David G. Lewallen, Randall R. Kinnick, James F. Greenleaf, and Mark E. Bolander. "Exposure to Low-Intensity Ultrasound Increases

- Aggrecan Gene Expression in a Rat Femur Fracture Model." *Journal of Orthopaedic Research* 14, no. 5 (1996): 802–809.
- Young, Barbara, Phillip Woodford, and Geraldine O'Dowd. *Wheater's Functional Histology: A Text and Colour Atlas*. Elsevier Health Sciences, 2013.
- Yu, Tinghe, Jin Bai, Kai Hu, and Zhibiao Wang. "The Effect of Free Radical Scavenger and Antioxidant on the Increase in Intracellular Adriamycin Accumulation Induced by Ultrasound." *Ultrasonics Sonochemistry* 10, no. 1 (2003): 33–35.
- Yu, Tinghe, Shugang Li, Jie Zhao, and Timothy J. Mason. "Ultrasound: A Chemotherapy Sensitizer." *Technology in Cancer Research & Treatment* 5, no. 1 (2006): 51–60.
- Yudina, Anna, Matthieu Lepetit-Coiffé, and Chrit T. W. Moonen. "Evaluation of the Temporal Window for Drug Delivery Following Ultrasound-Mediated Membrane Permeability Enhancement." *Molecular Imaging and Biology* 13, no. 2 (June 3, 2010): 239–49. doi:10.1007/s11307-010-0346-5.
- Yuldashev, P. V., and V. A. Khokhlova. "Simulation of Three-Dimensional Nonlinear Fields of Ultrasound Therapeutic Arrays." *Acoustical Physics* 57, no. 3 (2011): 334–343.
- Yumita, Nagahiko, Ryuichiro Nishigaki, Koshiro Umemura, and Shin-ichiro Umemura. "Hematoporphyrin as a Sensitizer of Cell-Damaging Effect of Ultrasound." *Japanese Journal of Cancer Research* 80, no. 3 (1989): 219–222.
- Yumita, Nagahiko, Nobuo Okuyama, Kazuaki Sasaki, and Shin-ichiro Umemura. "Sonodynamic Therapy on Chemically Induced Mammary Tumor: Pharmacokinetics, Tissue Distribution and Sonodynamically Induced Antitumor Effect of Gallium-porphyrin Complex ATX-70." *Cancer Chemotherapy and Pharmacology* 60, no. 6 (2007): 891–897.
- Yumita, Nagahiko, Kazuaki Sasaki, Shin-ichiro Umemura, and Ryuichiro Nishigaki. "Sonodynamically Induced Antitumor Effect of a Gallium-Porphyrin Complex, ATX-70." *Japanese Journal of Cancer Research* 87, no. 3 (1996): 310–316.
- Yumita, Nagahiko, and Shin-ichiro Umemura. "Sonodynamic Antitumour Effect of Chloroaluminum Phthalocyanine Tetrasulfonate on Murine Solid Tumour." *Journal of Pharmacy and Pharmacology* 56, no. 1 (2004): 85–90.
- Zabolotskaya, E. A., and R. V. Khokhlov. "Quasi-Plane Waves in the Nonlinear Acoustics of Confined Beams." *Sov. Phys. Acoust* 15, no. 1 (1969): 35–40.
- Zhao, Ying-Zheng, Yu-Kun Luo, Cui-Tao Lu, Jing-Feng Xu, Jie Tang, Mei Zhang, Yan Zhang, and Hai-Dong Liang. "Phospholipids-Based Microbubbles Sonoporation Pore Size and Reseal of Cell Membrane Cultured in Vitro." *Journal of Drug Targeting* 16, no. 1 (2008): 18–25.
- Zhou, Yun, Ronald E. Kumon, Jianmin Cui, and Cheri X. Deng. "The Size of Sonoporation Pores on the Cell Membrane." *Ultrasound in Medicine & Biology* 35, no. 10 (2009): 1756–1760.





## List of publications

Lafond M, Prieur F, Chavrier F, Mestas J-L, Lafon C. Numerical study of an Ultrasonic Confocal Setup for Cavitation Applications. *Journal of the Acoustical Society of America*, Under review, October, 2016.

Chettab K, Mestas J-L, Lafond M, Djamel Eddine, Dumontet C, High Doxorubicin Delivery into Tumor Cells by Ultrasound Without Contrast Agents, *Molecular Pharmaceutics*, Under review, October, 2016.

Lafond M, Aptel F, Mestas J-L, Lafon C. Ultrasound-Mediated Ocular Delivery of Therapeutic Material: a Review. *Expert Opinion on Drug Delivery*. Invited paper, published online. June, 2016.

Lafond M, Mestas J-L, Prieur F, Chettab K, Geraci S, Clézardin P, Lafon C. Unseeded Inertial Cavitation for Enhancing the Delivery of Chemotherapies: A Safety Study. *Ultrasound in Medicine and Biology*, vol. 42, No 1, pp. 220–231, January, 2016.

Prieur F, Pillon A, Mestas J-L, Cartron V, Cèbe P, Chansard N, Lafond M, Lafon C. Enhancement of Fluorescent Probe Penetration into Tumors In Vivo Using Unseeded Inertial Cavitation. *Ultrasound in Medicine and Biology*, vol. 42, No 7, pp. 1706–1713, July, 2016.

Chettab K, Roux S, Mathé D, Cros-Perrial E, Lafond M, Lafon C, Dumontet C, Mestas J-L. Spatial and Temporal Control of Cavitation Allows High In Vitro Transfection Efficiency in the Absence of Transfection Reagents or Contrast Agents. *Plos One*. p.0134247, August, 2015.

Prieur F, Zorgani A, Catheline S, Souchon R, Mestas J-L, Lafond M, Lafon C. Observation of a cavitation cloud in tissue using correlation between ultrafast ultrasound images, *IEEE Transactions On Ultrasonics Ferroelectrics and Frequency Control*, Vol. 62, No 7, pp. 1256–1264, July, 2015.